SENSOR AND DATA FUSION OF REMOTELY SENSED WIDE-AREA GEOSPATIAL TARGETS

STEPHEN CHURCHILL

SENSOR AND DATA FUSION OF REMOTELY SENSED WIDE-AREA GEOSPATIAL TARGETS

by

© Stephen Churchill

A thesis submitted to the

School of Graduate Studies

in partial fulfillment of the

requirements for the degree of

Master of Engineering

Faculty of Engineering and Applied Science
Memorial University of Newfoundland

January 2009

St. John's Newfoundland Canada

Abstract

This thesis consists of the examination of methodologies for sensor fusion and data fusion of remotely sensed, sparse geospatial targets. Methods for attaining an increased awareness of targets in both tactical and strategic roles are proposed and examined. The example methodologies are demonstrated, and areas for further research noted. Discussions of the proposed methods are carried forth in the context of iceberg detection.

Amongst the difficulties associated with the combination of sensor parameters and sensor data are the wide variety of technologies, performance ability, coverage, and reliability that are available to those users of remote sensing technology. Typical sensors include airborne search radars, marine search radars, surface wave radar, and satellite synthetic aperture radar. The ability to mitigate the related parametric variances is the test of an appropriate sensor or data fusion algorithm.

Documented herein are the efforts to find such an algorithm using various statistical methods. Primary among these is Bayes Theorem combined with tracking systems

such as the multiple hypothesis tracker. This and other methodologies are explored and evaluated, where appropriate. It will be demonstrated that such a methodology can combine sensor data returns to provide high performance, wide-area, situational awareness with sensors considered to have poor performance.

Acknowledgements

The author would like to acknowledge the financial support of C-CORE, the Natural Sciences and Engineering Research Council of Canada, and the proponents of the joint industry projects; the Integrated Ice Management Research and Development Initiative, and the Ice Management Joint Industry Program.

Also the author would like to thank Provincial Airlines Environmental Services Division for the use of their Ice Management Control Centre and access to their Ice Data Network System and its data.

Finally the author would like to thank his supervisors Charles Randell, Ph.D., P.Eng., and Eric Gill, Ph.D., P.Eng., as well as Desmond Power, M.Eng., P.Eng., C-CORE Director of Remote Sensing, for their guidance and advice.

Portions of this material have previously been published in the following reports.

C-CORE, *Ice Management JIP Year 2003*, C-CORE Report Number R-03-059-226 v1, December, 2003.

C-CORE, *Integrated Ice Management R&D Initiative, 2002*, Section 9, C-CORE Report Number R-02-026-110 v1.1, May, 2003.

C-CORE, *Integrated Ice Management R&D Initiative, 2001, Vol 1 – Iceberg Detection*, C-CORE Report Number R-01-24-605-V2, December, 2001.

Various published papers containing portions of this material are listed below:

Churchill, Stephen, Charles Randell, Des Power, Eric Gill, "Data Fusion: Cumulative Effects of Discrete Fusion on Target Detection Probability", *Proceedings of the International Geoscience and Remote Sensing Symposium (IGARSS'06)*, July 31-August 31, 2006, Denver, Colorado.

Churchill, Stephen, Charles Randell, Des Power, Eric Gill, "Data Fusion: Remote Sensing for Target Detection and Tracking", *Proceedings of the International Geoscience and Remote Sensing Symposium (IGARSS'04)*, September, 2004.

Churchill, Stephen, "Remote Sensing Data Fusion", *Graduate Symposium Proceedings Session – II*, December 3rd, 2003, Memorial University, St. John's, NF, Canada.

Churchill, Stephen, Charles Randell, Eric Gill, Desmond Power, "Data Fusion: Associations of Detections for Multiple Hypothesis Tracking using Remote Sensing", *Proceedings of NECEC 2003*, November 12, 2003, St. John's, NF, Canada.

Churchill, Stephen, Charles Randell, Eric Gill, Desmond Power, "An outline of Fusion and Sensor Combinational Methodologies for Disparate, Sparse Multi-Sensor Networks for Detecting Icebergs", *Proceedings of the International*

Geoscience and Remote Sensing Symposium (IGARSS'02), June 24th, 2002, Toronto, ON, Canada.

Churchill, Stephen, Charles Randell, Eric Gill, Desmond Power, "Toward Fusion of Satellite SAR and other Remotely Sensed Marine Data for Wide-Area Operational Monitoring", *Proceedings of NECEC 2001*, November 13, 2001, St. John's, NF, Canada.

Table of Contents

List of Tables

List of Figures

List of Abbreviations and Symbols

AIMR	Airborne Imaging Microwave Radar
CIO	Coupled Ice Ocean (Iceberg Drift Model)
CIS	Canadian Ice Services
CPBS	Carcinogenicity Prediction and Battery Selection
ESRF	Environmental Studies Revolving Fund
f(x)	A quantity derived as a function of the variable 'x'
FLAR	Forward Looking Airborne Radar
FLI	Fluorescence Line Imager
GIS	Geographical Information System
GNN	Global Nearest Neighbor
HF	High Frequency (3–30 MHz)
IDNS	Ice Data Network System
IIMI	The Integrated Ice Management Initiative Program
IIP	International Ice Patrol
IPIX	Ice Multi-Parameter Imaging X-band Radar
LORAN	Long Range Navigation
MHT	Multiple Hypothesis Tracking
MIROS	Microwave Radar Observing System
MTT	Multiple Target Tracking
OTH	Over-The-Horizon (Radar)

PAL	Provincial Airlines Limited, particularly the Environmental Services Division
PDF	Probability Density Function
Pr(X)	The statistical probability of some random variable X
Pr(X|Y)	The statistical probability of variable X given the occurrence of Y
SAR	Synthetic Aperture Radar
SLAR	Side Looking Airborne Radar
SLDMB	Self-Locating Datum Marker Buoy
SWR	Surface Wave Radar
UHF	Ultra High Frequency (300 MHz–3 GHz)

List of Appendices

Chapter 1 Introduction

This manuscript describes the research, application, and development completed towards finding appropriate methodologies for sensor and data fusion of remotely sensed targets. Within the context presented here, sensor and data fusion refer to the combination of sensors parameters and detection data, respectively. Similarly, remote sensing refers to the observation of a phenomenon via either active or passive means. The phenomena being sensed are referred to as targets. For our purposes, the targets are physical objects presumed to exist in some broad geographical location; however, the reader should not presume that the theory and methods presented here are limited to this specific application.

While the body of work presented could have been applied to a broad range of targets, a specific target set was chosen due to the application that motivated the development of these methods. Specifically, the availability of a diverse set of independent sensors used for the remote sensing of icebergs provided the opportunity to produce methods for combining these sensors, and their data.

This work, being driven with this specific application in mind, focused on combining disparate, sparse sensors producing temporally sporadic data. These sensors vary parametrically with respect to geographical coverage, detection capability, and reliability. Thus, the body of work presented here limits itself to the mitigation of the challenges posed by the use of these discordant sensors.

For the reader's reference, Figure 1.1 (Petro-Canada, 2002) provides a map of the offshore region of Eastern Canada; the geographical area of interest. Icebergs frequent this area to varying degrees from March to July each year as they drift with the Labrador Current. The motivating factors behind the monitoring of icebergs in this region stems from the desire to protect the shipping routes that pass through the area and the oil and gas fields located on the north-eastern Grand Banks of Newfoundland. The safe operation of shipping vessels, and of oil rigs and platforms, requires knowledge of the iceberg locations.

1.1 Icebergs and Iceberg Management

Icebergs are sections of glacial ice, set adrift when broken from the glacier at the ocean edge. The International Ice Patrol (IIP) provides a brief description of the iceberg process (IIP, 2003a). About 90% of all icebergs encountered in Canadian waters are calved from the glaciers of Western Greenland, accounting for 10,000 to 40,000 icebergs annually (CIS, 2002a).

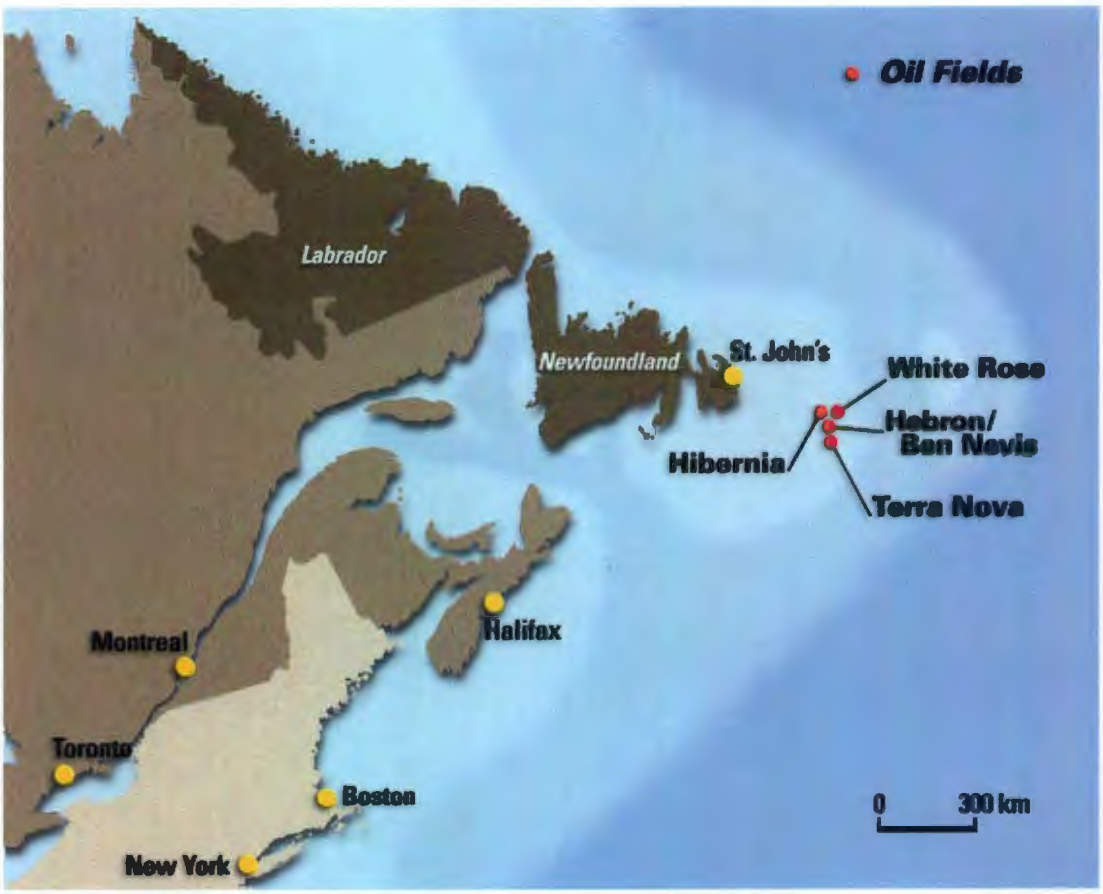

Figure 1.1: Oil and Gas Operations Map (Petro Canada, 2002)

The major glaciers of Greenland are shown in Figure 1.2 (IIP, 2003b). Ocean currents carry the icebergs through Baffin Bay and the Labrador Sea. The icebergs eventually following the Labrador Current south to Newfoundland (Figure 1.3, CIS, 2002a). In the North Atlantic, the water temperature ranges from −1.7 °C in the Labrador Current, to 20 °C in the Gulf Stream. South of the Grand Banks, the cold Labrador Current mixes with the warm Gulf Stream. Generally, icebergs melt rapidly once they encounter the Gulf Stream; however, in 1926 an iceberg was reported 275 km from Bermuda, and they have been know to travel as far east as the Azores (IIP, 2003a).

Icebergs range in size from less than 1 m in waterline length (maximum dimension in the plane of the water surface) to hundreds of meters. Their mass generally ranges from hundreds of tons to tens of millions of tons. Icebergs have been known to exceed kilometers in length with associated increases in mass (CIS, 2002b).

Icebergs are classified on waterline length, and mass ranges are associated with these. Table 1.1 (CIS, 2002b) shows the standard IIP classifications.

Figure 1.4 shows yearly iceberg frequency (IIP, 2003c) as determined by the IIP. The numbers are determined from reports of icebergs south of the 48th Parallel in each year. This accounts for an average of 480 icebergs per year.

Figure 1.2: Iceberg Producing Glaciers (IIP, 2003b)

Figure 1.3: Iceberg Affecting Currents (CIS, 2002a)

Table 1.1: Iceberg Classifications			
Classification	**Height Above Water (m)**	**Waterline Length (m)**	**Approximate Mass (Mt)**
Growler	less than 1 m	less than 5 m	0.001
Bergy Bit	1 m to less than 5m	5 m to less than 15 m	0.01
Small Berg	5 m to 15 m	15 m to 60 m	0.1
Medium Berg	16 m to 45 m	61 m to 120 m	2.0
Large Berg	46 m to 75 m	121 m to 200 m	10.0
Very Large Berg	Greater than 75 m	Greater than 200 m	Greater than 10.0

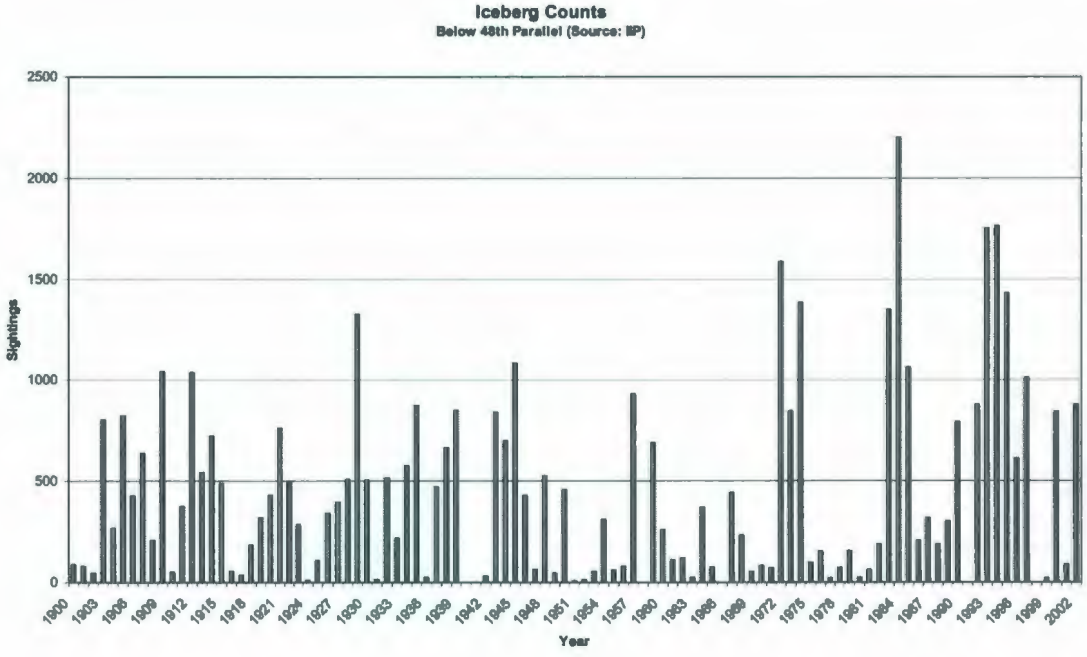

Figure 1.4: Iceberg Frequency

While both shipping and oil and gas recovery require knowledge of iceberg locations, it is the oil and gas industry that requires wide-range, accurate data that can only be supplied by advanced remote sensing devices. For its part, shipping relies mainly on reported southern 'ice limits' and the use of commercial marine radar systems for detection.

The oil and gas operators must be concerned with the probability that a drifting iceberg may impact a platform, tanker, or supply vessel, or scour undersea facilities such as wellheads and pipelines. Thus, since the discovery of oil and gas deposits in the region in the late 20th century, a fair amount of effort has been placed in determining means of long-range detection and physical management of icebergs.

To protect their installations from the potential of iceberg collisions, operators of offshore oil and gas development and recovery programs use a variety of remote sensing technologies for the detection of icebergs. The subset of icebergs that could pose a threat to installations can then be physically managed to remove the threat imposed by their presence.

The main detection techniques currently used for ice management are aerial patrol, visual sightings from vessels and platforms, marine radar, satellite synthetic aperture radar (SAR), and surface wave radar (SWR). Almost all of these, except human vision, rely on radar systems. These and other means of detecting icebergs will be discussed in Chapter 2.

With every sensor currently in use or available for remote sensing, there are trade-offs between sensor performance and coverage. For operations where large regions must be searched, a balance must be struck between using sensors with high coverage ability and lower detection performance, and sensors with low coverage ability and high detection performance.

1.2 The Need for Advancement in Fusion Ability

Ideally, a single sensor that is better in all respects to any combination of the existing sensors could be sought; however, practical technological and financial limitations dictate that such a sensor will not likely exist in the near future. Instead, the appropriate combination of information from the existing individual sensors provides the best means to achieving a data product that provides better coverage, continuance, detection ability, and mitigates false positives in a manner beyond the capabilities of any single sensor.

The lacking performance of the current sensor regime has been apparent for many years. Rossiter et al. (1995) pointed out several flaws in the iceberg detection systems in use at the time:

- A lack of a continuous iceberg detection capability within the near-platform zone precipitating the need for iceberg re-identification.
- A lack of utilization of all available data.

- A lack of drift direction information, such as iceberg keel data.
- Reliable and timely information is critical: otherwise the information will lack credibility.

As well, requirements were noted which are still relevant:

- Ships require only positional information of icebergs to avoid collision, platforms desire heading and speed information in addition to positional, since they lack the ability to maneuver or maneuver quickly.
- Ships, especially tankers, do not consider growlers less than 200 t a threat, however bergy bits with masses greater than 10,000 t can do damage, therefore the detection system should be capable of detecting approximately 1000 t icebergs, or 10 m × 10 m × 10 m.
- Ice information that is required for tactical decisions should be on the bridge or in the platform control room for direct and immediate use.

The cost of developing new sensors is seen as prohibitive; however, the remote sensing technologies in use are continually being improved. The need exists to make the most of the information available from the current sensors and to deploy these sensors effectively.

These sensors should be combined parametrically in order to provide the means for advanced risk modeling. Offshore structures must be designed to withstand the loads they may experience; for structures that are exposed to icebergs this load is determined from risk analysis models. With previous risk models, detection schemes incorporate a

rudimentary sensor scheme—often consisting of only one marine radar sensor. This does not take into account the many other radars and types of sensors being used in offshore iceberg management. Taking these other sensors into account, their different types and the assessment of their implementations, will result in more accurate and realistic risk assessments. Furthermore, a method for combining detection data from the many different sensors in use for iceberg detection could provide a better, real time, wide-area view of the ice conditions on the East Coast for efficient use of the ice management resources. A system that accounts for the uncertainty associated with each sensor type will provide the means to utilize even wide-area low-confidence sensors and increase the accuracy and coverage of the sensor network.

1.3 Statement of Challenges

In a broad sense, defining a methodology for the combination of sensor parameters and sensor data satisfies a need that exists in a wide range of applications. In terms of remote sensing technologies, the need to monitor large geographical expanses is a challenge. In a country, such as Canada, with an extensive coastline that is largely unguarded and mostly unmonitored, the application of a system capable of combining data collected over large geographical areas has significant security applications.

The challenges, in particular to iceberg detection, are numerous. Icebergs present poor radar targets (Rossiter et al., 1995) compared to the approximate radar cross section of other objects and standard references. The effective target area of icebergs is affected by their irregular shape and the conductivity of ice. Table 1.2 compares small icebergs to other typical offshore targets.

The complexity of the iceberg detection problem is not limited to iceberg size or reflectance of radio waves. The solution must consider the type of sensor being used, its ability to detect targets, minimize false alarms, and discriminate between icebergs and other targets. As well, the applicability and tasking of any sensor within a sensor hierarchy is dictated by its reliability, availability, coverage, and data latency. The ability of any sensor to detect targets is further a function of the target size, environmental conditions, and range.

Table 1.2: Radar Cross-Section Comparison		
Classification	**Radar Cross-Section (m^2)**	**Actual Projected Cross-Section (m^2)**
Growler	0.01–0.1	2
Bergy Bit	0.5–1.0	60
Small Iceberg	5–10	400
Supply Vessel	150	400
Life Raft	0.25–0.5	3
Steel Sphere	1	1

In terms of an overall strategy for offshore hydrocarbon recovery and offshore platform safety, the designed iceload of the platform must be considered along with its safety perimeter and its ability to avoid collision. This combined with the ice management strategy—the towing of icebergs to avoid collisions with surface and subsea structures, and the ability of these operations to succeed—define the threat to the structure. An examination of all of these influences is beyond the scope of this document.

When focusing on providing safe operation of offshore installations and vessels, the key is knowledge of iceberg existence and location. This knowledge also promotes effective sensor resource deployment, such as the dispatching of ice management vessels and surveillance aircraft, or the acquisition of satellite imagery.

The need exists for a system that can monitor both the immediate (tactical) and upstream (strategic) areas so that ice management operators can make informed decisions on the use of ice management resources. A knowledge of the sensor network's ability to detect icebergs, through the parametric combination of sensors, and the assimilation of data to form a most-certain analysis of the current iceberg positions, would give the ice management operators insight into what is really happening in the ocean regions that influence industry safety and operational decisions.

There are two aspects to the integration of information from iceberg sensors. First, the challenge is to define ways of combining current remote sensing capabilities such that a set of sensors can be viewed as a 'single' sensor network. This view of the sensors as a whole would provide detailed knowledge of areal coverage and the ability to detect targets in this coverage area. The network could be adjusted for areas deficient in ability to detect targets by introducing new or reallocating existing sensors. This provides the means for theoretical risk analysis and planning.

Second, a methodology must be defined for the combination of the sensor-derived data. Represented in a state space paradigm, iceberg data should include factors such as position, size, keel depth, and the level of confidence associated with the target. Subsequently from these the attributes such as risk to surrounding structures can be estimated. The association between targets could be determined from of the target, if available, along with knowledge of the sensors and the environment.

1.4 Definitions: Sensor Fusion vs. Data Fusion

As discussed above, the methods examined here can be divided into two categories:

- a methodology for combining sensor performance characteristics: Sensor Fusion; and,
- a methodology for combining data obtained from a sensor: Data Fusion.

The challenge of combining sensors' performance is concerned with the combination of performance curves spatially and temporally. The methodology to achieve this is not concerned with individual data points, only with the combination of the sensors' statistical performance parameters.

Alternately, the combination of sensor data is concerned only with the combination of data, not performance statistics. The combination of detection data makes use of performance statistics to determine the validity of those detections.

The two strategies are summarized in the following definitions:

- Sensor Fusion: From individual performance curves, overall sensor network performance must be devised using a method that accounts for the various parameters of each sensor. In doing so, the value of each sensor can be assessed on an incremental basis to determine optimal configurations for existing and future installations. Thus, this fusion serves a long-term strategic purpose.

- Data Fusion: With detection data coming from multiple sources, a means to fuse the detection data into a combined detection database is necessary. The fusion methods must account for variations in the different sensors such as detection confidence metrics and latency times between detections. Through rigorous utilization of sensor knowledge, sensor derived data can be combined in a statistical manner, allowing even low confidence data to be combined effectively. This fusion serves both strategic and tactical purposes, and is sometimes referred to as data integration.

1.5 Thesis Contributions

The focus of this thesis is the combination of sensors and sensor data. The thesis applies existing theory and techniques to the areas of sensor parameter combination with emphasis on spatial-temporal combination, and detection ability of combined sensors. As well, the integration of detection data from sensors is accomplished in terms of detection coverage, the current position of previously detected targets, and confidence in this resultant information. It is demonstrated that combining detection information provides an improved detection ability through efficient use of all available information.

This approach is unique in its application of these theories to iceberg detection. It is of particular interest at this time, when effective satellite observation is becoming a commercial possibility. The number of remote sensing instruments is now reaching a

quantity that will allow for wide-area coverage and sufficient revisit rates to support the algorithms herein described.

Chapter 2 Current Solutions and Techniques

2.1 Iceberg Detection

Presented in this chapter is a historical perspective of iceberg detection, followed by an overview of theory and algorithms deemed applicable to the challenges described in Chapter 1.

2.1.1 Iceberg Detection Sensors

A large variety of remote sensing technologies have been examined for their applicability to the iceberg detection problem.

There are a variety of sensors currently used to detect icebergs off the Canadian East Coast:

- human visual observation;
- airborne frequency-agile search radars;
- ship-mounted search radars (X-band and S-band);
- ship-mounted enhanced search radars;

- platform-mounted search radars (X-band and S-band);
- platform-mounted enhanced search radars;
- satellite-borne SAR; and,
- surface-wave radar.

These are compared parametrically in Appendix A, and a summary is presented in Table 2.1 and Table 2.2. As well as those listed, other technologies have been previously evaluated for iceberg detection (Rossiter, et al, 1995):

- coherent radar systems, providing:
    - target velocity from Doppler info; or
    - enhanced imaging from phase shift;
- imaging radar:
    - Side Looking Airborne Radar (SLAR); and
    - airborne SAR;
- Forward Looking Airborne Radar (FLAR), such as AN/APS 137;
- Ice multi-Parameter Imaging X-band Radar (IPIX);
- Airborne Imaging Microwave Radar (AIMR), passive microwave technology; and,
- Fluorescence Line Imager (FLI), visual spectrum technology.

None of these systems are currently used for iceberg detection off Canada's East Coast for reasons including cost, availability, and applicability.

Detailed analysis of ice detection using the sensors mentioned above can be found for marine radar in Environmental Studies Revolving Fund (ESRF) Report 008 (Ryan, Harvey, Kent, 1985), enhanced marine radar in ESRF Report 035 (Harvey, Ryan, 1986), and airborne radar in ESRF Report 045 (CANPOLAR, 1986). C-CORE has also evaluated current and promising techniques. A partial list of the reports containing an evaluation of relevant sensors is given below:

- C-CORE IIMI Report 1999 (C-CORE, 1999)
    - 'SeaScan' enhanced marine radar
    - RADARSAT-1 iceberg detection
    - Physical management concepts
- C-CORE IIMI Report 2000 (C-CORE, 2000)
    - High Frequency (HF) surface wave radar
    - RADARSAT-1 iceberg field trials
    - Physical management evaluation
- C-CORE IIMI Report 2001 (C-CORE, 2001)
    - RADARSAT-1 iceberg field trials

- 'SeaScan' enhanced marine radar

- C-CORE IIMI Report 2002 (C-CORE, 2003a)
  - HF surface wave radar validation
  - Ultra High Frequency (UHF) coherent radar system
  - ENVISAT satellite SAR detection
  - Improved 'SeaScan' enhanced marine radar

- C-CORE IIMI Report 2003 (C-CORE, 2003b)
  - Satellite SAR iceberg detection in sea ice
  - ENVISAT ship/iceberg discrimination
  - Physical management with nets

- ESRF 008: The Assessment of Marine Radars for the Detection of Ice and Icebergs (Ryan, Harvey, Kent., 1985)
  - Testing of X and S-band radar off Labrador
  - Some mathematical treatment of RCS and signal to clutter ratio

- ESRF 045: Iceberg Detection by Airborne Radar: Technology Review and Proposed Field Programs (CANPOLAR, 1986)
  - Examines feasibility of studies into real aperture SLAR, SAR, etc.
  - Statistical target and clutter return distributions
  - Litton APS-504V(5) SAR system

- Signal processing, scan to scan integration, CFAR processing

- Mobil Oil, Assessment of Iceberg Management for the Grand Banks Area: Analysis of Detection and Deflection Techniques (Bishop, 1989)
  - Litton APS-504 V(5), pulse compressed, frequency agile SAR
  - The BiStar radar system
  - IPIX Doppler radar

- ESRF 132: Remote Sensing Ice Detection Capabilities—East Coast (Rossiter et al., 1995)
  - Exhaustive treatment of support vessel and platform needs
  - SLAR vs. SAR
  - Overviews of SARs: STAR1, STAR2, Litton APS 504V(5), and FLAR AN/APS 137, marine pulse radar, HF SWR, IPIX Doppler radar, AIMR microwave radiometer, FLI optical imager, and other acoustic systems and optical systems

Table 2.1: Sensors, Part I

Sensor	Visual			Surface Wave Radar	Satellite Radar	Airborne Radar	Enhanced Marine Radar	Marine Radar	
	Airborne	Platform	Ship	HF SWR	RADARSAT/ ENVISAT	Litton SAR Search	SeaScan/Titan	S-band	X-band
Coverage	Horizon based on height of observer	*id.*	*id.*	450km range, 120° wide, 200,000km²	Works best in 300km or 150km swath width modes	Most effective between 150 to 450m altitudes, hence 50 to 87km swath width	Same as Marine Radar	Dependent on Radar Height. Support Vessels 17km, Hibernia 48km [1]	*Id.*
Probability of Detection	No data	No data	No data	Small bergs (>15m) out to 450km[3]	For these modes, can only detect bergs over 30m, but does this very well.	Growlers (<5m) detectable up to 29km in calm seas	Capable of detecting growlers (<5m) at 7km	Bergy Bits (5–15m) detectable up to 13km [2]	Capable of detection of 20m bergs upto 23km in calm seas [2]
Probability of False Alarms	No data	No data	No data	No data	No data	No data	No data	No data	No data
Resolution	Spatial resolution .3mrad, ~5.1m @ 17 km	*id.*	*id.*	600m, 3.6° Azimuth	50m or 30m resolution respectively.	2% of range used for detection. Beamwidth 2.3 °	Dependent on the marine radar used (X or S-band)	1% of range used for detection. Beamwidth 2°	1% of range used for detection. Beamwidth 0.8°
Cost	$4500 to $5000 per hour	Salary	Salary and any ship costs	Operational Costs	$2k to $4k per image for commercial.	$4500 to $5000 per hour	Additional setup cost of processor	Setup low, plus operators salary.	*id.*
Update Freq	1–2 days weather permitting	Real time	Real time if in region of interest	Real time less any post processing	An ascending and descending pass every 3 days	1–2 days weather permitting	Real time if in region of interest	Real time if in region of interest	Real time if in region of interest

Table 2.2: Sensors, Part II

Sensor	**Visual**			**Surface Wave Radar**	**Satellite Radar**	**Airborne Radar**	**Enhanced Marine Radar**	**Marine Radar**	
	Airborne	Platform	Ship	HF SWR	RADARSAT/ ENVISAT	Litton SAR Search	SeaScan /Titan	S-band	X-band
Data Latency	None, if sighting relayed by radio	None	None	From 6 to 20 minutes processing time	3 hours minimum	None, if sighting relayed by radio	None	None	None
Availability	Only when a flight has been chartered.	Constant	Constant	Daytime operation due to ionosphere 'F' Layer	Constant, note update frequency	Only when a flight has been chartered	Constant	Constant	Constant
Reliability	Susceptible to low visibility	*id.*	*id.*	No weather limitation	Penetrates most weather conditions, has a dependency on sea state for ocean target detection	Works in X-band therefore somewhat susceptible to rain and fog. Flights can only occur in appropriate weather	Dependent on the marine radar used (X or S-band)	Better than X, adversely affected by heavy rain [1]	Affected by moderate rain and fog [1]
Ability to Classify	Excellent identification, some size information, no accurate velocity information due to range ambiguity	*id.*	*id.*	Long period tracking available. Some size information	Detection software developed. Isolates targets from clutter and speckle. Size detection excellent. No velocity information	Human interpretation of Radarscope. Some ability to detect size. No velocity information	Same as Marine Radar, software may make tracking easier	Human interpretation of Radarscope. Some ability to detect size, and if monitored, direction and speed	*id.*

[1] Rossiter et al., 1995
[2] C CORE, 1992
[3] C CORE, 2000

2.1.2 Other Approaches to the Ice Problem

Other approaches to iceberg management include attempts to modify, mark or destroy icebergs.

In Ryan (1985), the issue of the radar cross section of icebergs (radio frequency reflectivity of icebergs) is addressed. Several previous attempts to detect icebergs are noted, including methods for marking icebergs for re-identification:

- dye via various delivery systems, documented in Allen (1971), Grant (1979), and Robe (1978); and,
- floating tags, documented in Robe (1977).

The floating tags described above were attached with lines to icebergs, and included a radar reflector and radio direction finder transmitter. It is reported that most icebergs broke away from their line during stormy conditions or rolling events.

In 1975 the US Coast Guard Research and Development Center attempted to tether an instrument package to an iceberg using a large steel dart and trailing line. The method effectively solved the rolling and melting problems; however, calving could still dislodge the dart. Tests were apparently carried out in 1975 and 1977 with success. As well, research was conducted in 1971 to define an electronics package for deployment on or near icebergs to transmit position derived by Long Range Navigation (LORAN) or other navigational systems (Ryan, 1985).

Proposed in Ryan (1985) is the deployment onto icebergs of the following passive and active materials and devices; the purpose of which is to make icebergs easier to detect:

- resonant filaments (a.k.a. chaff);
- reflective mesh;
- off-berg reflectors (kites or balloons);
- radar transponders;
- radio direction finders;
- LORAN transmission equipment;
- HF radar transponders; and,
- satellite tracking transponders.

Of these methods, only satellite tracking transponders, such as Self Locating Datum Marker Buoys (SLDMB), are currently used. Not addressed in Ryan (1985), is the prohibitive cost to deploy these technologies, or the reliability of their application to icebergs. The primary user of satellite transponder technology is the IIP, which deploys them from aircraft.

Also worth noting are the attempts at reducing iceberg mass. Amongst others, the IIP attempted this using conventional bombs, thermite, lampblack and mining (IIP,

2003d). Figure 2.1 shows the result of a thermite test. These methods have proven ineffective against icebergs.

Figure 2.1: Thermite used on an Iceberg by the IIP

2.2 Techniques Applicable to Sensor Fusion

This section describes common statistical techniques that are deemed appropriate to the combination of iceberg detection sensor parameters. These methods will be examined further in Chapter 3, where they are applied to sensor fusion. They are presented here only as a reference to the basic theory.

2.2.1 Probability Theory

The most apparent method of combining any statistical parameter is through traditional statistical combination. What follows is an explanation of the mathematics of classical statistics, as illustrated here by Venn probability trees.

Possibly the simplest method of combining any set of probability parameters is classical statistics. Because each parameter from the set can be treated as an independent probabilistic test, they are combined using the intersection function for independent variables (Peebles, 2001). In Figure 2.2 this is demonstrated by using a Venn probability tree for three consecutive trials. For simplicity, the same probability of success is used for each trial.

In these trials, the probability of success of any single test is defined to be 60% (0.6), hence the probability of failure is 40% (0.4). Success is termed a positive outcome and failure a negative outcome. All possible outcomes of three consecutive tests can be seen in the Venn tree.

Combining all three tests into a single trial requires defining some criteria that represents success or failure of the three tests as a whole. For example, the criteria of success could be defined as at least two positive results from three trials, thus two or all three of the trials must have a positive outcome for this set of trials to be viewed as a success. This introduces a new probability of success for the set of tests. Effectively,

an external confidence limit has been imposed on the outcome of the set. The success of two of the three tests is required for the minimum confidence to be satisfied.

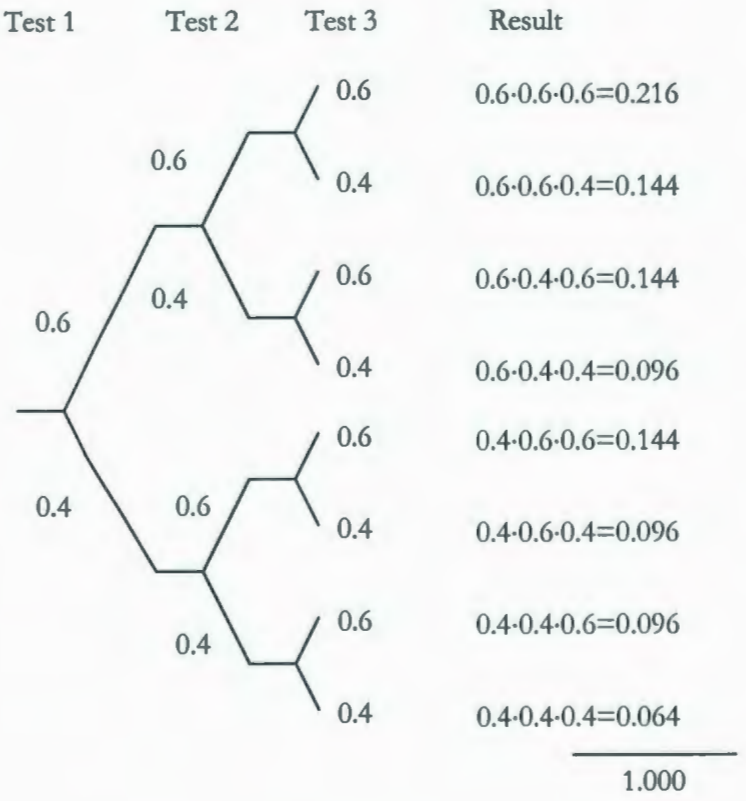

Figure 2.2: Venn Trees

For example, presuming a 60% probability of success of each trial, and requiring at least two successes of three trials for a 'conclusive' level of confidence, the probability

of success of the complete set can be found from the sum of the probability of each trial that meets the 'two-of-three' criteria or better:

$$\begin{aligned} 2of3 &= 3(\Pr(success)^2 \cdot \Pr(failure)) + \Pr(success)^3 \\ &= 3((0.6)^2(0.4)) + (0.6)^3 \\ &= 0.648 \end{aligned} \qquad \text{Eq. 2.1}$$

Thus the probability of success increases from 60% (0.6) to 64.8% (0.648) when the three attempts are treated as one. It is clear at this early stage that a clearer definition of confidence is warranted; better methods of determining confidence will be discussed further in Section 2.2.3 and illustrated in Chapter 3.

If the qualitative measure of required confidence is less, the quantity of negative results allowed may be increased. For example, an individual test repeated three times, requiring only one 'success' for the test to be considered successful, provides a result with less confidence of representing the actual state space than one requiring at least two out of three. Using the one of three criteria, the chances of this combination of individual trials being successful is increased significantly from 60% to 93.6%.

In essence this is the well-known 'M out of N' radar filtering technique (Bogler, 1990). The effect of using an m-of-n combination on a probability of success depends on the initial value of the probability of success, and the values of m and n. Applying a 1-of-n overall success criterion will increase the probability of success regardless of its previous value; a positive result from either sensor will be counted as a valid outcome,

even if success occurs in only one trial but not the others. Similarly, if the results from 2-of-3 tests are required to be correct then those sets with only a single positive are eliminated. This increases the chances of success of a set with an individual probability of success greater than 0.5, but will lower the chances of success of a set with individual probability of success less than 0.5.

A series of graphs are attached (Figure 2.3, Figure 2.4, Figure 2.5), which can help illustrate the results of combining different iterations of tests with various success criteria. In these, all trials have the same probability of success.

The total probability of success, given a method of 'best m-of-n' with a success rate of S among all the trials, can be written as below:

$$\Pr(OverallSuccess) = \sum_{x=m}^{n} {}_{n}C_{x} S^{x} (1-S)^{n-x} \qquad \text{Eq. 2.2}$$

The most advantageous method would be to require only one successful event to include the set of trials as an overall success. At this point it appears that this method is very effective at increasing the probability of success of a trial; however, the tradeoff lies in the effect on the confidence, which can be shown to decrease. This is discussed in Chapter 3.

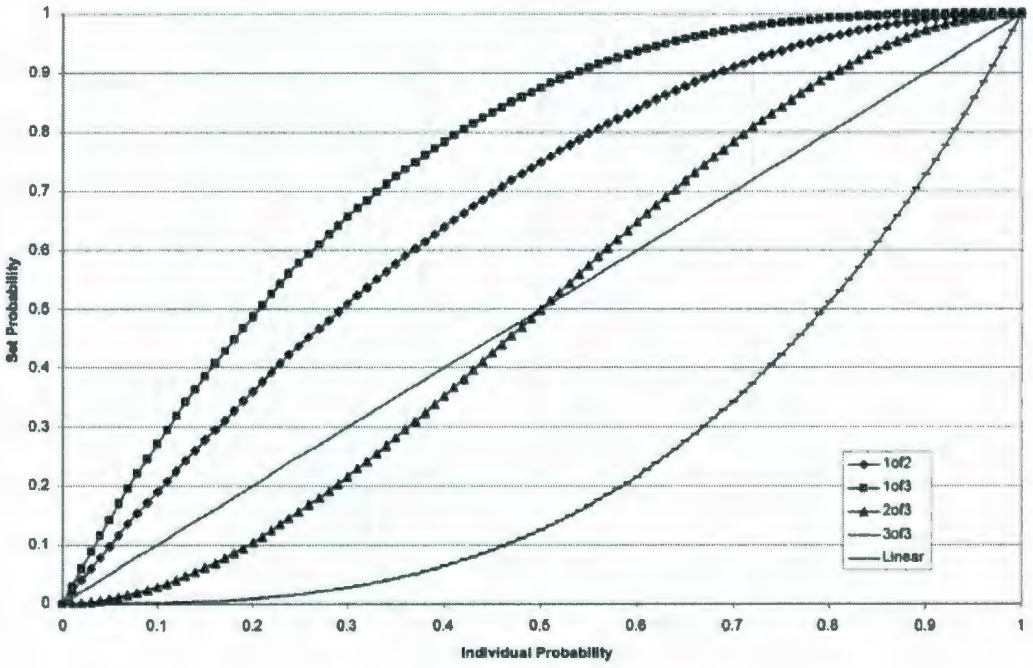

Figure 2.3: Example M-of-N Combinations

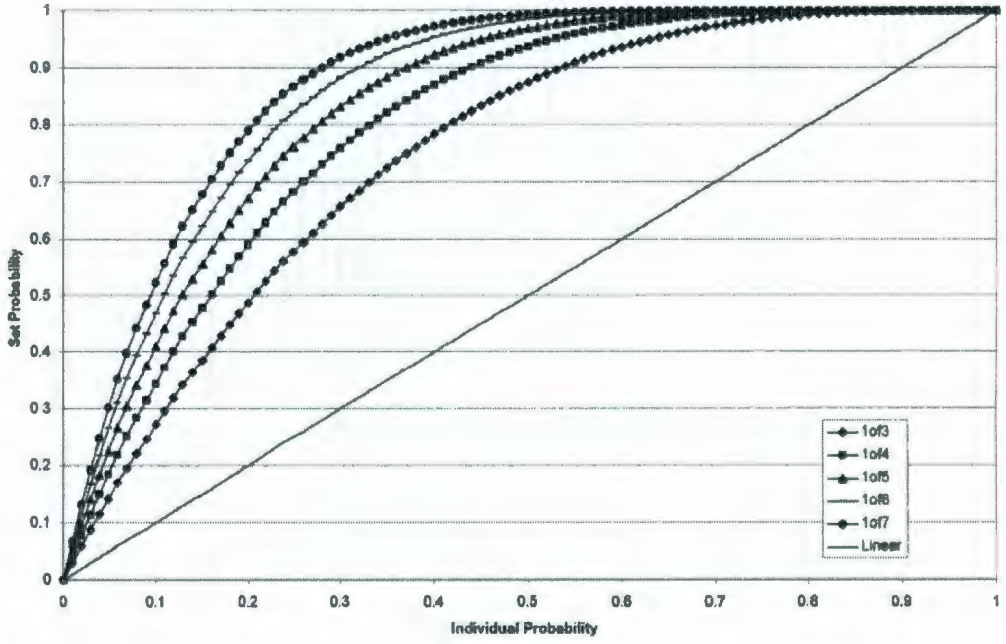

Figure 2.4: 1-of-N Combinations

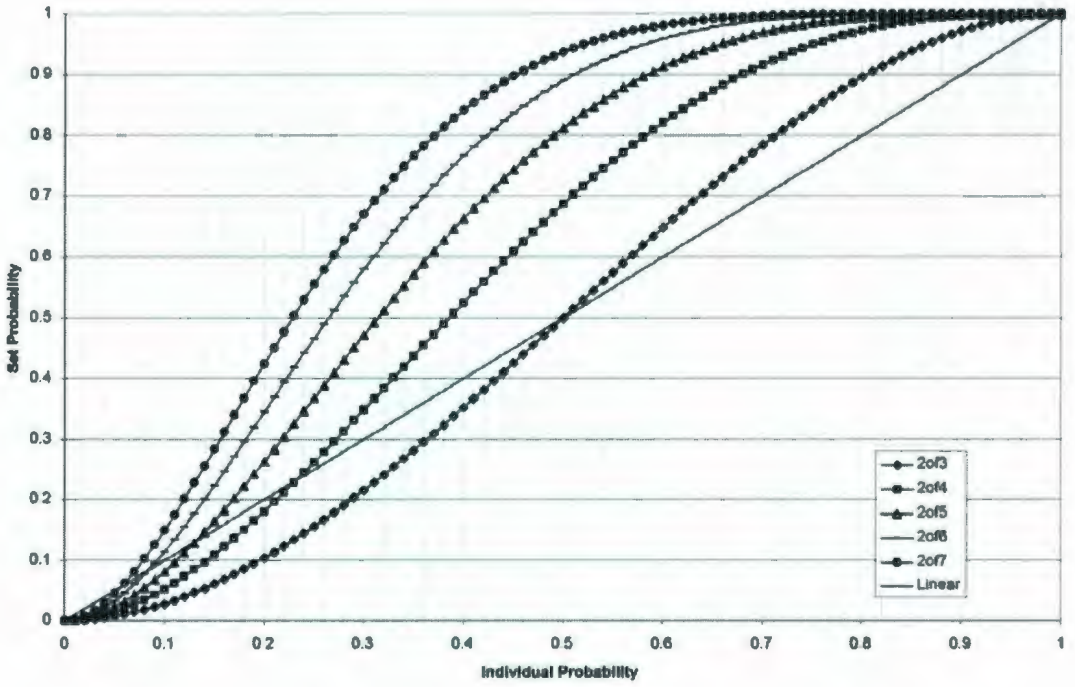

Figure 2.5: 2-of-N Combinations

2.2.2 Conditional Probability and Bayes Theorem

The classical method described above deals with independent probabilistic measures. This is insufficient for multivariate problems with dependent variables. One way of depicting dependent problems is through use of a joint probability table (Brown and Hwang, 1992) as shown in Table 2.3. This table is known as a confusion matrix in classification theory. Here an unknown state space is referred to, where the phenomenon being investigated is present, 'positive', or not present, 'negative'.

Table 2.3: Two-Way Table			
	Positive Test Result	**Negative Test Result**	
Positive State	Correct Test Result	False Negative Result	Probability of an Actual Positive
Negative State	False Positive Result	Correct Test Result	Probability of an Actual Negative
	Probability of a Positive Result	Probability of a Negative Result	1.0

The two-way table can be expressed in equation form, as in Table 2.4.

Table 2.4: Two-Way Table with Equations			
	Positive Test Result	**Negative Test Result**	
Positive State	Correct Test Result	False Negative Result	Pr(*PS*)
	Pr(*PS* & *PR*)	Pr(*PS* & *NR*)	
Negative State	False Positive Result	Correct Test Result	Pr(*NS*)
	Pr(*NS* & *PR*)	Pr(*NS* & *NR*)	
	Pr(*PR*)	Pr(*NR*)	1.0

Where we use the definitions below:

- PS = Positive State
- NS = Negative State
- PR = Positive Test Result
- NR = Negative Test Result

The conditional probabilities are $\Pr(PR \mid PS)$, $\Pr(NR \mid PS)$, $\Pr(PR \mid NS)$, and $\Pr(NR \mid NS)$, where $X \mid Y$ indicates the likelihood of some condition X given Y. The joint probabilities are shown in Table 2.4, they include $\Pr(PS \,\&\, PR)$, $\Pr(PS \,\&\, NR)$, $\Pr(NS \,\&\, PR)$, and $\Pr(NS \,\&\, NR)$. The marginal probabilities are $\Pr(PR)$ and $\Pr(NR)$.

Bayes theorem is a method for dealing with a problem that relies on some *a priori* knowledge. Where the initial state—the marginal probability $\Pr(PS)$—is known or approximated and a test is performed on the system. Bayes Theorem provides a method to update the marginal probability with the new information from the result of the test. Bayes theorem can be stated as in Joyce (2003):

$$\Pr(A \mid B) = \frac{\Pr(A \,\&\, B)}{\Pr(B)} \qquad \text{Eq. 2.3}$$

In the above table, the 'state' is the prior condition of the system, and the $\Pr(PS)$, or the probability of the state being 'positive'. Thus, given a result of the test, the estimate of the state is redefined. The updated estimate is termed the 'posterior'.

In cases where not all of the joint and marginal probabilities are known, the other probabilities may be determined through calculation. The multiplication law of probability states for dependent probabilities is shown in Eq. 2.4.

$$\begin{aligned} \Pr(A \,\&\, B) &= \Pr(A \mid B) \times \Pr(B) \\ &= \Pr(B \mid A) \times \Pr(A) \end{aligned} \qquad \text{Eq. 2.4}$$

The significance of the two-way table for determining the actual state of some system is in its ability to provide a confidence metric. This is further elaborated on in the following sections. Its relationship to sensor fusion is illustrated in Chapter 3.

2.2.3 Statistical Confidence

As discussed in Section 2.2.1, a measure of confidence is required for evaluating the combination of statistical parameters. It can be defined, for the purposes of this treatise, that confidence is the statistical representation of the ability of some test or trial, or set of trials, to return the true value of the state space being observed.

There are four parameters of interest returned from the conditional probabilities of the two-way table (Section 2.2.2); these can be termed as in Chankong et al. (1985):

$$selectivity\ (sensitivity) : \Pr(PR \mid PS) \qquad \text{Eq. 2.5}$$

$$selectivity\ (specificity) : \Pr(NR \mid NS) \qquad \text{Eq. 2.6}$$

$$predictivity(+) : \Pr(PS \mid PR) \qquad \text{Eq. 2.7}$$

$$predictivity(-) : \Pr(NS \mid NR) \qquad \text{Eq. 2.8}$$

Thus, a test can be defined—not simply as its likelihood of returning positive or negative—but on its ability to represent the true state space: to return a positive result when the state is positive, and to return a negative result when the state is negative.

The confidence in the trial is the likelihood that the test result represents the state of that being observed:

$$Confidence\ Given\ PR = \Pr(PS \mid PR) = \frac{\Pr(PS\ \&\ PR)}{\Pr(PR)} \qquad \text{Eq. 2.9}$$

and,

$$Confidence\ Given\ NR = \Pr(NS \mid NR) = \frac{\Pr(NS\ \&\ NR)}{\Pr(NR)} \qquad \text{Eq. 2.10}$$

These conditional probabilities of predictivity should be maximized, as they vary proportionally with the confidence in the information returned from the test. Note that the confidence in a test's ability to determine a positive state is not necessarily equal to its ability to determine a negative state.

Often the Pr(PR|PS) and the Pr(PR|NS) are the parameters used in examining the worthiness of a test as a detector for some phenomenon. In these cases the formula for predictivity can be derived from Bayes theorem as a function of Pr(PR|PS) and Pr(PR|NS):

$$\Pr(PS \mid PR) = \frac{\Pr(PS \,\&\, PR)}{\Pr(PR)} \qquad \text{Eq. 2.9}$$

$$= \frac{\Pr(PS)\Pr(PR \mid PS)}{\Pr(PR)\Pr(PS + NS)}$$

$$= \frac{\Pr(PS)\Pr(PR \mid PS)}{\Pr(PR \,\&\, PS) + \Pr(PR \,\&\, NS)}$$

$$= \frac{\Pr(PS)\Pr(PR \mid PS)}{\Pr(PS)\Pr(PR \mid PS) + \Pr(NS)\Pr(PR \mid NS)} \qquad \text{Eq. 2.11}$$

The formula for Pr(PS|NR), Pr(NS|PR), and Pr(NS|NR) can be similarly determined:

$$\Pr(PS \mid NR) = \frac{\Pr(PS)\Pr(NR \mid PS)}{\Pr(PS)\Pr(NR \mid PS) + \Pr(NS)\Pr(NR \mid NS)} \qquad \text{Eq. 2.12}$$

$$\Pr(NS \mid PR) = \frac{\Pr(NS)\Pr(PR \mid NS)}{\Pr(NS)\Pr(PR \mid NS) + \Pr(PS)\Pr(PR \mid PS)} \quad \text{Eq. 2.13}$$

$$\Pr(NS \mid NR) = \frac{\Pr(NS)\Pr(NR \mid NS)}{\Pr(NS)\Pr(NR \mid NS) + \Pr(PS)\Pr(NR \mid PS)} \quad \text{Eq. 2.14}$$

These equations are dependent on the prior state of the state space. In keeping with Bayes Theorem, the Pr(PS|PR) or the Pr(PS|NR) can be used as posterior values to update the Pr(PS) prior value. The implication of this will be examined further in Section 2.3.1.

2.3 Techniques Applicable to Data Fusion

This section describes common statistics techniques that are deemed appropriate to the combination of iceberg detection data. These methods will be examined further in Chapter 4, where they are applied to data fusion. They are presented here only as a reference to the basic theory.

2.3.1 Iterative Bayes

As briefly mentioned in Section 2.2.2, Bayesian Theory may be used for the modification of a prior probability value using a conditional posterior calculation. This update may be done using the formula derived in Section 2.2.3, or iteratively as shown below.

This iterative method provides a means of combining multiple statistical tests. The terminology used here is based on Chankong et al. (1985). In each iteration, where the test returns either a positive or a negative, the prior value is updated:

- given a positive result:

$$\Pr(PS)_{updated} = \Pr(PS \mid PR) \qquad \text{Eq. 2.15}$$

- or, given a negative result:

$$\Pr(PS)_{updated} = \Pr(PS \mid NR) \qquad \text{Eq. 2.16}$$

To simplify the equations, the notation is changed as shown below:

- the following define the selectivities (specificity and sensitivity):

$$\alpha^{+} = \Pr(PR \mid PS) \qquad \text{Eq. 2.17}$$

$$\overline{\alpha^{+}} = \Pr(NR \mid PS) \qquad \text{Eq. 2.18}$$

$$\alpha^{-} = \Pr(NR \mid NS) \qquad \text{Eq. 2.19}$$

$$\overline{\alpha^{-}} = \Pr(PR \mid NS) \qquad \text{Eq. 2.20}$$

- and, the following define the predictivities:

$$\theta^{+} = \Pr(PS \mid PR) \qquad \text{Eq. 2.21}$$

$$\overline{\theta^{+}} = \Pr(NS \mid PR) \qquad \text{Eq. 2.22}$$

$$\theta^{-} = \Pr(NS \mid NR) \qquad \text{Eq. 2.23}$$

$$\overline{\theta^{-}} = \Pr(PS \mid NR) \qquad \text{Eq. 2.24}$$

The recursive formulae can be generated for the predictivity equation above by defining θ_0 as the *a priori* knowledge of the probability of a positive state, and θ_1 as the subsequent predictivity after the result of the test has been obtained. For example, the positive predictivities for the first iteration are defined as follows:

$$\theta^{+}_{0} = \Pr(PS) \qquad \text{Eq. 2.25}$$

$$\theta^{+}_{1} = \Pr(PS \mid PR) \qquad \text{Eq. 2.26}$$

The formulae for recursive calculation of predictivity can be derived using the above notation:

$$\Pr(PS \mid PR) = \frac{\Pr(PS)\Pr(PR \mid PS)}{\Pr(PS)\Pr(PR \mid PS) + \Pr(NS)\Pr(PR \mid NS)} \qquad \text{Eq. 2.27}$$

$$\theta^{+}_{1} = \frac{\theta^{+}_{0} \cdot \alpha^{+}}{\theta^{+}_{0} \cdot \alpha^{+} + \overline{\theta^{+}_{0}} \cdot \overline{\alpha^{-}}} \qquad \text{Eq. 2.28}$$

$$= \frac{\theta^{+}_{0} \cdot \alpha^{+}}{\theta^{+}_{0} \cdot \alpha^{+} + (1-\theta^{+}_{0}) \cdot (1-\alpha^{-})}$$

$$= \frac{\theta^{+}_{0} \cdot \alpha^{+}}{\theta^{+}_{0} \cdot \alpha^{+} + 1 - \theta^{+}_{0} - \alpha^{-} + \theta^{+}_{0} \cdot \alpha^{-}}$$

$$= \frac{\theta^{+}_{0} \cdot \alpha^{+}}{1 - \alpha^{-} + (\alpha^{+} + \alpha^{-} - 1)\theta^{+}_{0}}$$

$$= \frac{\theta^{+}_{0} \cdot \alpha^{+}}{\overline{\alpha^{-}} + (\alpha^{+} + \alpha^{-} - 1)\theta^{+}_{0}} \qquad \text{Eq. 2.29}$$

In a similar manner Pr(NS | NR), Pr(PS | NR), and Pr(NS | PR) can be found:

$$\Pr(NS \mid NR) = \theta^{-}_{1} = \frac{\theta^{-}_{0} \cdot \alpha^{-}}{\overline{\alpha^{+}} + (\alpha^{+} + \alpha^{-} - 1)\theta^{-}_{0}} \qquad \text{Eq. 2.30}$$

$$\Pr(PS \mid NR) = \overline{\theta^{-}_{1}} = \frac{\overline{\theta^{-}_{0}} \cdot \overline{\alpha^{+}}}{\alpha^{-} - (\alpha^{+} + \alpha^{-} - 1)\overline{\theta^{-}_{0}}} \qquad \text{Eq. 2.31}$$

$$\Pr(NS \mid PR) = \overline{\theta^{+}_{1}} = \frac{\overline{\theta^{+}_{0}} \cdot \overline{\alpha^{-}}}{\alpha^{+} - (\alpha^{+} + \alpha^{-} - 1)\overline{\theta^{+}_{0}}} \qquad \text{Eq. 2.32}$$

These recursive formulae allow for the calculation of the probability that a positive result represents a positive state. This is significant, since it can be used to illustrate

that the results obtained from the recursive analysis are the same as that obtained from analysis of the Venn tree depiction of the problem using the intersection function for independent variables on the separated Pr(PR | PS) and Pr(PR | NS), as seen below.

The example below demonstrates that there is no difference between evaluating a battery of tests as one and evaluating these tests as individual iterations. In this example sensitivities of 0.6 and 0.7 are used. Both test iterations have a probability of false positive of 0.01. The calculations are shown in Figure 2.6.

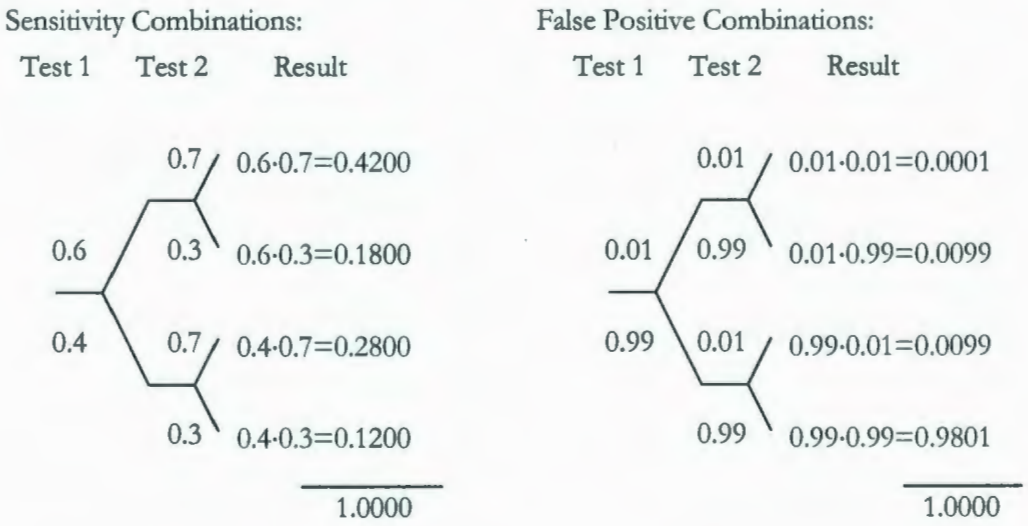

Figure 2.6: Intersection Calculation of Multiple Tests

The probability of a success in both iterations is 0.42. The chance of a false positive decreases to 0.0001 in this case. Using the results of the combined tests we can find the predictivity for positive and negative results as below.

- The predictivity for positive results of both tests, combined:

$$\begin{aligned}\Pr(PS \mid PR) &= \frac{\Pr(PS)\Pr(PR \mid PS)}{\Pr(PS)\Pr(PR \mid PS) + \Pr(NS)\Pr(PR \mid NS)} \\ &= \frac{0.05 \cdot 0.88}{0.5 \cdot 0.88 + (1-0.5) \cdot 0.0001} \\ &\approx 0.99976\end{aligned} \qquad \text{Eq. 2.33}$$

- The predictivity for negative results of both tests, combined:

$$\begin{aligned}\Pr(NS \mid NR) &= \frac{\Pr(NS)\Pr(NR \mid NS)}{\Pr(NS)\Pr(NR \mid NS) + \Pr(PS)\Pr(NR \mid PS)} \\ &= \frac{(1-0.5) \cdot 0.9801}{(1-0.5) \cdot 0.9801 + (0.5) \cdot 0.12} \\ &\approx 0.89091\end{aligned} \qquad \text{Eq. 2.34}$$

These can be compared to the results of iterating over the two individual tests. The same analysis is performed recursively on the first test and then the second, both with positive results:

$$\begin{aligned}\Pr(PS \mid PR) &= \frac{\Pr(PS)\Pr(PR \mid PS)}{\Pr(PS)\Pr(PR \mid PS) + \Pr(NS)\Pr(PR \mid NS)} \\ &= \frac{0.5 \cdot 0.6}{0.5 \cdot 0.6 + (1-0.5) \cdot 0.01} \\ &\approx 0.98360\end{aligned} \qquad \text{Eq. 2.35}$$

$$\Pr(PS \mid PR)_{new} = \frac{\Pr(PR \mid PS)\Pr(PS \mid PR)_{prev}}{\Pr(PR \mid NS) + (\Pr(PR \mid PS) + \Pr(NR \mid NS) - 1) \cdot \Pr(PS \mid PR)_{prev}} \quad \text{Eq. 2.36}$$

$$= \frac{0.7 \cdot 0.983606557}{0.01 + (0.7 + 0.99 - 1) \cdot 0.983606557}$$

$$\approx 0.99976$$

Likewise, the predictivity calculation for negative results is done in two steps when using the recursive formula:

$$\Pr(NS \mid NR) = \frac{\Pr(NS)\Pr(NR \mid NS)}{\Pr(NS)\Pr(NR \mid NS) + \Pr(PS)\Pr(NR \mid PS)} \quad \text{Eq. 2.37}$$

$$= \frac{(1 - 0.5) \cdot 0.99}{(1 - 0.5) \cdot 0.99 + (0.5) \cdot 0.6}$$

$$\approx 0.71223$$

$$\Pr(NS \mid NR)_{new} = \frac{\Pr(NR \mid NS)\Pr(NS \mid NR)_{prev}}{\Pr(NR \mid PS) + (\Pr(PR \mid PS) + \Pr(NR \mid NS) - 1) \cdot \Pr(NS \mid NR)_{prev}} \quad \text{Eq. 2.38}$$

$$= \frac{0.99 \cdot 712230216}{0.3 + (0..7 + 0.99 - 1) \cdot 0.712230216}$$

$$\approx 0.89091$$

These two results provide identical posterior probabilities: illustrating that either batch or iterative means can be used to determine confidence in test results. As well, using this iterative approach, out of sequence calculations should ultimately provide the same results as test calculations performed in sequence, which will help to resolve any issues with data arrival times.

2.3.2 Association and Tracking

Extensive volumes have been written on fusion systems, tracking, and association algorithms. Various authors treat the subject with different levels of abstraction, examinations of architecture, and inferences and extrapolations of the target features.

For a broad-based, exhaustive examination of the topic see Hall (1992), where many aspects of general data fusion are addressed including the relationship between the system and the users, the types and levels of inferences that the system should make, the types of sensors and their outputs in terms of pre-processing of data, characterization of sensor parameters, and definition of the state vector.

Hall defines three levels of fusion. The first level is physical combination of the parameters measured. The second level of fusion is the processing of situation assessments, seeking a higher order of inference such as meaning or patterns in time or space. The third level would be a further abstraction from situational assessments, to determining a level of threat or adversarial intention for military or intelligence applications.

Heistrand et al. (1983) describe three basic architectural approaches to data fusion for tracker-correlation systems:

1. A centralized architecture that transmits raw, unprocessed data from several sensors to a central fusion process, which performs data

alignment and association, followed by correlation, tracking and classification.

2. A fusion process that receives state vector and declaration of identity information generated by preprocessing performed at each sensor. Here, alignment, association, correlation, filtering, and classification are performed on state vectors rather than raw data.

3. A hybrid approach of the above methods. Presumably with more or less preprocessing and/or a combination of processed and raw data transmitted to the central process.

Haykin et al. (1994) also discuss distributed systems. Within the distributed system Haykin et al. describe three approaches: majority vote, fusion of statistics, and fusion of feature vectors.

Majority vote systems integrate data by a simple vote. If the majority of systems believe a feature to exist, then it is reported. A weighting factor can be added to provide a more sophisticated integration. Haykin et al. point out that this system is in actuality lossy. Information is being discarded when the vote on a feature does not make the majority. For this reason, majority vote systems are not recommended.

The fusion of statistics can be done through the integration of sufficient statistics computed by the preprocessors of the individual sensors. In this manner, processed information is combined based on the information altered by the preprocessor of the

sensor. This includes position and time information, along with other information stored in a feature vector.

Fusion of feature vectors integrates feature vectors generated from the raw data by the preprocessors of the individual sensors. The feature vector is a set of target parameters that may or may not be completely defined at the time of detection. The feature vector may prove more intuitive in the extrapolating of future events since it may contain information that can be used for determining the type or intent of the target. Events can be extrapolated and then confirmed to provide evidence of target existence, population of the feature vector and increased certainty of the validity of the information. Confidence values associated with the data will provide feedback, providing a means for the focusing of the sensor array to areas of particular interest.

The choice of the system will most likely depend on the sensors available, specifically on the location where processing and interpretation of raw data are completed.

Hall's definition contains four parts for the first level of fusion:

- Data alignment: transformation of data into a common spatial and temporal reference frame.
- Data association: sorting or correlating observations from sensors into groups representing data related to a single distinct entity; this determines which observations belong together as being from the same entity, object, event, or activity, or whether they constitute a new entity.

- Tracking: estimating target position and velocity.
- Identification: combining identity information—may include clustering methods, adaptive neural networks, templating methods, and Dempster-Shafer and Bayesian inference.

Of the processes mentioned above, data association is one of the most complex, particularly if the state space represents non-physical information, such as analysis of financial trends, or sociological phenomena. Aldenderfer and Blashfield (1984) describe four categories of association measures:

1. distance measures, for example Euclidean, Weighted Euclidean, City Block, Minkowski, Mahalanobis, Bhattacharyya, and Chernoff;
2. correlation coefficients, for example Pearson Product-Moment Correlation and Spearman's Rank Correlation Coefficient;
3. association coefficients, measures of agreement such as Jaccard's Coefficient, Gower's Coefficient, Cohen's K-Coefficient; and,
4. probabilistic similarity coefficients.

Selecting the association metric depends on the nature of the state space, such as for continuous, discrete, or binary variables. Hall reports that Brown, Pittard, and Spillane (1990) developed a test bed to compare association metrics.

Further decisions that must be made in the design of a data fusion architecture include the time at which associations will be made, either when they are received, or at some

later time in a batch mode of processing, as well as whether multiple associations will be allowed for single targets: multiple versus single hypothesis systems.

At a more practical level Blackman and Popoli (1999) review multiple target tracking (MTT) systems. Such a system can be broken down into several parts, namely: Sensor Data Processing, Observation-to-Track Association, Track Maintenance, Filtering and Prediction, and Gating Computations.

As illustrated in the block diagram of Figure 2.7 (Blackman and Popoli, 1999), the fusion system employs an iterative process of updating tracks and positions.

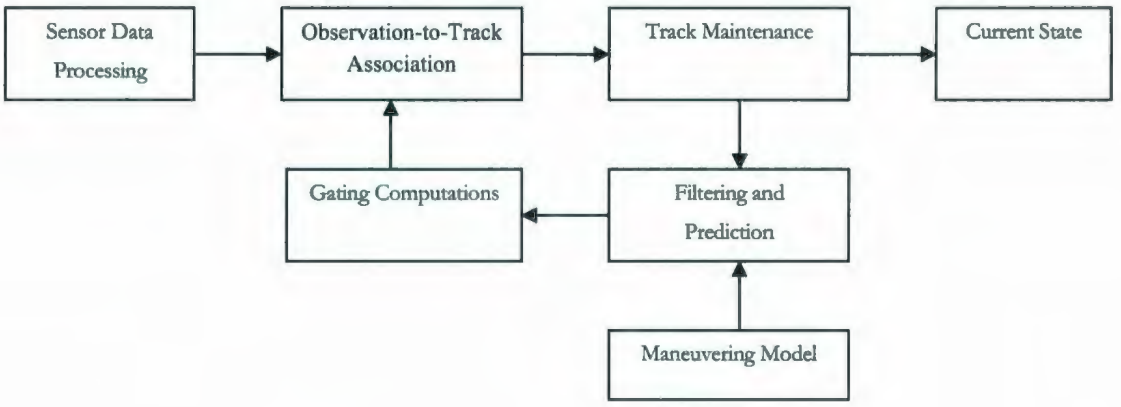

Figure 2.7: Tracking-Fusion System Diagram

The individual blocks in this diagram are elaborated on below:

- Sensor Data Processing and Measurement Formation: Performed at the sensor or at a centralized location. Observation data are derived from the sensors raw data through manual or automated means.

- Observation-to-Track Association: Observations are associated with existing tracks. Gating computations eliminate impossible detection/track associations, speeding up automated processing. Association improves the quality of information about the tracks.

- Track Maintenance: Tracks are given a score based on their reliability. Unreliable tracks may represent 'false positives', and are deleted when their score is reduced to below a preset threshold. Targets not associated with tracks start a new track with an appropriate score-track initiation.

- Filtering and Prediction: Given refined estimates of the tracks being monitored, estimates are made of the position of the target at a time when future data will arrive.

- Gating Computations: From the estimates of its future position a 'gate' is determined. This 'gate' is the possible position for the target given what is known of its current state. This simplifies association of the next target observation data to the updated track database.

The tracking system would step through this process every time new information becomes available.

Track initiation algorithms depend on the type of association being used. In global nearest neighbor (GNN), new tracks would be started for all observations that are not assigned to a previous track, whereas in multiple hypothesis tracking (MHT) new tentative tracks are started on all observations and subsequent data are used to determine which of these tracks are valid. For tentative track confirmation, the lifetime of the track without confirmation is limited. As well, the gate size can be chosen as a function of the confidence of the original detection. The decision as to whether a tentative track is deleted or kept is based on some metric. A track score function modifies the initial tracks and deletes the appropriate tracks.

An example of a track score function would be the log-likelihood ratio for use in evaluating a hypothesis:

- H_1: A single target produced the observations contained in the track. Result: Track Confirmation.
- H_o: The observations contained in the track were produced by unrelated events, such as false positives. Result: Track Deletion.

Alternatively a Bayesian updated score could be used (such as presented in Section 2.3.1), with the threshold set either by some basis in calculation or empirically.

The filtering and prediction aspect of the tracker is used to incorporate the assigned observations into the updated track parameter estimates. The output of the prediction defines the center of the gating region used in the next iteration. Blackman and Popoli

(1999) suggest Kalman filtering as the most applicable if the underlying target dynamics and the measurement processes can be assumed to be Gaussian. In this case, estimation of the mean target state and the associated covariance matrix is all that is required to define the probability density function (PDF) from the target position in state space. However, if these Gaussian assumptions are not justified, such as in the case of non-linear target dynamics, it may be preferable to propagate the PDF directly in target state space, rather than just using the mean and covariance from the Kalman filter to define a Gaussian PDF. Alternatively, interacting multiple models or Kalman filters may be used to approximate a non-linear dynamic.

Chapter 3 Sensor Fusion Method

This chapter examines the application of methodologies for sensor fusion specifically pertaining to the parameters that describe sensor capabilities to detect targets and avoid the generation of false targets.

The sensor fusion methodology should be such that the combination of parameters from multiple sensors can be represented as a single theoretical sensor. Hence, it is the combination of parameters that affects the fusion of sensors.

The focus of the discussion revolves around the intended application for these methods—detection of the icebergs that seasonally populate the waters along Labrador and Newfoundland coasts and infringe upon the areas of petroleum development in the Northwest Atlantic.

Since the intention of this section is to examine the combination of parameters without the associated sensor data, stochastic simulation techniques such as Monte Carlo will not be addressed; stochastic methods could be used in place of, or in association with

the methods presented here. Likewise, the combination of sensor data will not be discussed until Chapter 4.

3.1 Sensor Fusion Overview

Sensor fusion, as defined in Section 1.4, refers to the statistical combination of sensor parameters. The goal of sensor fusion is to provide the means of creating a single model that can be used in place of multiple models for simulation and theoretical sensor evaluations.

A useful sensor fusion system should provide a single sensor output based on multiple sensors with varying parameters (such as geospatial region, temporal interval, and data latency). This requires a method of combining the associated sensor parameters.

The resultant fused sensor provides the means to further the analysis of ice detection simulations and strategic evaluation of geographic and temporal placement of various combinations of sensors. In this section the basic theories outlined in Section 2.2 will be discussed within the context of their application to sensor fusion.

To begin, the variables affecting the combination of sensors parameters and data will be briefly reviewed, followed by the specific challenges affecting sensor combination and subsequently how these challenges are met.

3.1.1 Sensor Variables

A number of variables apply to the sensors that can be used in this remote sensing application. The variables are discussed briefly below, and the optimal result from any variation in the combination of sensor performance noted.

The parameters associated with the sensors are probability of detection, probability of false alarms, identification, coverage, resolution, latency, and confidence in results.

- Probability of detection refers to the capability of a sensor to correctly identify the target of interest from the sensor's area of coverage. This should be maximized in order to ensure maximum data acquisition.

- Probability of false alarms refers to a target datum that may be non-existent or an entity that has been incorrectly identified as a target of interest. This must be minimized to prevent undermining confidence in the system. Decreasing the probability of false alarms will improve the systems ability to handle data sources with a low probability of detection.

- Identification, referring to both target identity and target features, must be maximized, thus distinguishing the target icebergs from the other objects such as ships, metal or non-metal, moving under power or drifting, and platforms, and quantifying size, and shape characteristics.

- Coverage must be maximized. An effective system will have a wide area of analysis to give the most comprehensive picture of the monitored environment. Coverage may be a function of sensor location, for multiple non-coincident sensors.

- Resolution must be maximized. This ensures detection of the smallest of targets and their features. Within the context of iceberg detection, this should be of a degree where the smallest detectable target cannot prove a threat to ships, pipelines and platforms.

- Latency in data availability must be minimized. In wide-area strategic operations some latency can be tolerated. The amount of latency—delay from sensor to user—that a fusion system can handle is related to the coverage area. That is, a larger coverage area will allow for larger latencies due to the ability to detect targets at the extremities and still have time for a reaction. Latency does reduce the effectiveness of a sensor for detection near a facility, particularly in the tactical area.

- Confidence, as determined by the certainty of the results, must be maximized for the system to be of value. Where the output of any system has a confidence below the tolerable limit for the user, the system may be abandoned for other methods.

Sets of the above variables exist for each sensor in the sensor fusion system. Further to this, variations in the number, location, and type of sensor affect how the final sensor fusion system will perform. Some sensors have restrictions on their availability; however, the sensor fusion system output is presumed to always be available. Despite this, the availability of the sensor will limit the methods of combining them. The interaction of these parameters is depicted in Figure 3.1.

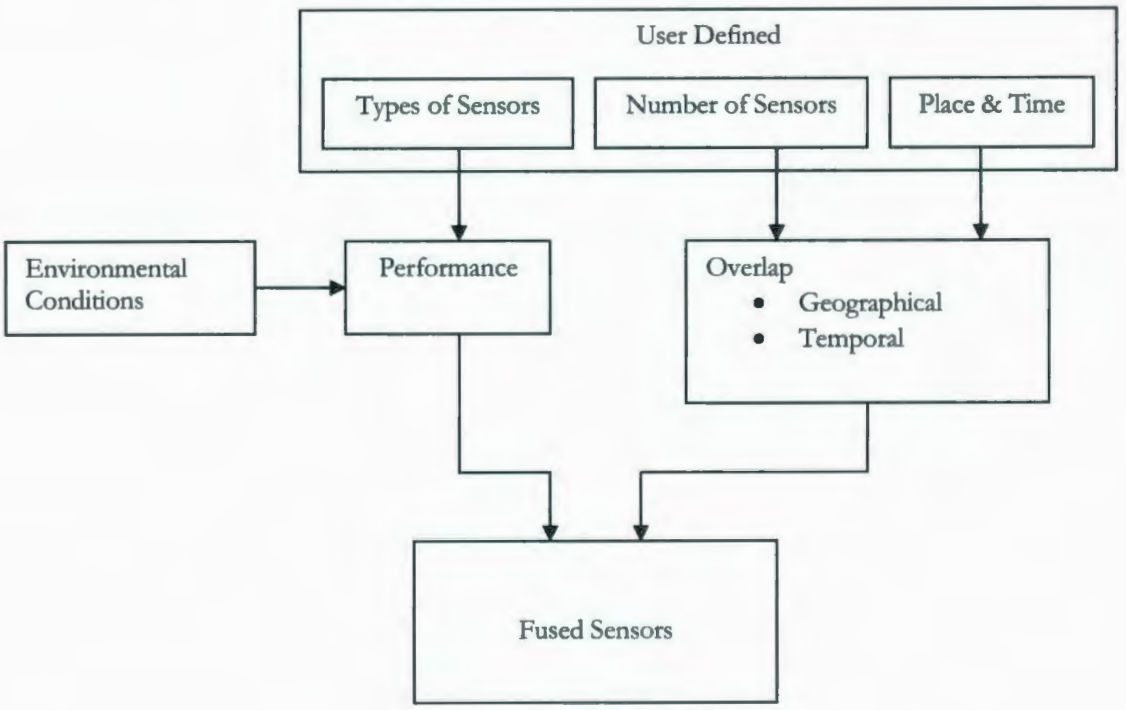

Figure 3.1: Sensor Fusion Variable Relationship

The combination of multiple sensors relies on the performance of each individual sensor and on the overlap, geographically and temporally, in the region being monitored.

It should be noted, in an evaluation of sensor performance and specifically with regards to risk analysis, that persistent adverse weather conditions which impact sensor performance may be relevant. However, this is beyond the scope of this investigation.

3.1.2 Sensor Fusion Challenges

Geospatially and temporally coincident sensors can have their performance combined with relative ease, as will be demonstrated in Section 3.3.1. Of a greater challenge is the combining of geographically and temporally spaced data.

The system for combining the sensor parameters must be capable of accommodating sensors with different sensor iteration rates, at different intervals, and observing from various locations.

There are three issues identified as challenges to the combination of the sensors parameters. Specifically, the combinational method must account for three items:

- the physical spacing of sensors, hereafter referred to as geospatial separation;
- the temporal separation between sensor data communications or report intervals; and,
- the temporal delay in receiving data from the sensors, hereafter referred to as data latency.

These challenges are addressed through the application of basic statistical theory, along with some exceptions necessary for handling data latency.

3.2 A Sensor Fusion Methodology

To address the challenges raised in Section 3.1.2, a methodology is proposed. At the most general level, the problem of parameter combination for sensor fusion will be examined from a statistical approach. By first decomposing the region of where sensors interact into a common grid from which each sensor can be referenced, and then applying each sensor's performance for that grid in sequence, a measure of the actual performance can be obtained. Hence, each grid unit has its own set of variables determined.

In Section 2.2 several techniques were described which are applicable to sensor fusion. The techniques consisted of two approaches:

- probability theory; and,
- conditional probability and Bayes theorem.

At a superficial level, probability theory techniques, such as those illustrated in Section 2.2.1, appear to have significant application to data fusion and are applicable to sensor fusion analysis. Indeed, for coincident sensors, the m-of-n technique (Section 2.2.1) would appear to be very useful. As seen in Figure 2.3, with the probabilities combined using a two-of-three criteria and a success probability of 0.7, they result in a probability of 0.784:

$$S_{Overall} = S^3 + 3 \cdot S^2(1-S) \qquad \text{Eq. 3.1}$$
$$\therefore \Pr(\text{det}) = 0.784$$

If available, false alarm probability data can also be included. Given the PFA for a single detection attempt is 0.022, then in the example directly above it becomes quite smaller:

$$S_{Overall} = S^3 + 3 \cdot S^2(1-S) \qquad \text{Eq. 3.2}$$
$$\textit{False Alarm Rate} \approx 0.00143$$

When examining the alteration of the probability curve, it was noted that above 50% the 'two of three' combination increases the probability of a 'successful' set, and below 50% the combination decreases the probability of a 'successful' set. In the above example, the Pr(det) is increased because it is above 50% and the PFA is suppressed because it is below 50%.

However, situations may exist where the Pr(det) and PFA rate are closer together or below the 0.5 probability, where the outcome of the methods such as two-of-three or three-of-five go from improving the likelihood of an overall outcome to decreasing it. Two-of-five or three-of-seven type schemes could be used in these cases as these have crossover points that are not at 0.5.

In this way the crossover point could be customized such that it falls between the false alarm rate and the sensitivity. This would allow us to increase sensitivity and decrease false alarm rates.

Notably, the m-of-n technique is not applicable to sensor fusion in general. The requirement to have multiple iterations of a positive sensor result implies an expectation of frequent sensor iterations—in the same location. In the case where fewer iterations might take place, this expectation would mean that results from a sensor fusion system could be delayed by days or weeks.

This shortcoming of the m-of-n techniques is not associated with the 1-of-n technique, making the 1-of-n technique more applicable to non-overlapping, geospatially separated sensors and to sensors with infrequent data updates.

The 1-of-n technique will be quite poor in its handling of false alarm targets. The m-of-n technique increases probably of detection and decreases the likelihood of detecting poorly detected targets. For sensors whose probability of false alarm is much lower than the probability of detection, this may be seen as a benefit. Unfortunately, processing by this method will prevent detection of 'faint' targets, for example, targets which have a probability of detection on the order of the probability of false alarm. Hence, this technique is limited to sensors whose probability of detection is significantly larger than the probability of false alarm.

Further to this, the Pr(det) and PFA parameters are not independent. When the detection problem is generalized, it is quickly discovered that these are conditional probabilities of the target existence problem. The following tables show the actual detection problem. Table 2.4 describes the problem using the terminology defined in Section 2.2.2. Table 3.1 shows the same table using industry nomenclature.

Table 3.1: Two-Way Table with Detection Vernacular

	Target Reported	**No Target Reported**	
Target Exists	Pr(det) (aka POD)	Missed target	Pr(Actual Target)
No Actual Target	PFA	Correctly observed non-target area	
	Pr(Target Reported)		1.0

Using the formulae for recursive Bayes, Section 2.2.3, a metric for confidence in the sensor result can be determined; this is useful in estimating the consequence of the combination method. The conditional probability of Pr(PS|PR) indicates the likelihood that the report of a target actually indicates a target and likewise Pr(NS|NR) indicates the absence of missed target. Using the iterative formulae defined in Eq. 2.29 and Eq. 2.30 and the target detection variables, Eq. 3.4 and Eq. 3.6 are produced.

$$\Pr(PS \mid PR) = \frac{\Pr(PS)\Pr(PR \mid PS)}{\Pr(PS)\Pr(PR \mid PS) + \Pr(NS)\Pr(PR \mid NS)} \quad \text{Eq. 3.3}$$

$$= \frac{prior \cdot \Pr(Det)}{prior \cdot \Pr(Det) + (1 - prior) \cdot PFA} \quad \text{Eq. 3.4}$$

$$\Pr(NS \mid NR) = \frac{\Pr(NS)\Pr(NR \mid NS)}{\Pr(NS)\Pr(NR \mid NS) + \Pr(PS)\Pr(NR \mid PS)} \quad \text{Eq. 3.5}$$

$$= \frac{(1 - prior) \cdot \Pr(Det)}{prior \cdot \Pr(Det) + (1 - prior) \cdot PFA} \quad \text{Eq. 3.6}$$

Notably, this requires the assumption of the prior statistic value with which to begin analysis. A non-informative prior value, such as 0.50 could be arbitrarily chosen for the purposes of sensor comparison. These two metrics indicate the likelihood that the information reported by the sensor correlates with the actual state of the phenomenon being observed.

Using Bayes, the outcome of each sensor iteration affects the estimate of the system state under observation. That is, the prior value estimate is replaced with the posterior (either of Pr(PS | PR) and Pr(PS | NR) given the detection result).

Given the methods elaborated on above, a methodology has been defined to address the issues raised in Section 3.1.2. Each of the three issues is addressed in turn: geographical separation, temporal separation, and data latency. The described method illustrates one approach, alternate approaches certainly exist.

To combine sensors that operate over different geographical areas, a 1-of-n criterion is recommended. Combining in such a statistical manner results is some increase in the probability of detection where the coverage area overlaps. This is achieved at a cost of increasing the probability of false alarms or false detections in the overlapping area. When looking strictly at non-coincident geographical coverage with no temporal component (repeating of sensor iterations), only the 1-of-n method will provide results.

To temporally combine sensor Pr(det) curves, consider that the detection curve represents an attempt to find an iceberg over a defined period. This time period is generally sensor dependent. For example the Pr(det) curve for the scan averaging marine radars can be derived from a minute or more of radar data while the Pr(det) curve from HF SWR radar in ice detection mode is derived from 5 minutes of radar data. To extend this to a longer period, a criterion is established for the minimum number of repeated observations to produce a detection (i.e. the m-of-n criterion). Once this is established, the combination of sensor probability curves can be done in the same manner as for geographical area. A knowledge of how the detection statistics were derived is required to prevent misapplication of this methodology. Furthermore, temporally combining sensors presumes that the target in question has remained in the same space with respect to the resolution of the system, thus limiting the time between observations or the maximum number of combined interactions.

Similarly, spatial and temporal separations can be combined, first temporally and then spatial. From the observation of different variations of the m-of-n parameters, it was determined that 2-of-n is the optimal combination criterion for typical marine radar systems; those sensors that have a very low PFA rate (see Figure 2.5). Given that the probability of a false alarm is generally much less than the probability of detection, this criterion applies the maximum increase in probability of detection while minimizing the probability of false alarms even for values of 'n' as low as three.

Data latency, often due to delays in data being processed, is taken into consideration insofar as the potential effect the delay would have on the risk to an offshore installation. Where the system of sensors is concerned, sensors that cannot provide observations of the area around the structure in time for effective management are not considered in the calculation of enhanced performance probability. This only affects areas around the installation to the extent that an iceberg could be present and have time to reach the installation before the data from the sensor is available. For example, RADARSAT-1 has approximately 2 hours turnaround time on processed data (1.5 hours turn around by a ground station and 0.5 hours processing time). In a worse case analysis, an iceberg traveling at its maximum possible speed (for illustration purposes 1.03 m/s, or 2 knots, is used here) would need to be within 14 km of the structure to be of any risk of not having been detected before impact, based on detection with this sensor alone (used only as an example). Hence, around the structure for a radius of 14 km, the RADARSAT-1 Pr(det) is reduced to zero in the analysis. That is, with respect

to the integration of the sensors, RADARSAT-1 contributes no detection information in this area; hence for immediate calculation purposes the Pr(det) is equal to zero in this region. In all other areas, the delay has no effect if the maximum travel is less than the system resolution and the RADARSAT-1 Pr(det) is considered in the overall performance of these outer regions. Significant data latency will impact the resolution of the system. Use of sensors with high data latency will require the use of coarse resolution to account for possible movement of the target.

Using the methodology outlined here, multiple sensors can be combined over a period of time, and with various delays in the availability of the data, to create a single probability of detection map over a geographical area. This can then be used to create more accurate and realistic risk analysis models.

3.3 Sensor Fusion Application

The methodology noted in the previous section can be used to combine sensor detection parameters for various sensors. First, an example of sensor iterations demonstrates the effect on the confidence metric derived from Bayes; subsequently a large scale application is presented.

3.3.1 Sensor Fusion Example

The combination of a set of detection parameters is illustrated with a simple example in Figure 3.2 and Figure 3.3. The effects on Pr(det) of the 1-of-n and m-of-n

combination of three iterations of the same sensor were shown previously in Figure 2.4. In this case, the cumulative probability of detection is depicted for the 1-of-3 case and the 2-of-3 case, along with the single event probability of detection for the example sensor. As can be seen in the two graphs, the use of 1-of-3 methods can dramatically improve Pr(det), but decrease confidence. The opposite is true for 2-of-3 methods.

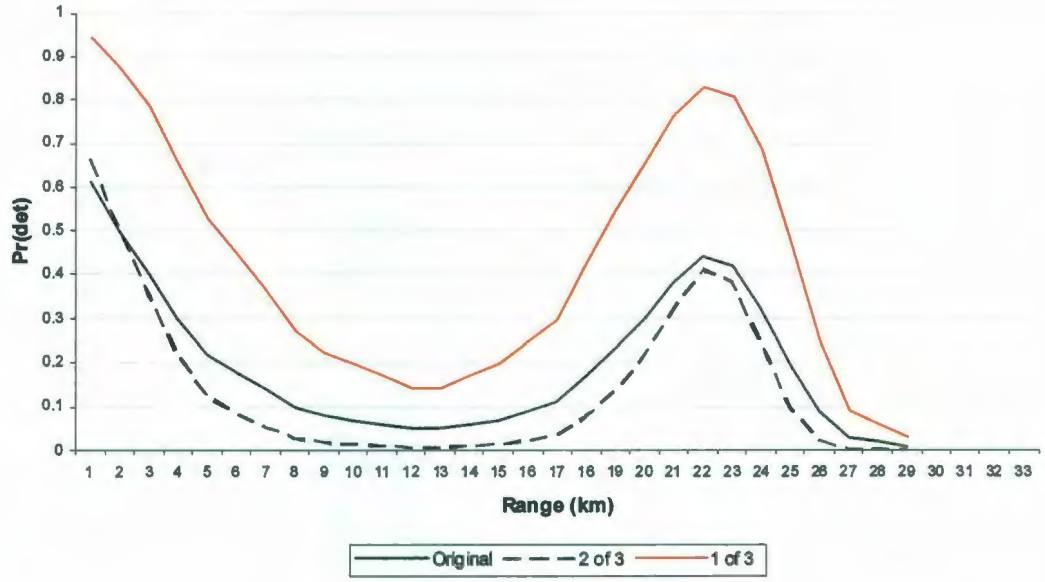

Figure 3.2: Pr(det) for Sensor Fusion

The plot of Figure 3.2 represents the detection of a 40 m iceberg in 5-m seas with S-Band marine radar mounted at platform height (~75 m). The PFA for this example is 0.01 and the prior value was 0.1. The figure shows the original Pr(det) in dark blue. This probability of detection is increased when a 1-of-3 criteria is applied. For 1-of-3, probability of detection is not limited by the original probability. For the 2-of-3

combination, the probability is only increased when the initial sensor Pr(det) is greater than 0.5. This illustrates that, while this method is applicable for sensors with a normally high Pr(det), it may hinder poorer performing sensors.

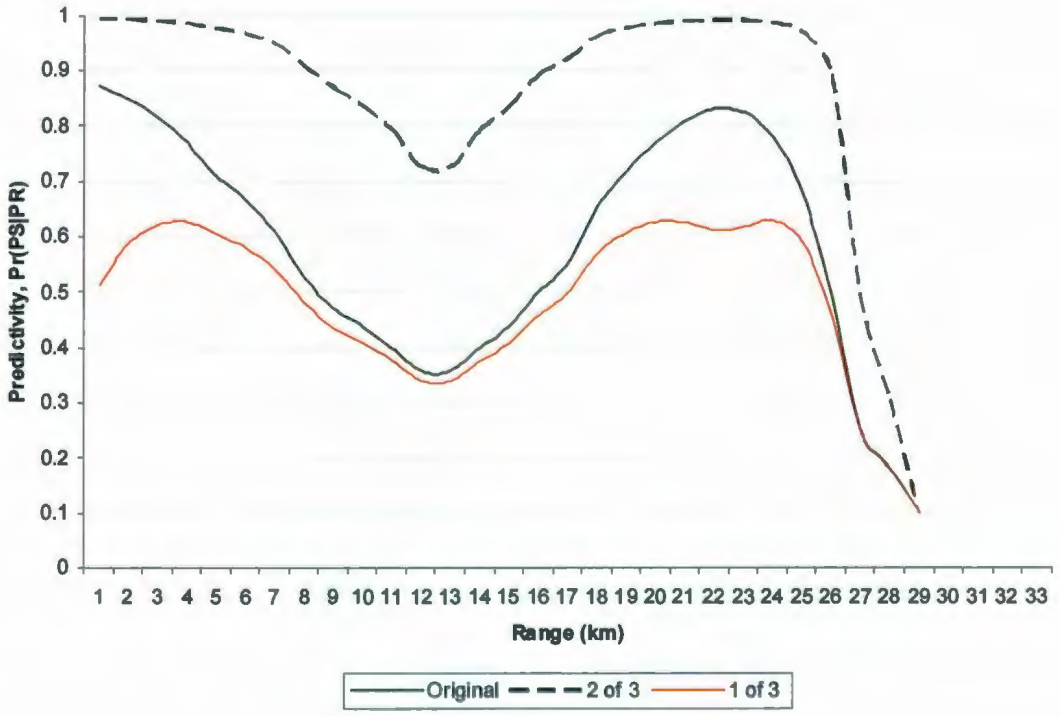

Figure 3.3: Certainty Result for Sensor Fusion

In Figure 3.3 the calculation of predictivity are shown for a simple positive iteration and for a 1-of-3 and a 2-of-3 case. This figure illustrates the confidence—the results of the predictivity calculations—is significantly higher for a 2-of-3 case than a 1-of-3 case. This illustrates the general trade off between increased Pr(det) and increased

confidence when selecting the m-of-n criteria. Also note that the low PFA provides a high confidence.

The next example illustrates the combination of parameters by the 1-of-n method. To perform the combination of parameters over a geographical area the sensors are referenced to a single relative reference frame in Cartesian coordinates. The sizing of the increments of the coordinate system would ideally be less than that of the resolution of the finest sensor, but may be restricted by processing requirements and the use of sensors with data latency.

In this example, the combined sensors are located in two locations. An attempt to detect 30-m icebergs with S-band radar is presented here. The S-band marine radars are positioned 35 km apart. Both radars are mounted at platform heights common to offshore oil and gas platforms—typically 35–45 m. Figure 3.4 shows the curve for target detection of each sensor. The effect of combining the two radar performances over a geographical area can be seen in Figure 3.5.

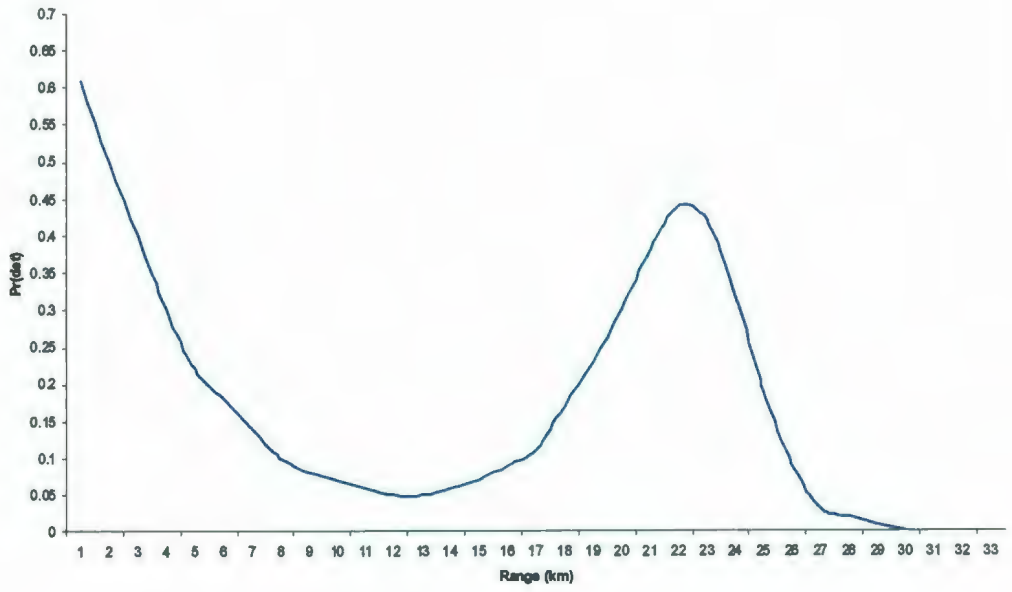

Figure 3.4: Example Pr(det) vs. Range

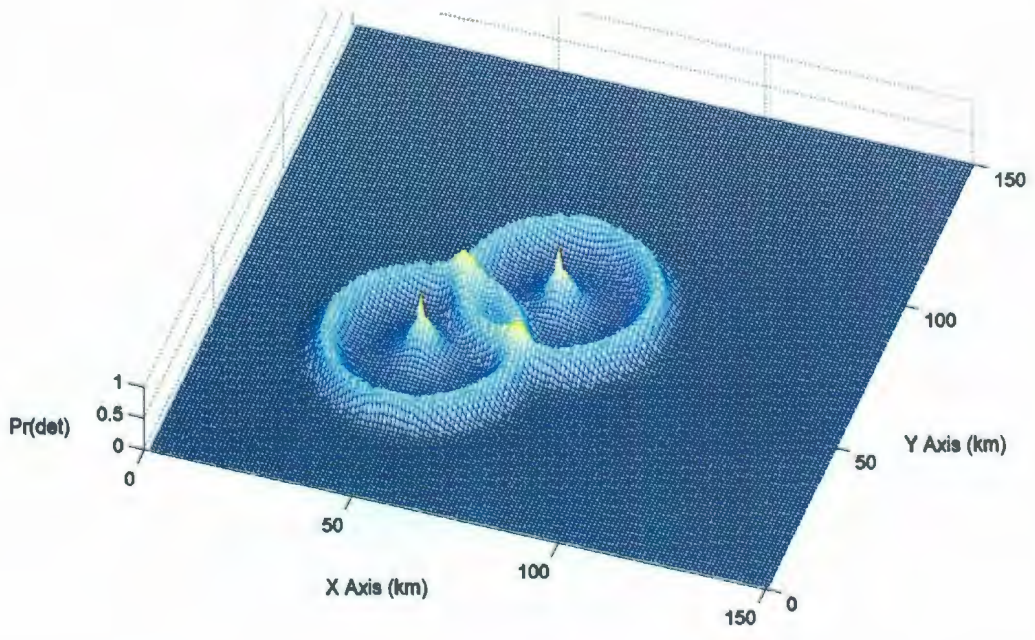

Figure 3.5: Example Pr(det) Combination over an Area

The benefit of combining geographically spaced sensors is clearly the area covered. A 1-of-n method must be used to do this, as any one sensor cannot detect outside its own range, negating the possibility of having two detections anywhere except where they overlap.

For combinations of events where multiple iterations are available over the same geographical region in a reasonable interval, it is presumed that at least some 2-of-n method is desirable; this is possible when the probability of false alarms is relatively low compared to Pr(det). The process is limited in 'n' by the amount of time available before de-correlation occurs. That is, the amount of time before the target has the opportunity to move to another resolution cell.

3.3.2 Sensor Fusion Sample Application

The following provides a sample application of the sensor fusion methodology described in Section 3.2. For the purposes here, it is assumed that the user has control, or at least knowledge, of the types of sensors in use, their number, location, and the parameters that define their performance.

Operators of sensor networks can typically place sensors spatially to provide relatively effective coverage of the area of interest to them. Each of these sensors types have varying parameters of performance. Each can, in turn, have its variations used to the sensor networks effective advantage within the confines of technology and cost.

The choice of coverage area and probability of detection required determines the sensor deployment configuration. Coverage area and probability of detection are functions of the type of sensors used. The frequency at which sensor sweeps are performed and the environmental conditions are independent variables.

At the time of writing, the offshore iceberg detection regime contained a variety of sensors with some used more frequently than others. These were described in further detail in Section 2.1.1. They consist almost exclusively of radar-based systems and are listed in Table 3.2.

Table 3.2: Offshore Sensor Regime	
Marine Radar	X and S-band non-coherent radar has been traditionally used in marine environments. X-band (10 GHz) provides better resolution due to its higher operating frequency and S-band (3 GHz) provides better penetration of fog and moderate (4 mm/hr) to heavy (16 mm/hr) precipitation (C-CORE, 1992). These are limited to the line-of-sight horizon or less depending on target size and environmental conditions. For a typical platform mounted unit at a height of 75 m this horizon is approximately 36 km.
Enhanced Marine Radar	Based on slightly modified conventional marine radar, enhanced marine radars effectively use data processing techniques to enhance the detection capabilities of marine radar, particularly for small targets or in poor conditions. These are restricted to the line-of-sight horizon.
Surface Wave Radar	Surface Wave Radar (SWR) is a variant of Over-The-Horizon (OTH) radar. Where microwave frequency systems are limited to very near the line-of-sight horizon, HF band (3–30 MHz) radars are capable of using the conductivity of the ocean to extend their range and provide detection capabilities up to 450 km. This coherent radar system is more susceptible to noise reflected by the ionosphere. The increased strength of this noise at night reduces the SWR performance for these periods of operation (C-CORE, 2000). Developments are underway to improve night time performance.

Airborne Radar	Airborne reconnaissance flights are routinely performed over the Grand Banks area of the East Coast of Canada where drilling and pumping operations occur. These aircraft use Litton APS-504 (V) 5 search radars. Varying altitudes provide a radar horizon of 50 to 87 km. Due to the use of frequency agility and higher incidence angles this system outperforms traditional marine radar (Rossiter et al., 1995).
SAR Satellites	Examples of SAR satellites include ENVISAT and the RADARSATs. The RADARSAT satellites are Canada's multipurpose space-borne SAR radars. Satellite SARs provide all-weather detection capability for 'small' or larger icebergs. Modes such as 300 km or 150 km swath width frames are useful for iceberg surveillance. These remote sensing satellites use polar orbits and are typically limited to multi-day revisit schedules per satellite (RSI, 2001).
Visual Observations	Visual observations are made from ships in transit, platforms, airplanes, and support vessels. These observations are obviously limited to the visible horizon and may be considered the most reliable. However they are the most afflicted by environmental conditions that decrease visibility.

For practical implementation purposes, the geographical area of interest has been broken into two parts: the tactical and strategic ranges.

The tactical range is the area in the immediate vicinity of the platform, typically extending outward on the order of 10 to 50 km (Rossiter et al., 1995). Sensors used in this area provide very quick update rates and very low latency. While SWR, satellite SAR and aerial sensing can be employed, the most utilized sensors in this region are conventional and enhanced marine radar, and visual observations from offshore production platforms or ships.

The strategic range encompasses a much wider area and is outside the tactical range. In this range, where data latency is not an issue, all sensors can be used. These include satellite SAR, airborne reconnaissance and SWR as well as marine radar and visual observations from ships and airplanes. The strategic area is vast, making it difficult to obtain accurate and frequent information updates about the region.

The following example shows a Pr(det) combination of these detection sensors for a 50-m iceberg in 5-m seas. There are six sensors used in the combination:

- enhanced marine radar with scan averaging at Hibernia;
- enhanced marine radar with scan averaging at Terra Nova;
- marine radar at the White Rose development with (capabilities assumed similar to the Terra Nova radar);
- typical aerial reconnaissance flight;
- RADARSAT-1 ScanSAR NarrowB frame; and,

- HF Radar.

First, consider the Pr(det) of the marine radars. Shown in Figure 3.6 is the probability of detection for an S-band marine radar of a 50-m iceberg in 5-m seas.

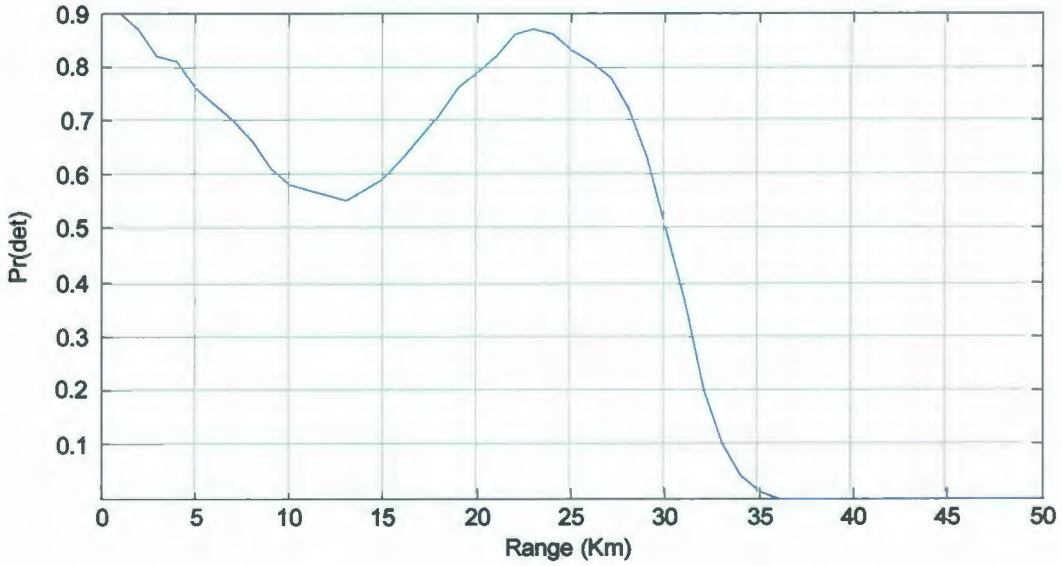

Figure 3.6: Probability of Detection Curve

This can be extended into three dimensions, assuming that the performance of the sensor is the same in all directions, by rotating the probability of detection in a full circle around the radar. This is shown in Figure 3.7.

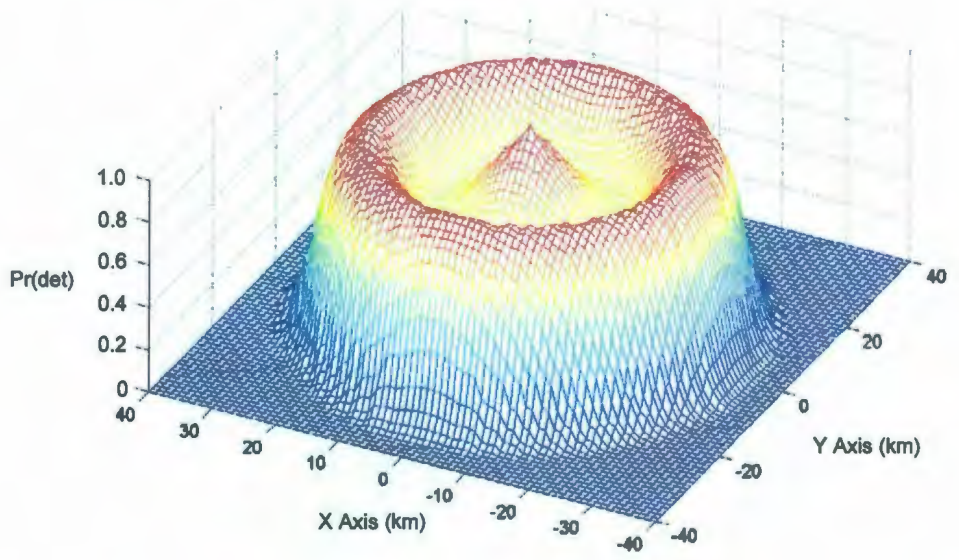

Figure 3.7: Pr(det) for a Single Radar in 3D

Taking the example of the two radars at Hibernia and Terra Nova, a second map of the probability of detection can be generated as in Figure 3.8. Scan averaging is excluded here so that the effect of the overlapping of the radars could be illustrated better, since the generally higher Pr(det) curves obtained with scan averaging benefit less from the combination method.

In Figure 3.8, it is possible to see that where the two radars overlap there is an increase in detection performance. It is noteworthy that the performance of each of the two radars in Figure 3.8 is different with respect to range and probability of detection. This is caused by the different heights of the radars (70 m for Hibernia and 45 m for the Terra Nova FPSO).

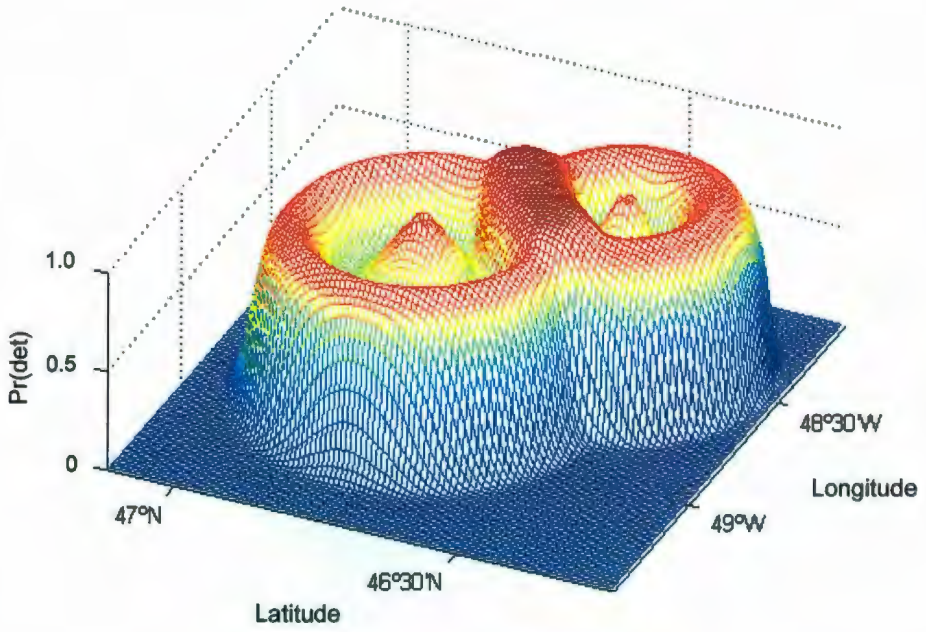

Figure 3.8: Interaction between Pr(det) for Two Marine Radar

In Figure 3.9, a top-down view of the area containing both marine radars is shown. The figure also contains a colour bar that shows the probability of detecting an iceberg, which is represented in colour in the image.

Figure 3.10 continues with adding detection performance of the radar system at White Rose, with similar capabilities as Terra Nova.

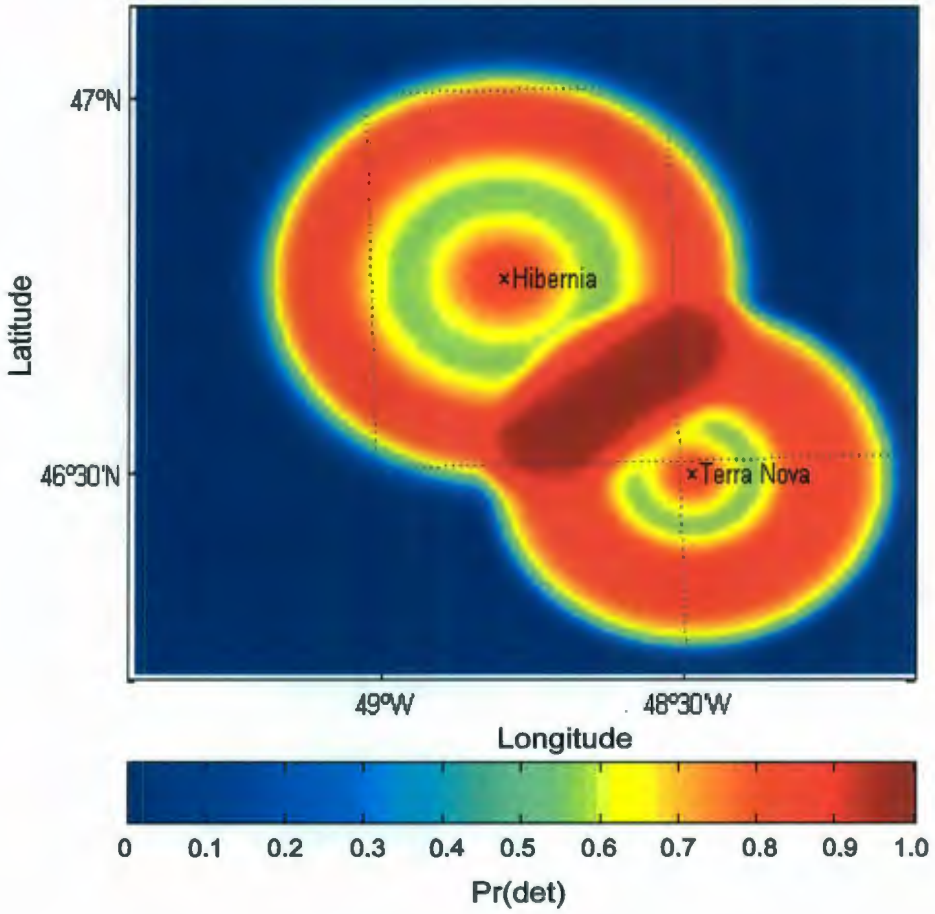

Figure 3.9: Top-down view of Hibernia and Terra Nova Radars

(Single Scan)

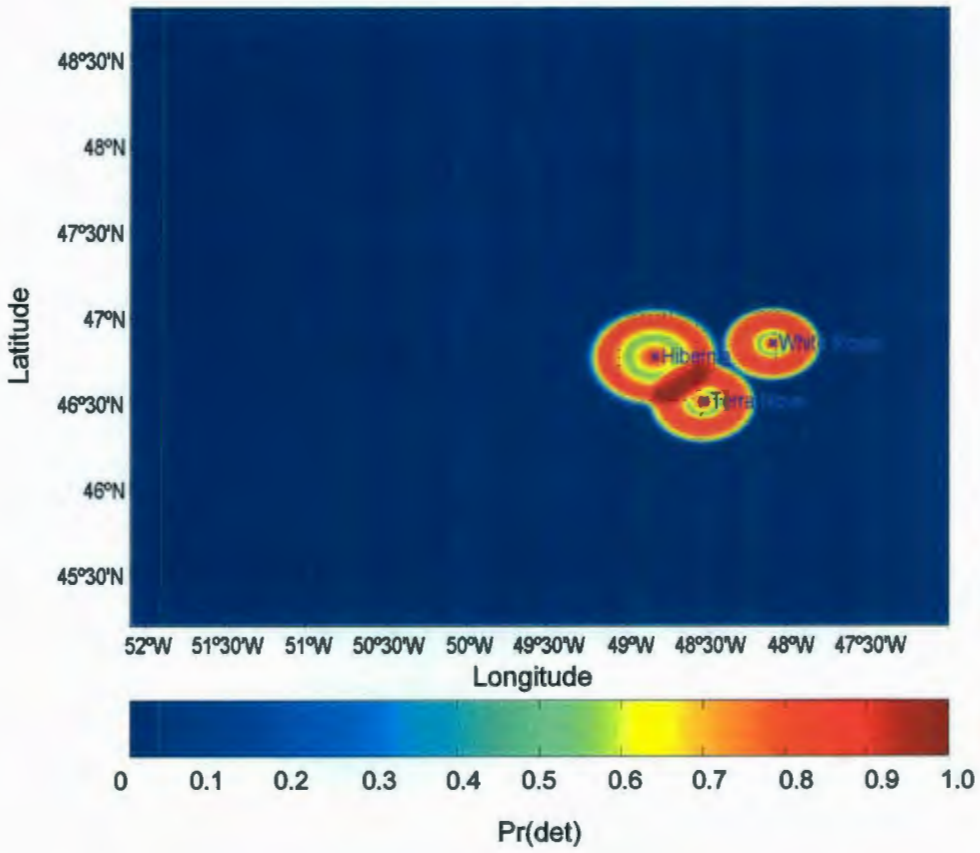

Figure 3.10: Pr(det) for Platforms with Marine Radar Installations

The contributions of HF SWR from Cape Race, a RADARSAT-1 ScanSAR frame, and an aerial search radar reconnaissance flight are added in Figure 3.11, Figure 3.12, and Figure 3.13 respectively. For the aerial flight, an example flight path is taken from an ice reconnaissance flight flown on April 23, 2001 by Provincial Airlines Limited (PAL). The RADARSAT-1 frame was taken directly from RADARSAT's planning software. The location of the frame with respect to the island of Newfoundland is seen in Figure

3.14. An ascending and descending RADARSAT-1 frame from subsequent days are shown in this figure.

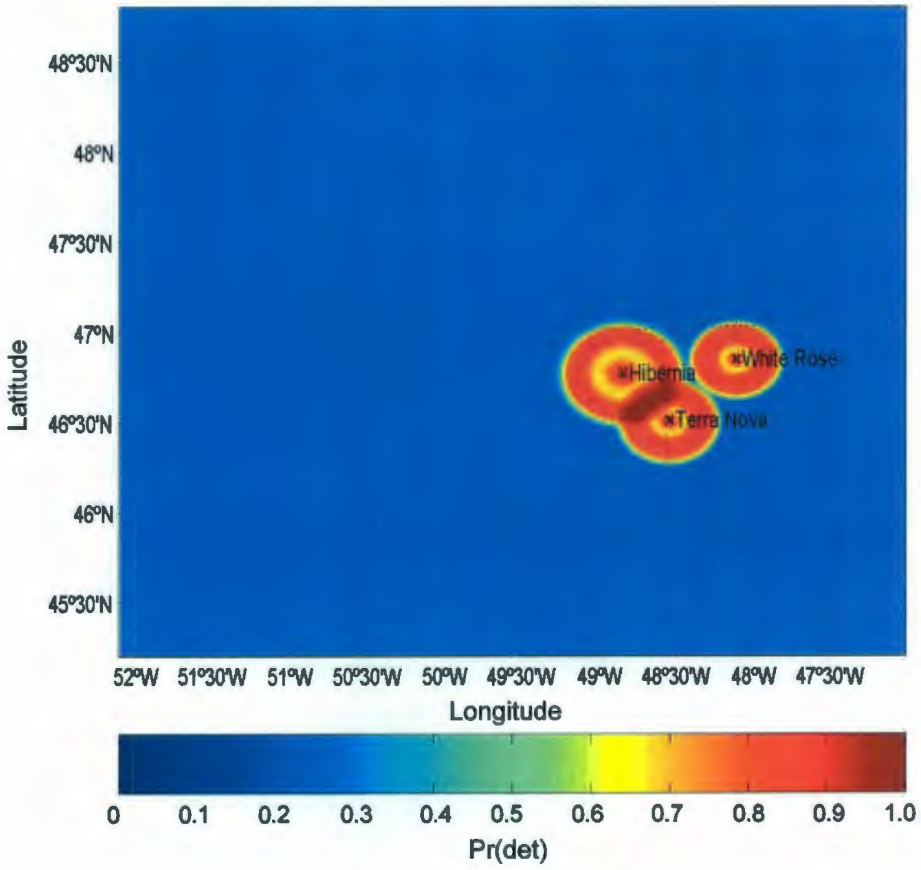

Figure 3.11: Pr(det) for Marine Radars plus HF SWR (2000)

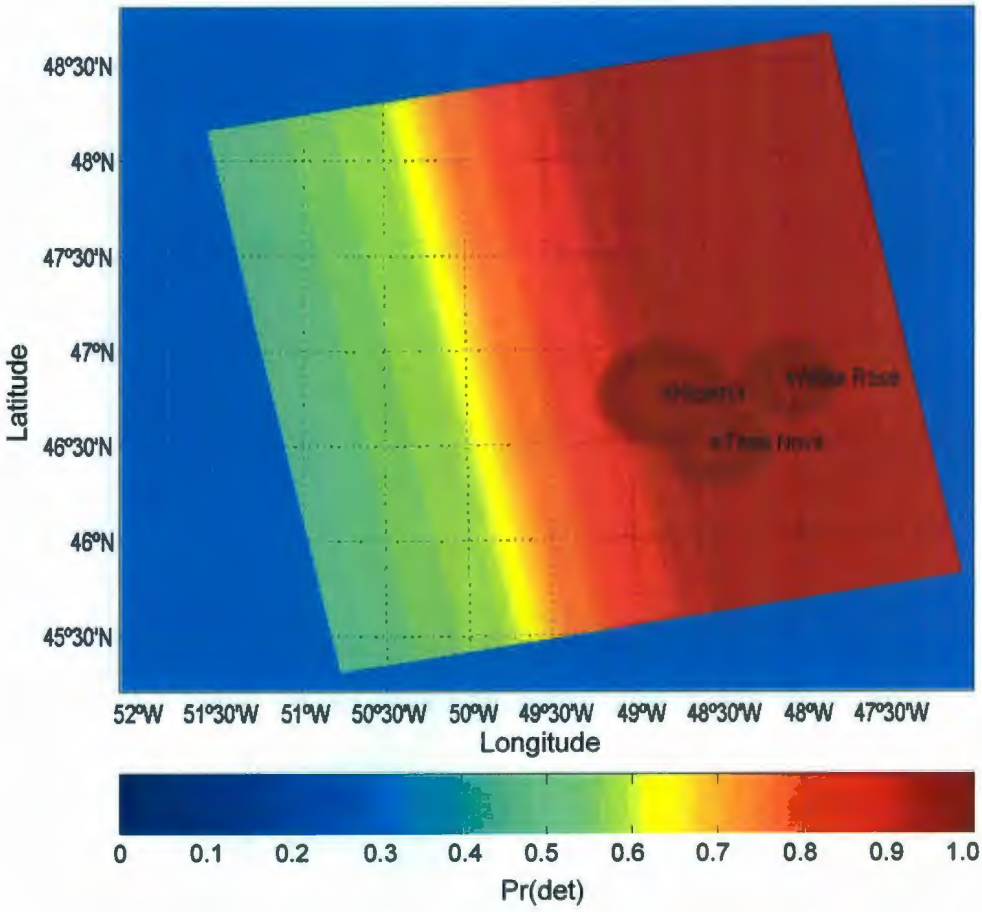

Figure 3.12: Pr(det) for Marine, HF SWR (2000), and RADARSAT-1

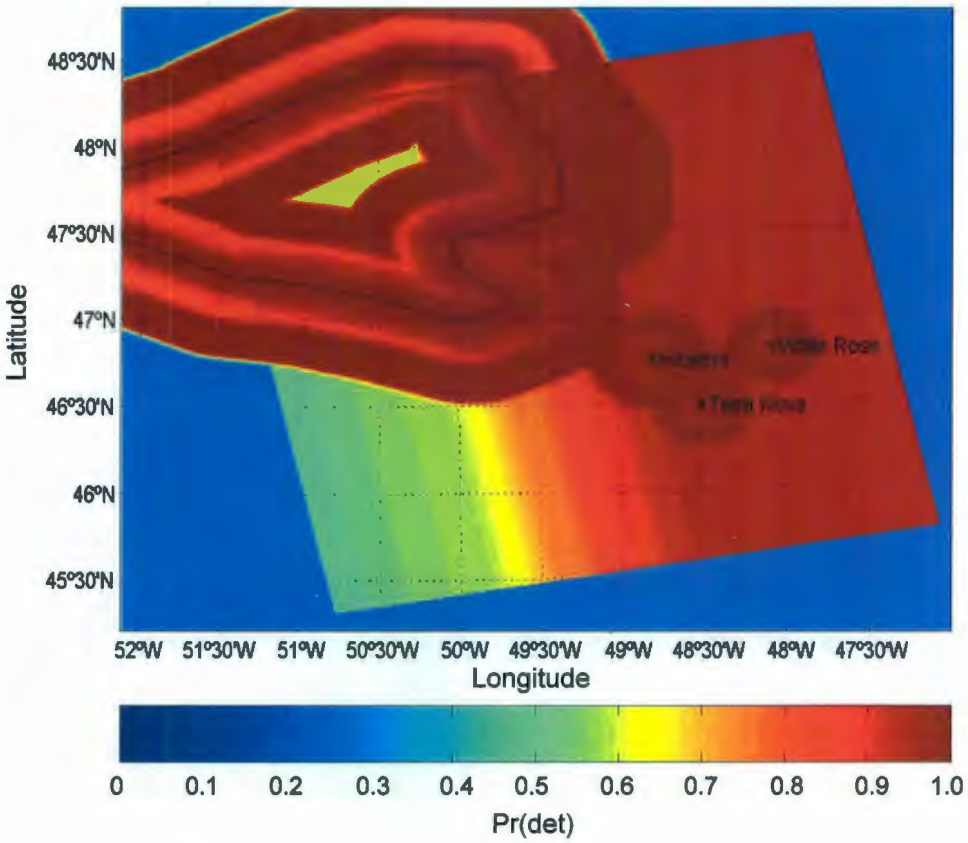

Figure 3.13: Pr(det) for Marine, HF SWR (2000), RADARSAT-1 and Aerial

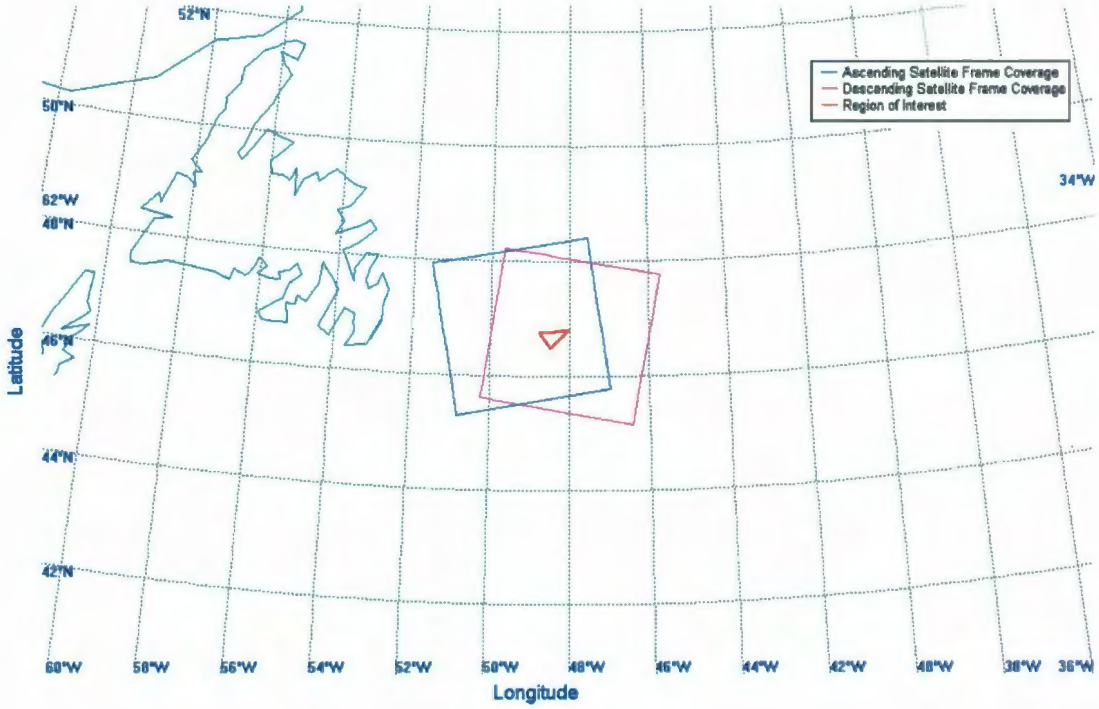

Figure 3.14: RADARSAT-1 Data Frame

3.3.3 Assessment of Results

This discussion on sensor fusion has provided a sensor fusion methodology. Described in this chapter have been techniques to assess multi-sensor performance based on well-known statistical methods. With this method, performance curves are added systematically to consider the influence of all the sensors in the geographical area of interest. In doing so, the value of each sensor can be assessed on an incremental basis to determine optimal configurations for existing and future platforms. The model of multi-sensor performance is compatible with existing ice load and risk analysis methods that apply individual iceberg target simulations around one or more platforms with modeled detection sensors.

3.4 Analysis

The multi-sensor method treats each sensor as a set of statistical tests over an area. This area is broken into small sections, and in each of these sections the probability of detecting an iceberg is determined. Using the methodology outlined here, multiple sensors can be combined over a period of time, with various delays in the availability of the data, to create a complete probability of detection map over a geographical area.

This method is useful in the implementation of sensor models for risk analysis. However, the method demonstrated here is limited in resolution. As well, the methodology has restrictions such as minimum number of iterations and the types of combinations that can be performed on spatially disparate sensors.

Though deliberately not addressed here, stochastic simulation techniques would likely be more feasible in the simulation of combined sensor performance. This is particularly true given the advances in computer technology in recent decades.

From an offshore oil and gas operational perspective, it is the handling of iceberg data on a day to day basis that is most relevant. For this analysis, tracking systems such as those discussed in Section 2.2 would be more relevant. The method for sensor fusion described here may provide benefit to sensor combination, but does not aid in the handling of target data. The remainder of this thesis thus focuses on what has been defined herein as data fusion.

Chapter 4 Data Fusion Method

This chapter examines the issue of data fusion methodologies specifically pertaining to the combination of detection sensor data with respect to target existence and non-existence, and the subsequent determination of target features.

It is intended that the proposed data fusion methodology be such that the combination of sensor reported data provides an increased likelihood of the determination of the existence of the target, along with an estimation of feature information derived or extrapolated in the process.

In recent years, data fusion systems have become an important element in offshore ice management due to the extreme importance of reliable detection predicating the availability of additional detection sensors. Examples of these sensors include multiple overlapping marine radars, and new long-range wide-area data sources such as HF SWR and satellite SAR.

Subsequently, the terminology and examples used in this discussion will revolve around the immediate application for these methods. In particular, the icebergs that seasonally populate the waters along Labrador and Newfoundland coasts and infringe upon the

areas of petroleum development in the Northwestern Atlantic are used to develop the application of the data fusion methodologies.

4.1 Data Fusion Overview

For the purpose of this analysis, data fusion refers to the combining of data from all available sources such as marine, enhanced marine, airborne, satellite and land-based radars and visual observations. Through the on-going collection and association of data from these, a single complete data product is generated.

While simple statistical methods can combine probabilities of detection for varying sensors, there are many applications were a more intuitive data-oriented system is desired. The goal is to provide a wide-area interpretation that is as accurate and current as possible. In a general context, this is a 'picture' of the state space that can then be used for other analysis. In the iceberg management application, the results of this combination can then be used to efficiently plan and manage the region close to the operation facilities (tactical zone).

There are many methods employed in data fusion and inference. For the purpose of this investigation, quantitative methods are more appropriate due to their basis in well understood mathematical and statistical techniques. These methods include, but are not limited to, 'weighted averaging' techniques, geometric methods, non-probabilistic methods, and probabilistic methods of inference such as Bayesian estimation, least squares method and Kalman filtering (Manyika and Durrant-Wyte, 1994).

4.1.1 System Variables

The parameters associated with the sensors are probability of detection, probability of false alarms, identification, coverage, resolution, latency, and confidence in results. These have been defined in 3.1.1. In addition to these definitions, note that where fusion systems rely on the features of targets to perform association the resolution of the sensors must be capable of detecting those features.

Sets of these variables exist for each sensor to be used in the sensor fusion system. Further to this, the variations in the number, location, and type of sensor affects how the final sensor fusion system will perform. The interaction of these parameters is depicted in Figure 4.1.

The combination of multiple sensors relies on the performance of the sensor and also on the overlap, geographically and temporally, in the region being monitored.

It should be noted in an evaluation of sensor performance, and specifically with regards to risk analysis, that persistent adverse weather conditions, which impact sensor performance, are relevant to the analysis. However, this is beyond the scope of this thesis.

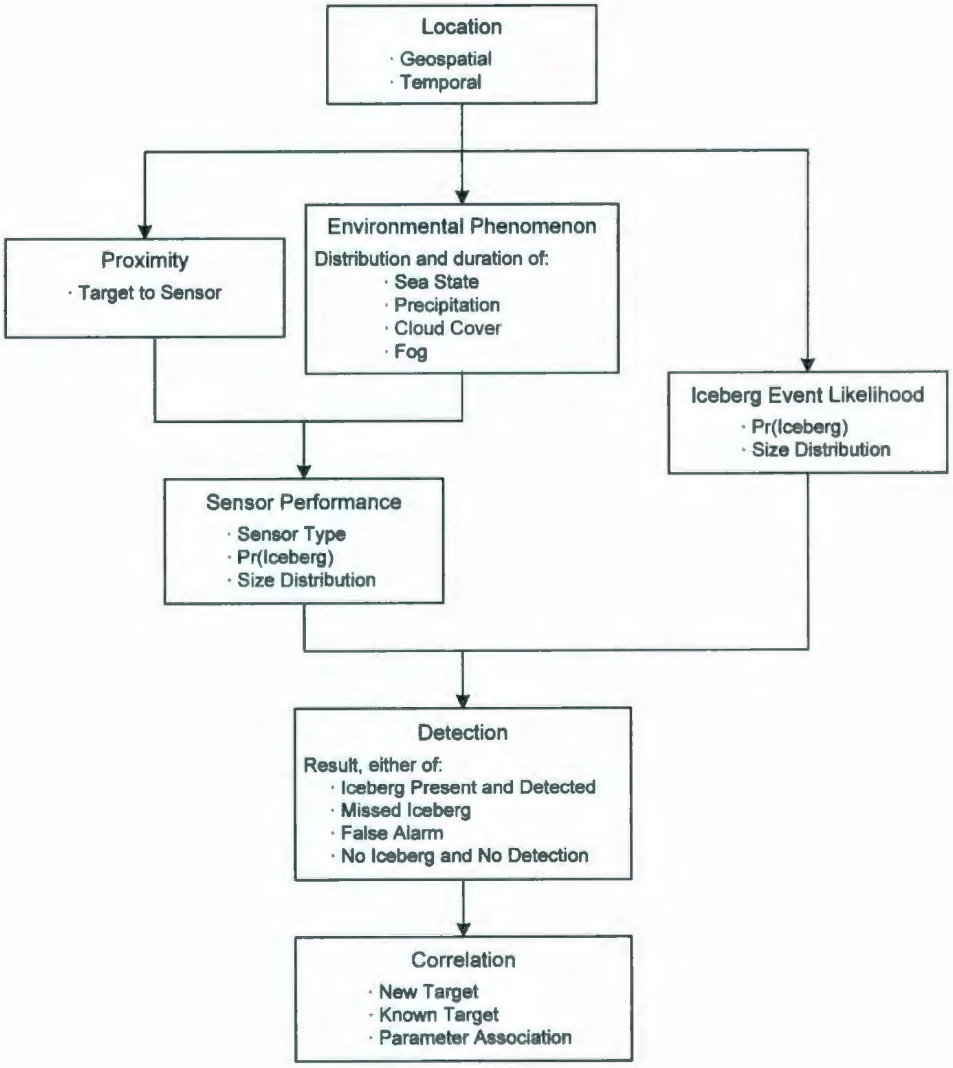

Figure 4.1: Data Fusion Variable Relationship

4.1.2 Data Fusion Challenges

The primary challenges facing a data fusion system are those of combining geographically and temporally spaced data. As well, the sensors described above have varying refresh rates, data latencies, probabilities of detection, and resolutions, which complicate the execution of data fusion.

The system for combining old and new data must be capable of incorporating data that arrives at different rates, at different times, and from various locations. Discussed below are the important aspects of data combination with respect to geographical and temporal combination of sensors and the effect of latent data. First a single sensor, or, sensor node is defined.

Sensor nodes are defined here as individual sensors. Most often these are radars on ships, platforms, aircraft, satellites, or onshore. As well, human observers on platforms, ships, and aircraft can be considered sensors for the purposes of this discussion.

Each sensor node consists of three parts. These include a sensor, raw data received from the sensor, and the interpretation of that data.

The primary performance parameter of a sensor is its ability to detect a target such as an iceberg. This is a probability curve, whose profile is defined by the technology of the sensor, the size of the target and environmental conditions.

Combination of data over a geographical area implies the requirement to associate data from one sensor with another. For detected targets to be combined over a period of time, the data must remain correlated for that period. That is, without knowledge of target movement, the data points of one moment in time must be such that they can be combined with the next iteration within the resolution of the sensor. Hence, the objects that are being detected from one period to the next are limited in the distance they can move from one sample to the next. For the information to be combined in the most simplistic manner, the time period elapsed must be smaller than the time required for the iceberg to move from one resolution cell to another.

The requirement for short-term correlation is very limiting to the data fusion method. To utilize other sensor nodes and combine multiple sensors over wide-areas, a method of associating new targets with old must be determined that does not require the target to be in the same location. A method of iceberg tracking must be established. To achieve this data fusion, a tracking system is employed.

4.2 A Data Fusion Methodology Using Tracker Theory

A useful data fusion system takes all available target information and combines it to create a single data product that is superior to what could be extracted from any of the individual datasets. In the selected application, this fusion system must be capable of combining available data on positions and possibly headings, speed and size of icebergs from many sensors, at irregular times and over a very large area. From these data, it must extrapolate a best estimate of the actual position, heading, speed and size of icebergs at any point in time. It must also account for errors in the measurement systems and for the reliability of the data.

Since extrapolating the position of the icebergs is necessary to both make the system useful and to reduce the computational requirements, it must have similar functionality to that of a radar tracking system. Consequently, a basic radar tracking system architecture is used as the framework for the fusion system. The overview of the fusion system presented in Figure 2.7 (Blackman and Popoli, 1999) is reproduced in Figure 4.2 for convenience.

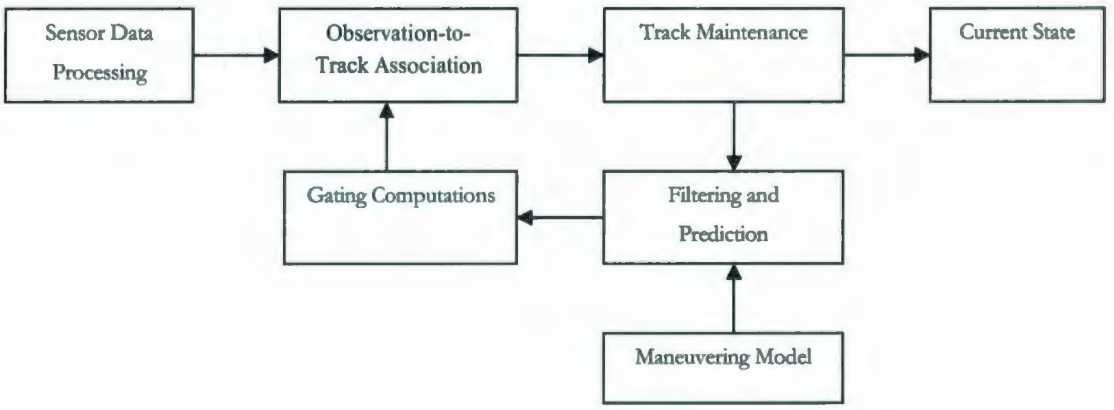

Figure 4.2: Tracking/Fusion System Diagram

With respect to the challenges noted in Section 4.1.2, this tracking system is deemed desirable. Geographical and temporally spaced data can be associated with one another given their prediction from one location to another. This association relies heavily on the availability of a maneuvering model. Reasonable latencies in data can be tolerated, but will have increasingly detrimental effects as targets near critical regions. Non-sequential data could be handled with varying degrees of inconvenience depending on the implementation and architecture of the system.

4.2.1 Architectures

The architecture of the data fusion system is most concerned with the transportation of data from the sensor to the user. This implies the processing of the data at the user or

at some point along this path. The location of the processing provides alternatives in the system implementation.

Two general approaches are applicable. They will be referred to here as centralized systems and distributed preprocessing systems. The descriptions are presented here based on Haykin et al. (1994).

Centralized systems immediately integrate the raw data into a common channel and then perform the necessary signal processing at a central location. This requires a high bandwidth communication link between all sensors and the central location.

Distributed preprocessing systems preprocess the raw sensor data at the sensor and then supply the interpreted output to some central integration system. The distributed method is more reasonable in this application, due to the geographic dispersion of the sensors and the cost associated with providing bandwidth for transmitting the raw data to a central location.

In the application which is the main focus of this thesis, the sources of the information to be fused are distributed over a wide-area. The data come from ships, platforms, airplanes, HF SWR stations, and Earth observation satellite ground stations. This tends to limit the methods of data processing, since each data source has varying degrees of processing and raw data are not available or difficult to access. The preprocessors in this case vary from human interpretation of radar displays to

sophisticated computer algorithms such as those used for satellite based SAR or HF SWR.

4.2.2 Tracking System Description

As illustrated in the block diagram of Figure 4.2, a system can be broken down into several parts, namely: Sensor Data Processing, Observation-to-Track Association, Track Maintenance, Filtering and Prediction, and Gating Computations.

The fusion system employs an iterative process of updating iceberg tracks and positions. A general description of the process is described in Section 2.3.2. To illustrate how the system will operate, a single iteration of the process is given below for a distributed pre-processing architecture.

- Sensor data consist of the processed data from a sensor or sensor array. The sensor array can be homogeneous (consisting of similar or identical sensors) or heterogeneous (disparate sensors). The use of heterogeneous sensors requires consideration of their individual abilities and may impact the track maintenance, gating, and filtering stages.

- Observation to track association is performed in either batch or iterative sequence. The association consists of matching new detected targets, or the lack of targets, to previous tracks; where tracks are a set of detections that are suspected of deriving from a single target.

- The track maintenance portion of the MHT provides for the generation of new tracks and/or association with available previous tracks.

Similarly, it accommodates the deletion of old tracks, such as those which are unsubstantiated by new detections. This case may arise in the presence of false alarms.

- Filtering can be used to reduce the error in position measurement. Many common filters, such as the Kalman filter, are well suited to this task. To determine the degree to which any new detection can be associated with a previous target, the estimated position of the previous target is calculated. A maneuvering model may be used at this point to provide the basis for statistical likelihood of position estimation, or for the reduction of computational load based on filtering using the gating region.

- The gating computation is used to remove improbable or impossible new detections from the association processing. The previous position prediction will carry with it an error variance that is used to define an area, or 'gate' at the time of the new detection. For each particular track, new targets outside of its gate area can be excluded from the association calculations, thus reducing processing time.

In an iterative implementation the system steps through this process each time new target information becomes available. The result is a picture of the current state of targets, utilizing all available data.

Data arriving out of sequence, that is after more recent information has been processed for a coincident area, may pose a problem based on the algorithms used. In the worst

case, an analysis will have to revert to a previous state and re-process the out of sequence information along with its subsequent previously processed data sets.

4.2.3 Data Fusion Example

A data fusion system should optimally combine data from sensors with excellent to poor detection ability, small to large coverage areas, and with varying false positive rates by using the information known about those sensors. These parameters will determine the confidence in the information from the sensors, and subsequent sensing iterations will adjust the confidence such that false positives are eliminated and confirmed detections are retained.

4.2.3.1 Track Scoring

A variety of methods can be employed to determine if an initial track should be propagated to the next iteration of the tracking system. The method used in any fusion or decision system is very subjective and is often based on the creator's preference and background. For the analysis presented here, Bayes statistics are employed. As introduced in Section 2.3, Bayes statistics operate in an iterative manner and modify some prior statistic value based on the negative or positive outcome of a statistically based test. For example, in a tracking system, the posterior result from an attempt to detect a target can be used to update the Bayes prior value; hence Bayes is useful as a track score method. There are quite a number of arguments for and some against the use of Bayesian decision theory and Bayesian inference.

When making decisions under uncertainty it makes a great deal of practical sense to use all the information available, old or new, objective or subjective. Humans make decisions using an intuitive process based on our experience and subjective judgments.

Classical statistical approaches consider the parameters of a model as fixed, but unknown, constants that are estimated using sample data taken randomly from the population of interest. The Bayesian approach treats these population model parameters as random quantities. The Bayesian approach uses old information or subjective data to construct an *a priori* distribution model for these parameters. This model expresses the starting assessment about how likely various values of the unknown parameters are. Current data is then applied via Bayes formula to revise this assessment, creating the *a posteriori* distribution model for the population model parameters. Parameter estimates and confidence intervals are calculated directly from the *a posteriori* distribution. These confidence intervals are legitimate probability statements about the unknown parameters, since these parameters are now considered random, not fixed (NIST, 2001).

The most frequent criticism of Bayesian analysis is that the *a priori* distributions which are 'improved' on every iteration can have various, reasonable distributions that will often yield different results. This is a supposedly unappealing lack of objectivity. However, Bayesian analysis with non-informative prior statistics (no or minimal *a priori* information) is objective. Berger (1985) points out, "When different reasonable priors

yield substantially different answers, can it be right to state that there is a single answer? Would it not be better to admit that there is scientific uncertainty, with the conclusion depending on prior beliefs?" That is to say, if reasonable prior statistics yield reasonable but different results, it should be acknowledged that uncertainty exists in the problem and not a deficiency within the method.

It is the ability to create an *a posteriori* distribution (the result of an iteration on an *a priori* distribution) and an associated certainty measurement that best lends Bayesian analysis to this application. The ability to use *a priori* information and iteratively add new information may provide a means around the problem of delayed data, if this can be done out of sequence. Non-sequential temporal processing is not address here.

Based on the distributed processing architecture (Section 4.2.1), the system would receive as input a list of iceberg observations and associated details. This information would include the type of sensor and the location of the observation. From the knowledge of the parameters of that sensor, and of existing icebergs already being tracked, the system updates its own tracking database. Details from this database would then be used to create estimations of iceberg positions, headings and speeds that would be used for the management of ice resources and subsequent improvement of safety for crew and facilities. Other inputs include environmental observations such as surface currents derived from radar and ocean current profile measurements taken from vessels and installations. In the absence of a more sophisticated predication

model, this information could also help provide short-term estimates of future iceberg positions.

The following Bayes iterative equations (Chankong et al., 1985) are convenient for use here. These are the same equations derived in Section 2.2.3. These become the basis for track score calculations.

$$\Pr(PS \mid PR) = \frac{\Pr(PR \mid PS) \cdot prior}{\Pr(PR \mid NS) + (\Pr(PR \mid PS) + \Pr(NR \mid NS) - 1) \cdot prior} \qquad \text{Eq. 4.1}$$

$$\Pr(PS \mid NR) = \frac{\Pr(NR \mid PS) \cdot prior}{\Pr(NR \mid NS) + (\Pr(PR \mid PS) + \Pr(NR \mid NS) - 1) \cdot prior} \qquad \text{Eq. 4.2}$$

The variables in these equations have been initially defined in Section 2.3.1; they are defined here specifically for target detection.

Pr(PS | PR) = Probability of a positive state (target exists) given a positive result (target detected).

Pr(PS | NR) = Probability of a positive state (target exists) given a negative result (target not detected).

Pr(PR | PS) = Probability of a positive result (target detection) given a positive state (target exists), typically referred to as probability of detection (Pr(det)) of a sensor.

Pr(NR | PS) = Probability of a negative result (target not detected) given a positive state (target exists), easily formulated as 1-Pr(det).

Pr(PR|NS) = Probability of a positive result (target detected) given a negative state (target does not exists), typically referred to as probability of false alarm (PFA) of a sensor.

Pr(NR|NS) = Probability of a negative result (target not detected) given a negative state (target does not exists), easily formulated as 1−PFA.

Prior = For the initial iteration the prior is set to a known or default value. Depending on the outcome of the iteration either the Pr(PS|NR) or the Pr(PS|PR) becomes the posterior value. At the beginning of the next iteration this is used as the prior value.

The outcome of this track score method is influenced by several key, typically preset, variables:

- Pr(det);
- PFA; and,
- the number of successive iterations.

As well, since the amount of processing resources is limited to some degree, a means of eliminating apparently false target tracks is required. For this, a limit is set on the posterior. Once a posterior value appears improbable to represent a target, that target (and/or its associated track), are removed from the system to free up processing resources for new detections.

The following example illustrates iterative Bayes and the influence of Pr(det) and PFA. Figure 4.3 depicts a positive detection followed by seven missed detections, followed by a detection and three more missed detections. In this case the non-informative prior value is 50% and the Pr(det) is 20% and the PFA is 5%. The initial detection raises the predictivity and maintains confidence in the detection, despite its lack of re-occurrence.

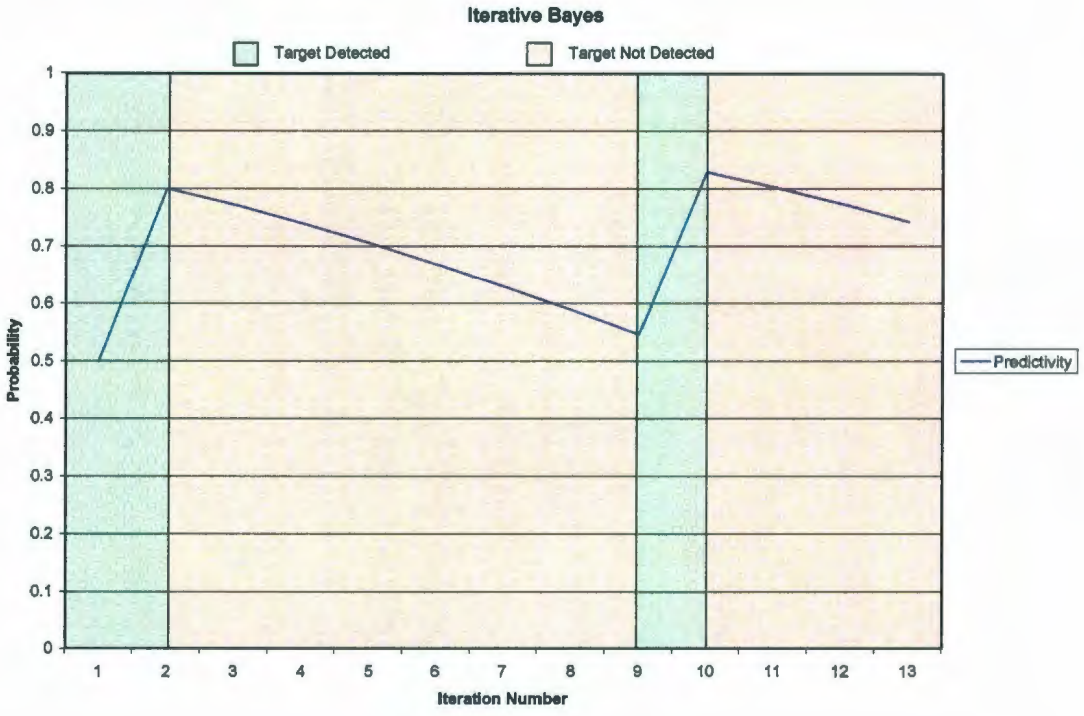

Figure 4.3: Iterative Bayes with Missed Detections, PFA = 5%

In Figure 4.4, the PFA is decreased to 1%. This shows the relationship between Pr(det) and PFA. The results are much improved; this is due to the interaction of PFA and predictivity.

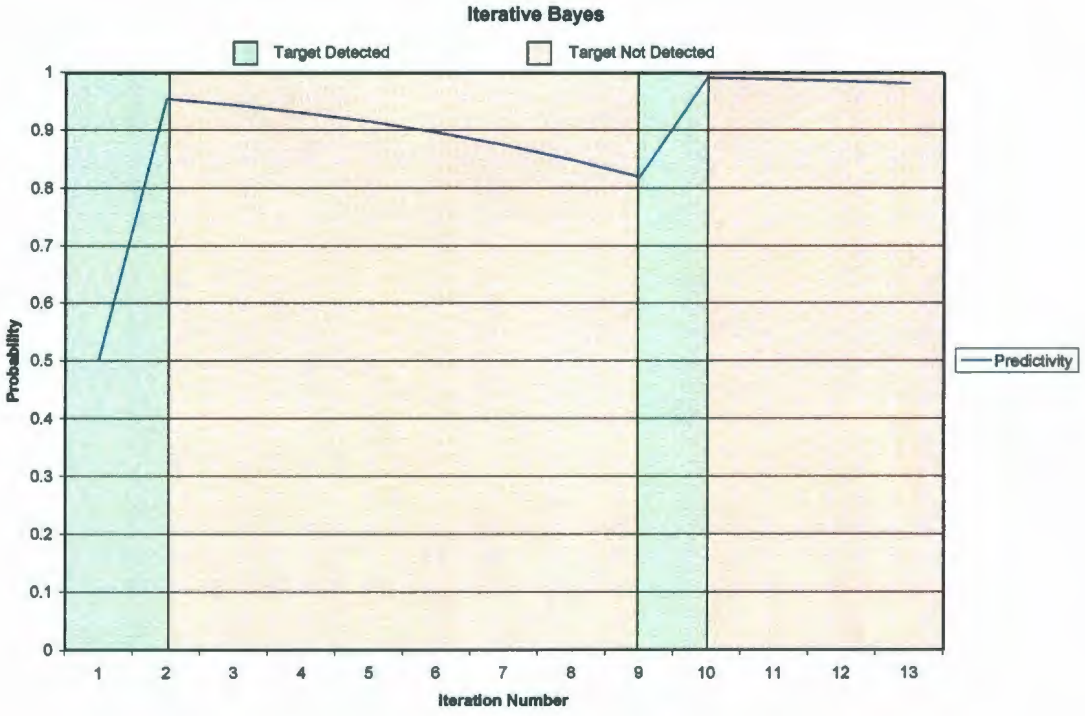

Figure 4.4: Iterative Bayes with Missed Detections, PFA = 1%

The detection is given merit by the low false alarm rate; likewise, the missed detections are moderated by the low likelihood of detection. A desirable PFA will ensure the propagation of a track through multiple iterations, even when the Pr(det) is poor. From this it is apparent that in a tracking system where Pr(det) may be low the role of PFA cannot be underestimated.

4.2.3.2 Bayes Iterative Simulation

To examine the influence of the track discarding value, the Bayes prior value and the Pr(det) and PFA on a tracking system, a simulation system was developed in MATLAB®. This system was based on Eq. 4.1 and Eq. 4.2. The system focuses on the detection aspect as opposed to the track aspect of MHT systems. The track quality is proportional to those targets which are known. Misidentification of targets is not dealt with here. Tracks and targets are referred to interchangeably since a valid target can only be found by sufficiently corroborating evidence of its track.

The key parameters in the simulation tests are briefly described in the following paragraphs.

- Gating: To simplify the analysis, it was assumed that the system was based on a reasonable maneuvering model with Gaussian distributed error, and the gating size was preset to two standard deviations of the model error.

- Bayes Prior: Several Bayes prior values were used throughout the analysis. While the choice of the prior value is debatable, early parametric experimentation with the simulation indicated that this initial value was quickly and significantly altered by the first iterations of the simulation. For the simulation, a value of 0.5 was used unless otherwise noted, as it represented a 'non-informative' value (Berger, 1985).

- Pr(det) & PFA: In practical implementations of tracking systems, the Pr(det) and PFA values will likely vary due to factors such as range, target

size, reflective properties, and environmental interference and noise. For this simulation, the Pr(det) and PFA are kept constant for each simulation test. Values for the Pr(det) and PFA are taken based on poor sensor performance (Pr(det) = 10 to 50% and PFA = 0.001% to 0.1%)

- Minimum Track Score: The value at which a track is discarded is critical to the reduction of false alarms within the system. This value was varied for several tests depending on the purpose as discussed below.

For each iteration of the simulation, several steps are followed:

1. Variable Initialization: The prior value chosen (0.5) was assigned to each element of a vector which represented a set of undiscovered targets.

2. Detection Attempt: Based on the Pr(det) and gate variance, a random number of vector indices were selected and determined to have been detected. Pr(det) is derated on the assumption that 95% of targets will be within the gating area; 5% will be missed. This is intended to represent imperfect target maneuvering models.

3. False Targets: Based on the PFA, a number of vector indices were created at each iteration corresponding to the PFA and the total number of target indices. The PFA rate was used for previous false alarms in a similar manner as the Pr(det) rate was for the target vector.

4. Bayesian Update: Using the corresponding Eq. 4.1 or Eq. 4.2, the posterior value was calculated based on whether the indices were contained in the 'detected' subset. False targets were also processed in this manner. Real target vector indices that had not been detected to this

point were not altered. If a previously detected target track was re-discovered after being discarded, it was reassigned the 0.5 prior.

5. Track Score Eliminations: For those posterior values that had fallen below the acceptable minimum to remain a valid track, the posterior values are set to zero. This is indicative that the vector indices were discarded and presumed invalid.

Subsequently, the posterior values become the prior values for the next iteration. All tracks with a score greater than the track score elimination limit are considered to be valid at this point.

Miscorrelation between targets is not accounted for. While cross-correlation of targets is possible, the intention of this simulation is to demonstrate the utility of the track score method. Cross-correlation of targets will be a function of the sensor resolution, maneuvering model accuracy and target density.

To examine the results of the simulation, the values at steady state are examined. As can be seen in Figure 4.5, the percentage of targets not deleted by the track maintenance function increases over the duration of the simulation. The time required to discover all of the targets is, in this case, about 50 iterations. For this example, a Pr(det) of 10% was used with a PFA of 1%. The track score elimination cutoff was a 0.1 probability value for the posterior. The number of false targets, as a ratio to real targets, is 0.154. At the steady state, 82.5% of all targets are represented as tracks in the system.

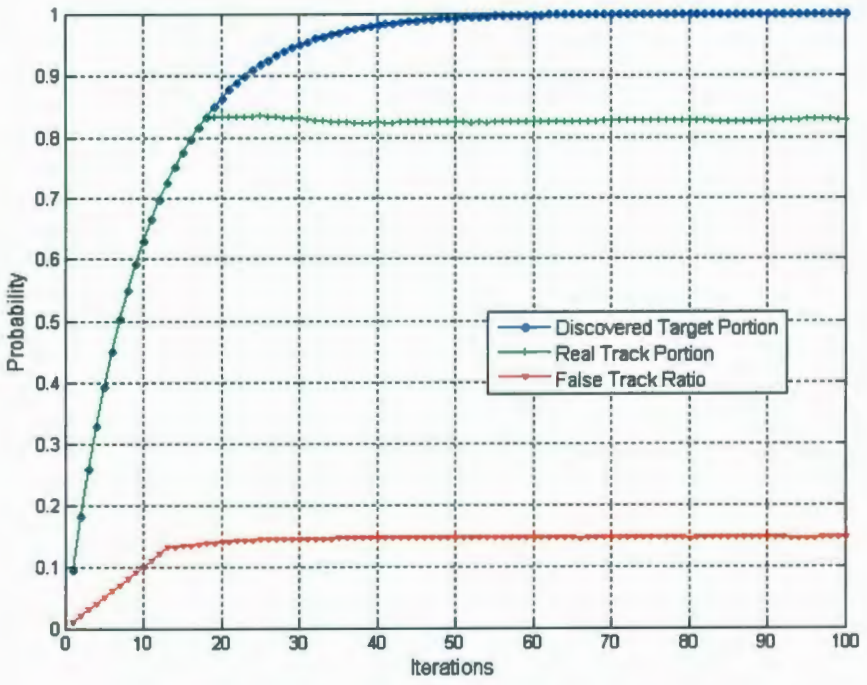

Figure 4.5: Simulation Steady State Values

The portion of simulated 'real' tracks that are maintained in the tracking system is primarily dependent on the track elimination value. Figure 4.6 shows the effects of various track elimination values on the percentage of real tracks maintained in the system. For this simulation, an initial prior value of 0.5 was used, along with a PFA of 0.1% and a Pr(det) of 15%. Variations on the prior value have little impact on the performance. Lower values of the track elimination value enhance detection performance.

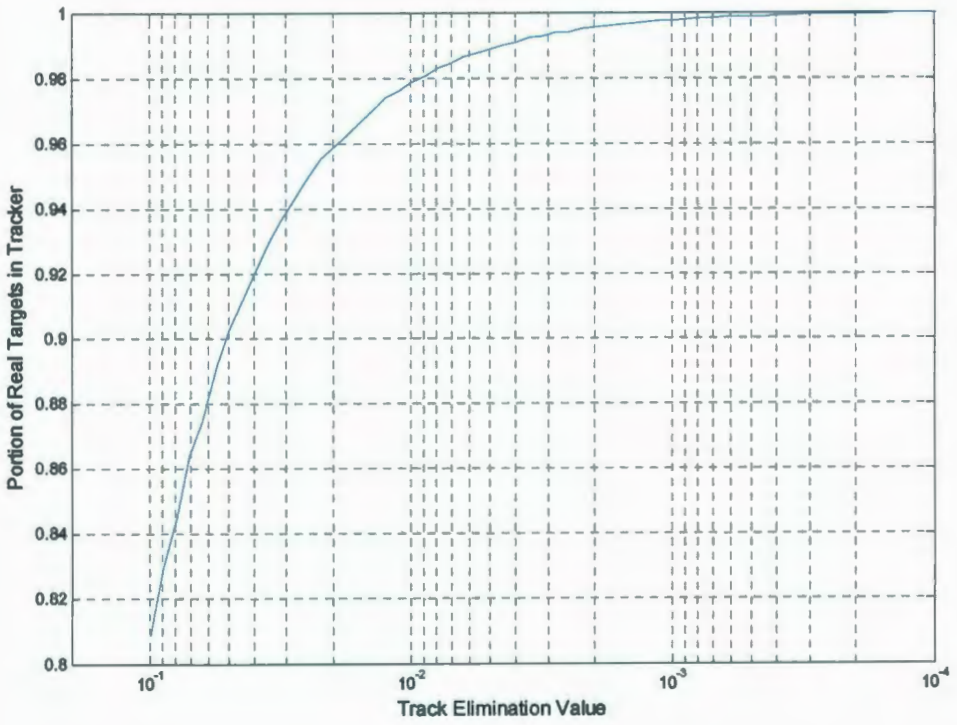

Figure 4.6: Real Targets in Tracker vs. Track Elimination Value

A tradeoff does exist with respect to the track elimination value and the false track ratio. Figure 4.7 shows the relationship between the prior value, the track elimination value and the ratio of false to real tracks in the system. For this example, a Pr(det) of 10% was used with a PFA of 0.1%

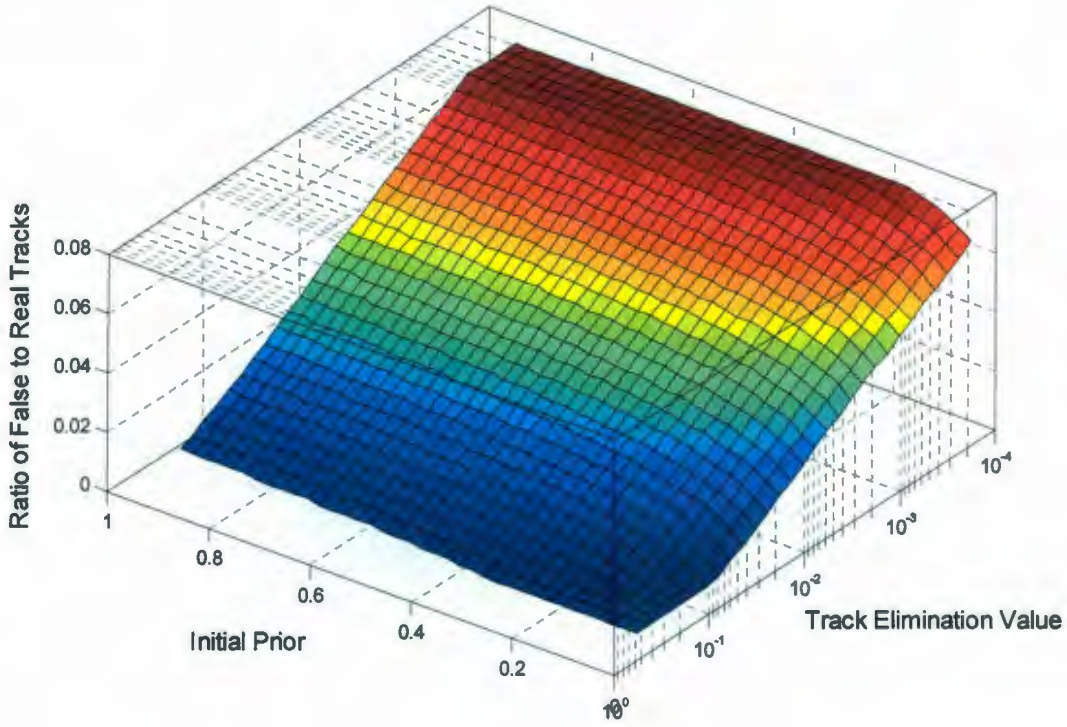

Figure 4.7: Ratio of False to Real Targets vs. Prior Value and Elimination Value

Given a sufficiently low track elimination value, a very high portion of the real targets will be represented as tracks in the system. This is achievable with very low Pr(det) rates. However, the system and sensor iterations required to detect all of the targets is dependent on the sensor Pr(det). Figure 4.8 shows the minimum number of iterations to reach 99% target discovery vs. Pr(det) value.

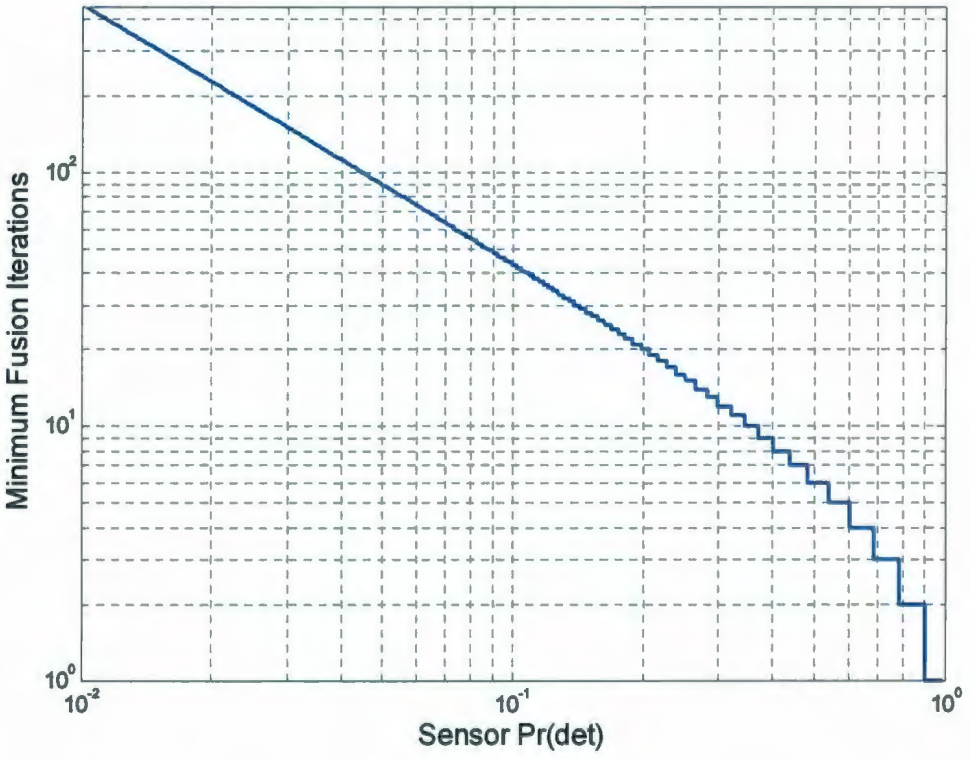

Figure 4.8: Iterations Required to Reach 99% Target Discovery

For reference, the interaction of PFA and Pr(det), with respect to the ratio of false tracks to real tracks that are maintained within the system, is shown in Figure 4.9. Note that as the system performance improves, the ratio of false to real tracks diminishes, quantization errors are created by the simulation.

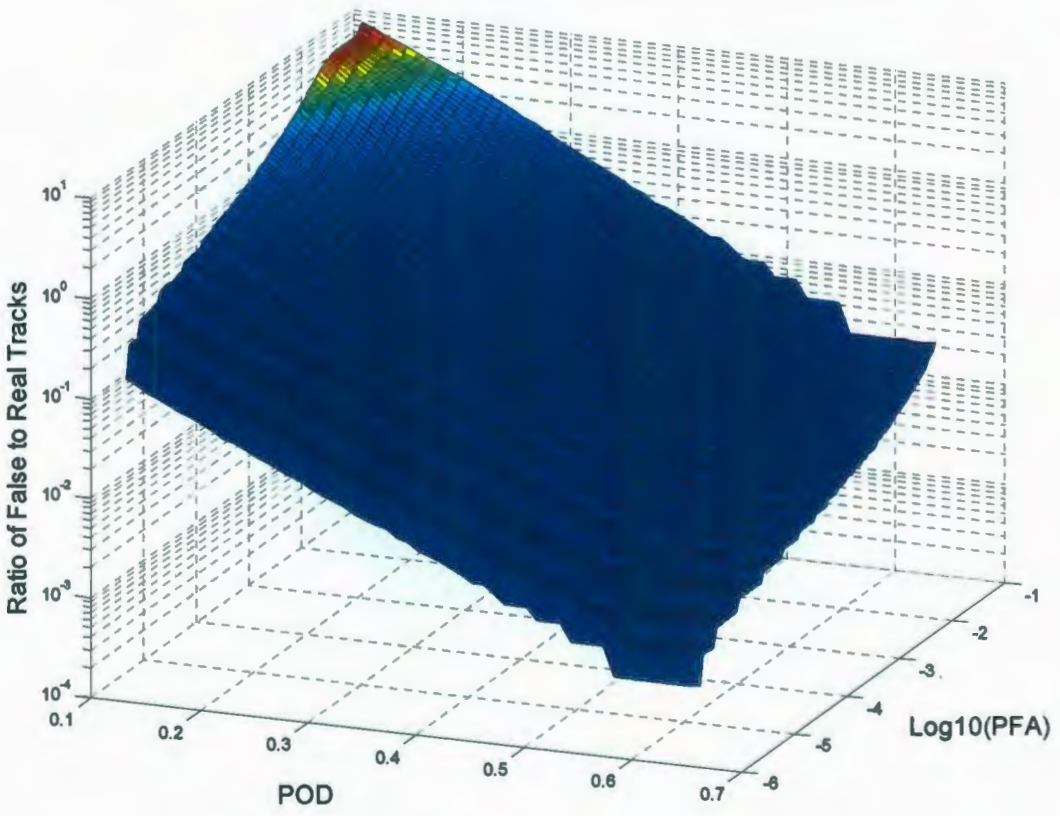

Figure 4.9: Ratio of False to Real Targets vs. PFA and Pr(det)

Bayes, as the basis for the track score component of the tracking system constructed here, dramatically improves the probability of detection in situations where some false tracks can be tolerated and sufficient iterations are available. These examples overlook the association portion of the system and presume a reasonable maneuvering and prediction model.

4.3 MHT Using Historical Maneuvering Statistics

Along with the track score component illustrated in Section 4.2.3, an association method is required to relate new target information to existing tracks, or create new tracks from previously undiscovered targets. The following is an example of this tracker fusion methodology implemented around the distributed architecture. In this first implementation, the target prediction estimates are related to the historical information on iceberg movement.

The facets involved in fusing iceberg data from multiple sources are illustrated schematically in Figure 4.10. The multiple hypothesis association examined here is the 'fusion' system at the center of the diagram. It uses the tracking system parameters, kinematics model, and knowledge of the sensors to accomplish data fusion.

Targets detected from sensor iterations must be associated with existing information in the database. To perform an association of targets detected from one sensor sweep to the next, the historical statistics of iceberg movement are examined and the likelihood of any new detection being attributed to a previous detection quantified. From this a hypothesis of most likely detections can be found. Additional methods of association are examined in Section 4.4.

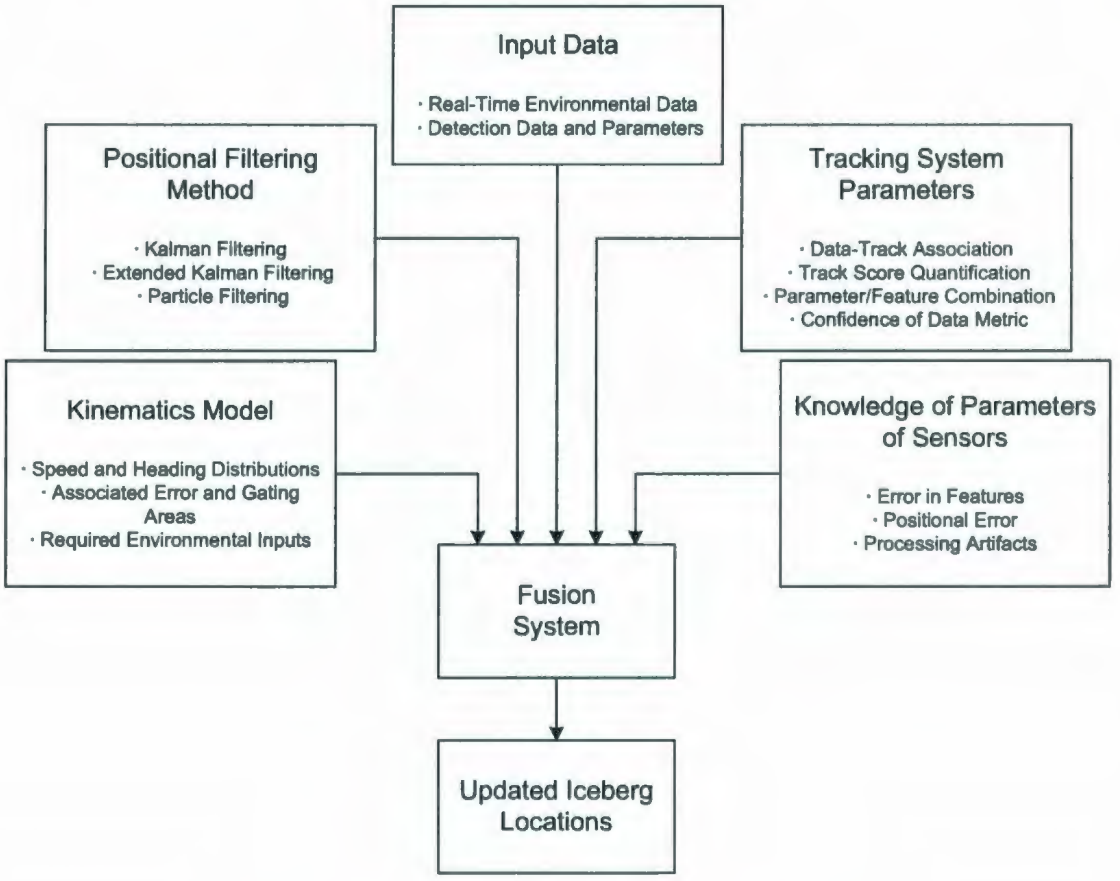

Figure 4.10: Fusion System with Broad Scope

This implementation is based on a multiple hypothesis tracker (MHT); information is retained in the system so that multiple theoretical solutions to the association challenge can be evaluated in parallel. Figure 4.11 shows a block diagram representing the algorithm.

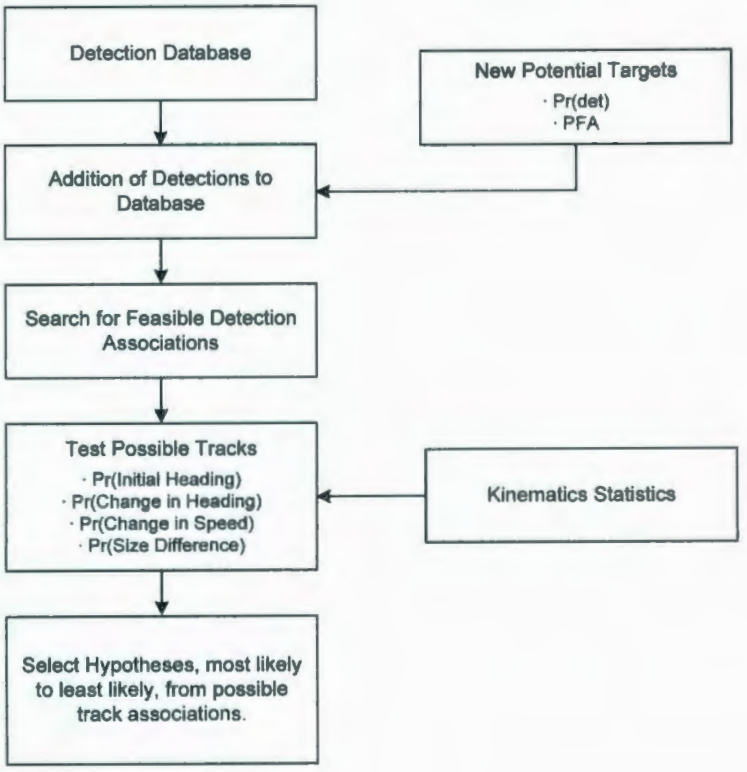

Figure 4.11: Multiple Hypothesis Tracker Outline

This multiple hypothesis tracker is written in MATLAB®. It collects iceberg detection information and stores it in a database containing information regarding the detection time, location, type of sensor (e.g. aerial reconnaissance, satellite data, SWR), the number of detections, and size and shape characteristics, if available. The detection information is input into this MHT in the MANICE file format (Environment Canada, 1989) since this is a common industry reporting method. Using the database and the kinematics statistics collected for icebergs, a likelihood is determined that detections from sequential sensor iterations are produced from a single iceberg. The greater the

likelihood value, the more confident the user can be that a group of detections, one from each of a several scans, are from a single iceberg detected at different times.

To increase the number of kinematic statistics that can be utilized, the system calculates the likelihood three detections—one from each of three scans—have come from the same iceberg. A group of three-detection sets that are not mutually exclusive constitute a hypothesis. Thus, if all available maneuvering statistics are to be utilized, three sensor scans, such as an aerial reconnaissance flight, a satellite frame, and another aerial reconnaissance flight, are needed to provide enough data for the creation of a hypothesis. Several statistics are utilized to provide a basis for the association of iceberg detections:

- probability of deviation from the wave and current direction;
- probability of turn rate for an iceberg per day;
- probability of the change in speed of an iceberg per day;
- probability of the heading of icebergs in an area (historical);
- probability of track speed between two detections; and,
- difference in size of detected icebergs.

The statistics that require three scans are conditional probabilities such as rate of change in heading or rate of change in speed. The rate of turn, change in speed, and historical heading statistics are broken into ¼ degree squares where sufficient historical

data (PERD, 2001) were available. Using these statistics, detections from three subsequent scans are compared. Every possible association of any three points, one from each of the scans, is evaluated and ranked by likelihood. A set of associations that do not conflict with one another constitute one hypothesis.

Inaccuracies in position measurements of detections during sensor sweeps are not specifically accounted for; however, since the statistics are arrived at from actual aerial flights the error inherent in this type of sensor is included. The iceberg tracks generated from the flights are the basis for the statistics detailed in Section 4.3.1. Areas where very little data have been collected may have statistics less representative of the actual drifting icebergs.

The number of possible associations between three sets of detections can be large. For example, for three scans with 50 iceberg detections each, the number of associations of any three detections, one from each scan, provides 125,000 track possibilities. From these, the set of mutually exclusive associations with the highest probability is selected; this is the most likely hypothesis. The number of possible hypotheses for 50 tracks from 125,000 possible exceeds billions of billions. To reduce this number, tracks with low probabilities can be eliminated. An algorithm that calculates hypotheses from most likely to least likely was developed and included in the MATLAB® implementation.

An example of the types of products that could be produced by such a MHT system can be seen in Figure 4.12 and in Figure 4.13. In the first diagram, associations are made from three consecutive days, the first in red, the second in yellow and the third in green. The depicted set of tracks represents the most likely hypothesis; to avoid confusion improbable associations are not shown.

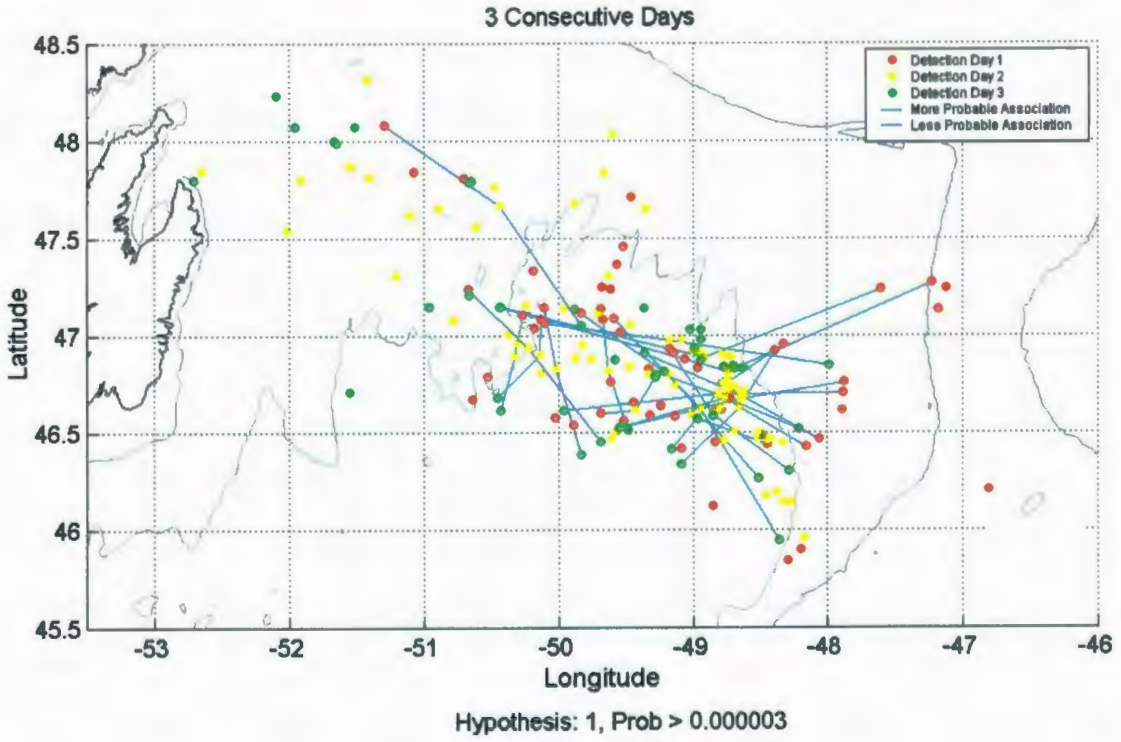

Figure 4.12: MHT Iceberg Association, Most Likely Hypothesis

In Figure 4.13, one iceberg detection (iceberg 72) from the scan iteration on day 2 is displayed with lines to all of its possible associations in the first and third scans. These

lines represent all of the possible tracks that include this detection from the second scan. Associated with this is a list of probable tracks ranked from highest to lowest that allows the operator to choose the most suitable track based on the operator's expert knowledge. This alternate system enables a human shepherded fusion system that may provide the operator with the information to choose a result they are more confident in, rather than the most probable result based on the statistics used. The numbers in the figure represent ID numbers from the database and the darker lines indicate associations that are more probable.

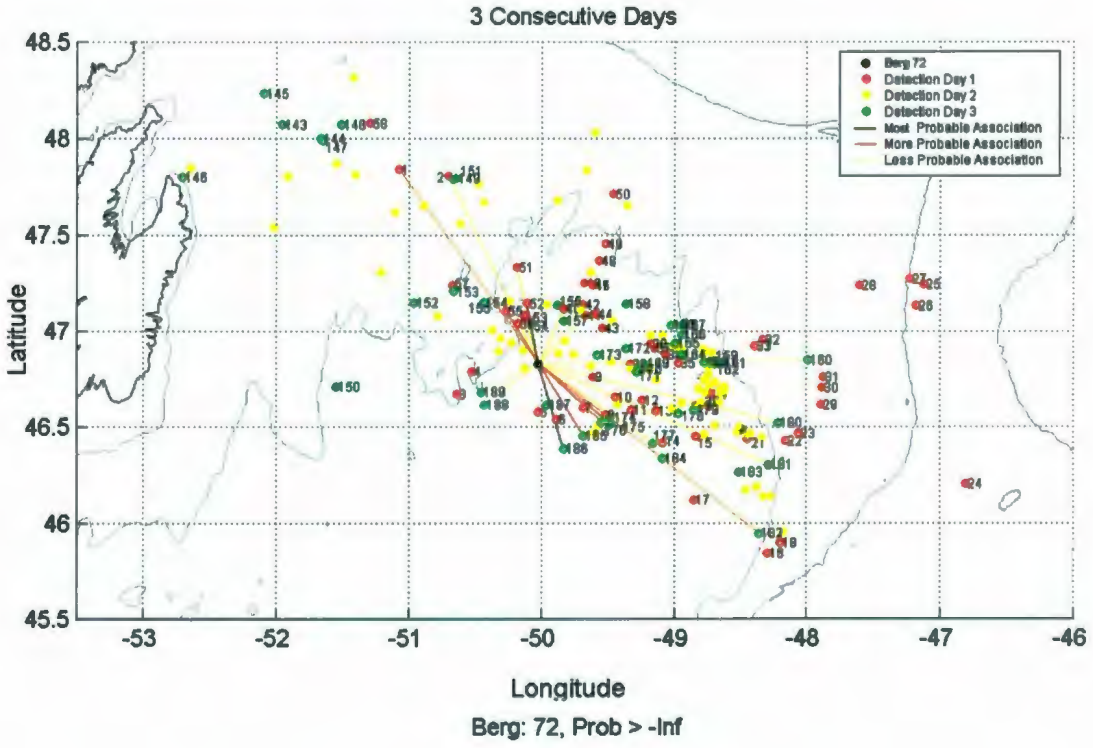

Figure 4.13: MHT Association, Single Iceberg

4.3.1 Supporting Analysis

Two sets of data were analyzed to generate the statistics used. The first were iceberg tracks from the IIP collected from 1960 to 2000 and covering a wide-area north east and south of Newfoundland (PERD, 2001). This dataset contained over 55,000 usable track fragments. The second dataset consisted of the tracks from the PAL Ice Data Network System (IDNS) database from the 2000 ice season (PAL, 2000). The IDNS is a geographic information system (GIS) based database system for monitoring discrete detections, mostly from aerial reconnaissance flights, for the hydrocarbon recovery companies operating on the Grand Banks of Newfoundland. The 2000 set contained tracks close to the Hibernia location and contained 627 usable track fragments. The IIP data set has a median of 62 hours between observations while the PAL data set has a much better median of 2 hours between observations, making its tracks much more representative of actual iceberg motion.

To make the previously described MHT system possible, drift data were analyzed to quantize the motion statistics of icebergs in the region of interest. Various regions have different currents and bathymetry. Hence, the area in which the iceberg was located can influence its motion and consequently the statistics were broken up into a grid measuring 0.5° latitude by 0.5° longitude. Two sets were generated, one set of statistics determine the average speed and direction of the icebergs from the data set in the 0.25° square, and the second determine the rate of change of speed and direction of

the iceberg by 0.25° square. The data set for this quantification of iceberg kinematics was further broken into icebergs that had an initial heading of north, east, south, or west in their 0.25° square.

4.3.1.1 Historical Drift Speed and Heading Statistics

For the historical drift speed and heading statistics, the IIP dataset tracks were broken down by 0.25° latitude and longitude squares, the drift speed and heading of the icebergs were calculated, and statistical models were generated from the accumulated data. An example of the modeled data is presented in Figure 4.14. The direction of the arrows of this diagram represent the average heading, while the size of the arrows represents the relative averaged speed.

Shown in Figure 4.15 and Figure 4.16 are examples of the modeled data for 0.25° square with the mean and standard deviation of the heading and the speed.

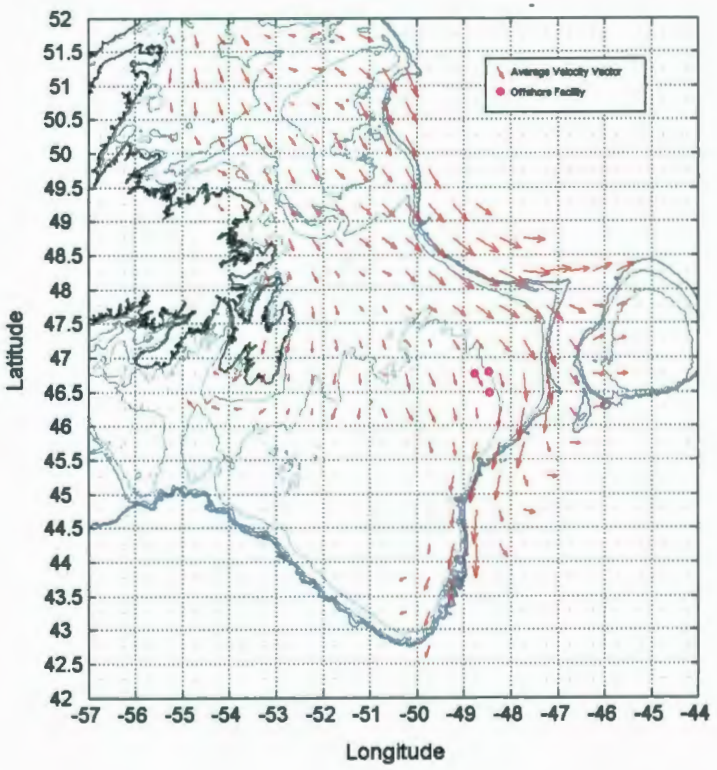

Figure 4.14: Average Heading and Speed Vector Plot

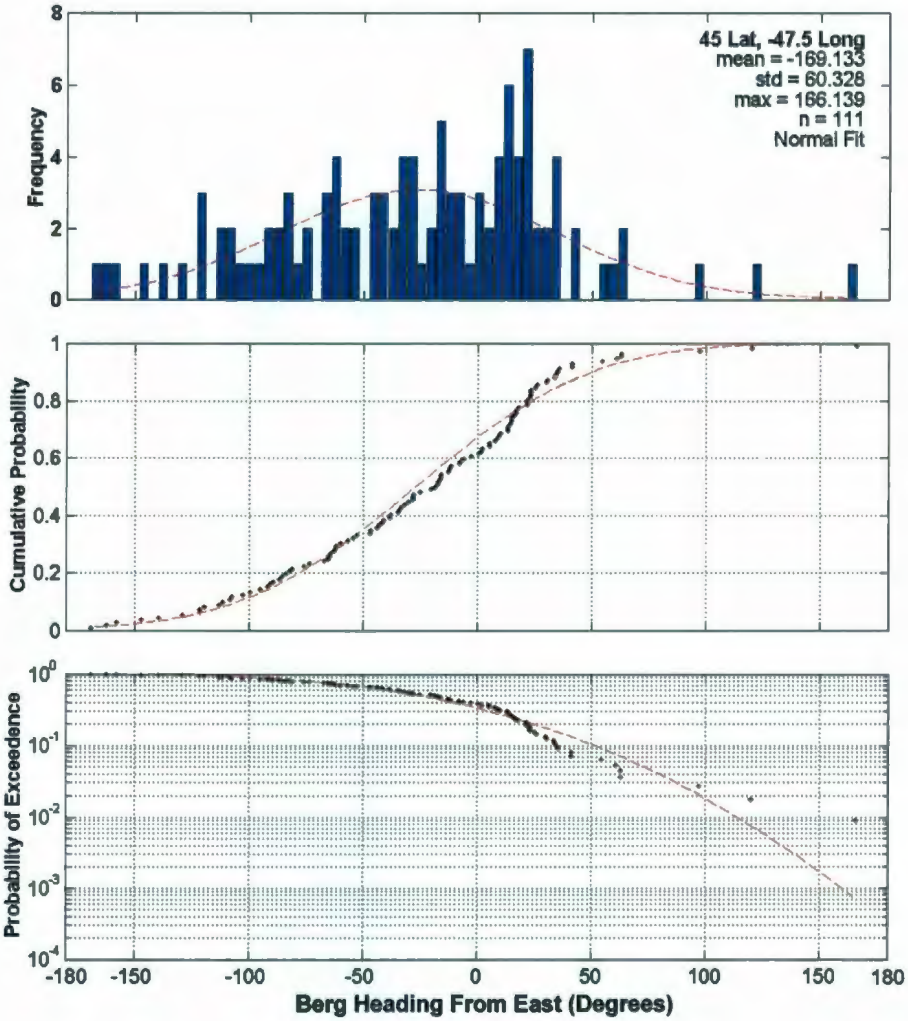

Figure 4.15: Average Heading Distribution

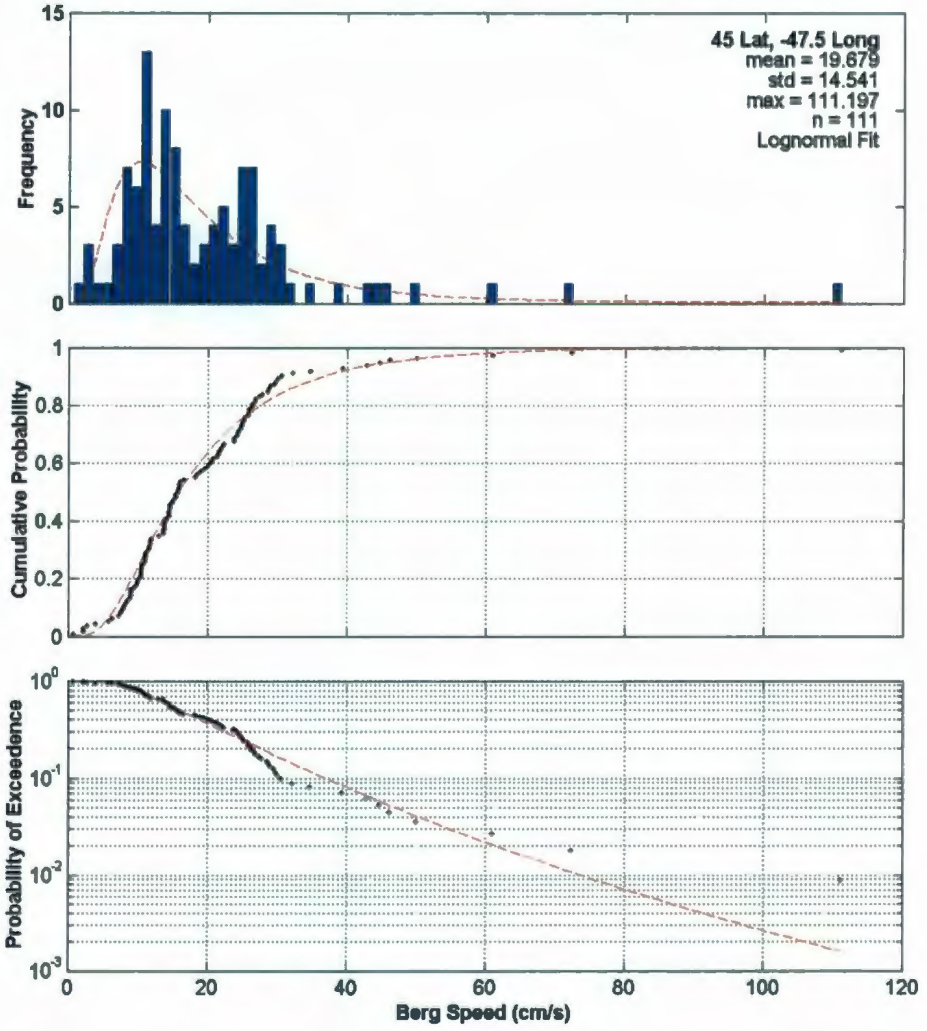

Figure 4.16: Average Speed Distribution

4.3.1.2 Historical Turning and Acceleration Statistics

Also using the IIP data set, the rate of change of the heading and speed data was analyzed. Given three points in an iceberg track, statistics for acceleration and rate of change of heading can be accumulated. That is, by examining the speed from the first to second sighting and from the second to third sighting, a set of data representing the average change of speed was found. As well, by measuring the change in direction from the first to second, and second to third points a set of data representing the average turning rate for an iceberg can be determined. These are normalized by day, and broken down into an additional four groups, one for each 0.25° square with initial north, east, west, and south headings.

Examples of these from the statistics accumulated are shown in Figure 4.17 and Figure 4.18 (note that $6 \cdot 10^{-6}$ m/s^2 equal 1 knot/day change in speed). These are the most important statistics for the MHT associations.

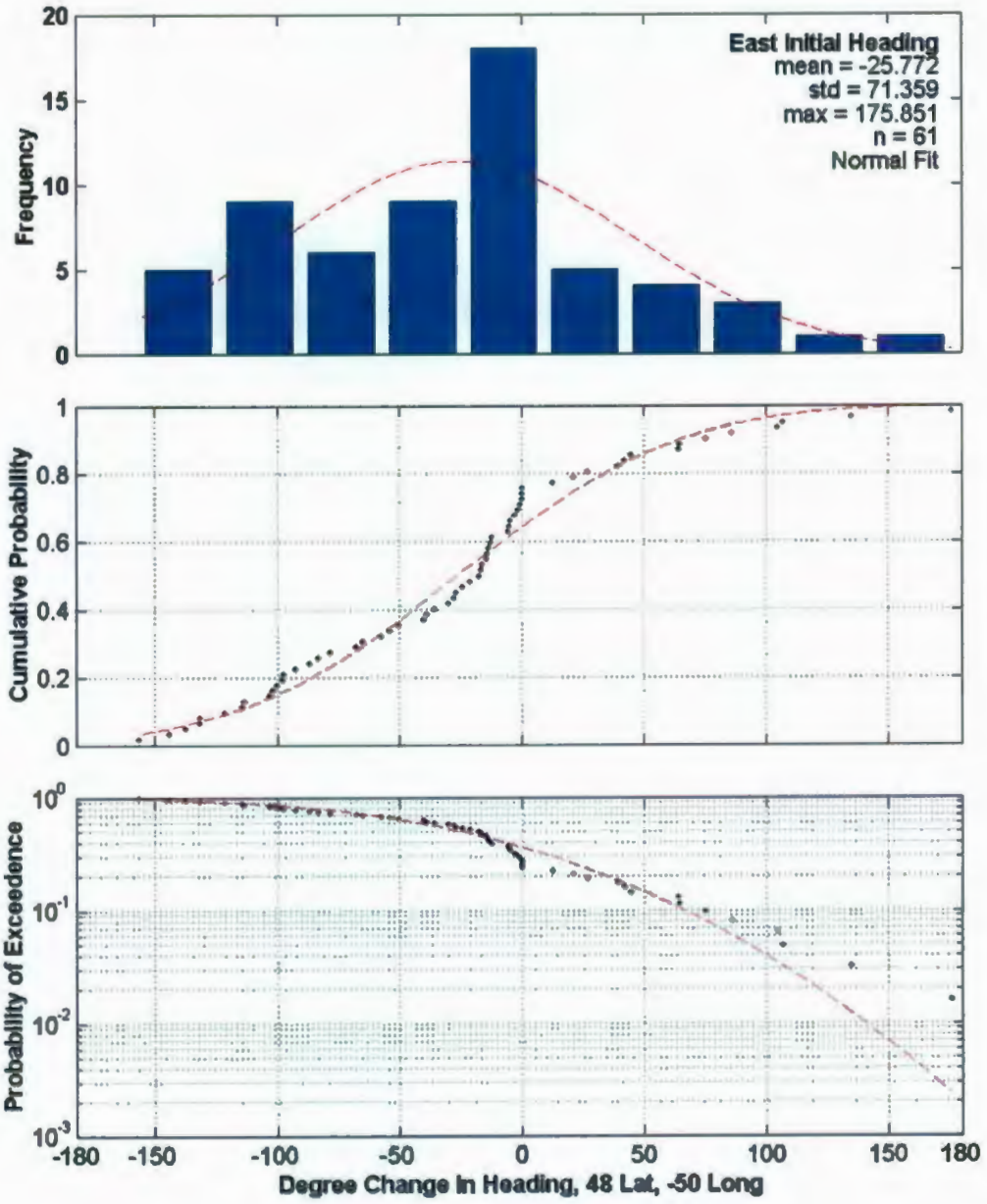

Figure 4.17: Average Change of Heading Distribution

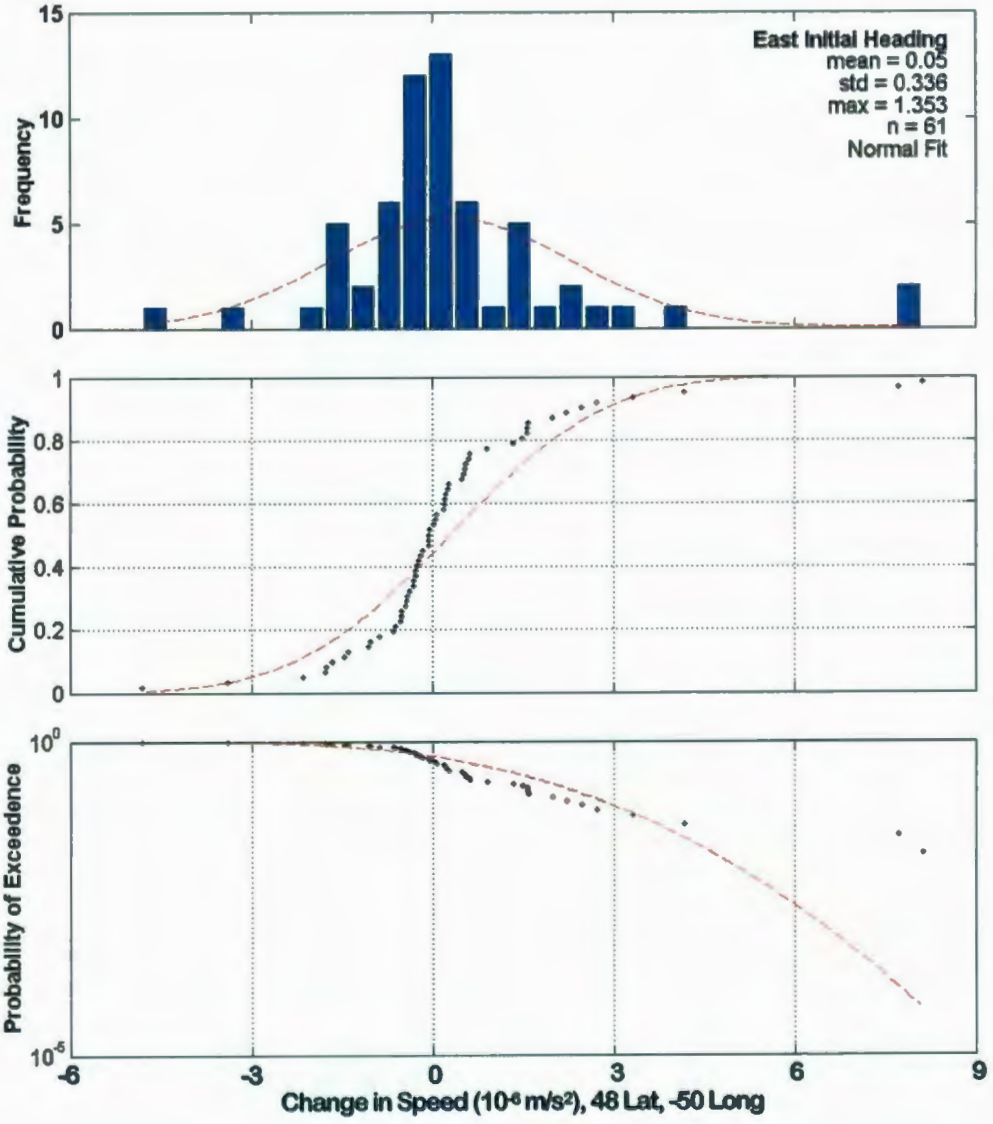

Figure 4.18: Average Change of Speed Distribution

4.3.1.3 Wave and Surface Current Direction vs. Heading Direction

Another supporting data set consists of iceberg heading and speed vs. wave and surface current heading. These conditional probabilities can be determined and used in the MHT association procedure. Given the environment conditions over the period between detections, a statistic is generated that represents the influence of the wave and surface current force on the icebergs motion. This affects the probability distributions of rate of turn and change in speed and subsequently the probability that any one iceberg is associated with any other two. This provides increased accuracy of results, since it incorporates real-time environmental information.

The analysis of these forces on iceberg motion was done using the PAL data set from 2000. This set was used due to its high temporal resolution. The environmental data was collected by the Microwave Radar Observing System (MIROS) onboard the Hibernia facility. The MIROS (2008) is a coherent radar that extracts Doppler information from the ocean surface producing directional wave spectra and surface current measurements.

An example of the heading correlation from a combination of the wave and surface current direction and iceberg direction is shown in Figure 4.19. This graph compares iceberg heading to the summation of wind or wave forces over the period between iceberg sightings. For a good correlation, the points should be in a straight line.

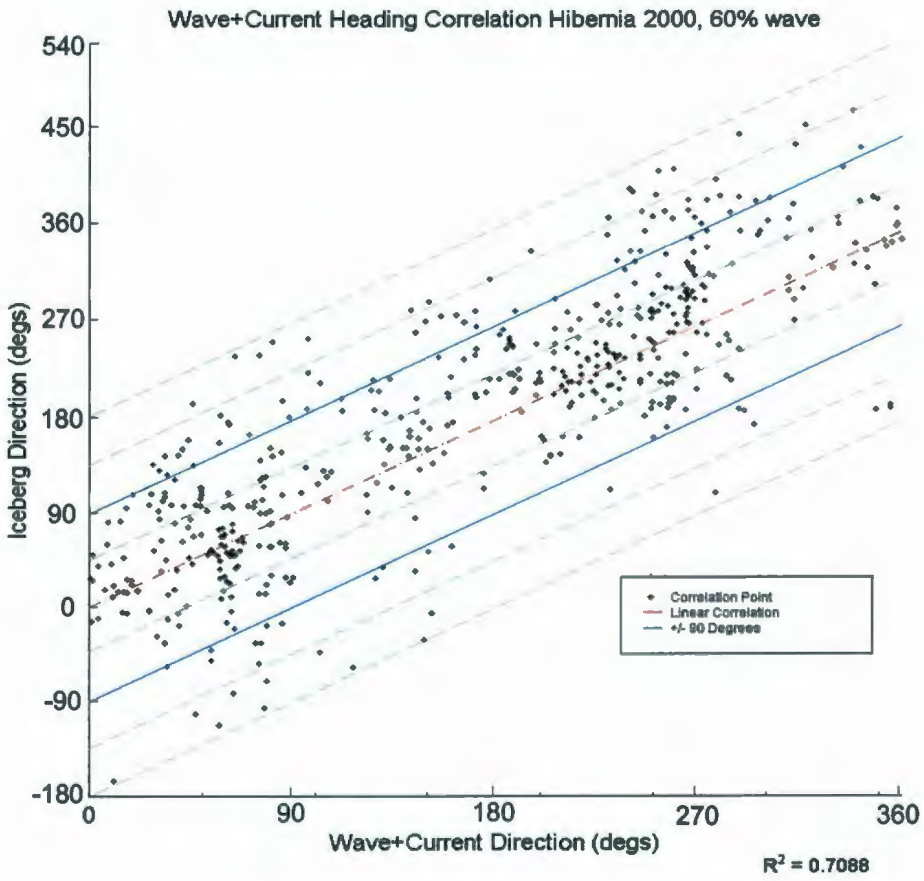

Figure 4.19: Wave and Surface Current Direction vs. Iceberg Direction

Also examined during this analysis was the influence of wind data collected at Hibernia and the correlation between significant wave height, wind speed, and surface current speed on iceberg speed. No correlation could be established in this analysis.

4.3.2 Statistical Maneuvering Application

A simulation was performed of the MHT system to test the ability to accurately associate iceberg detections to one another from sensor scans. In particular, scans that have significant periods between successive iterations, such as aerial reconnaissance flights, are of interest.

The accuracy of a set of iceberg tracks is determined by the frequency with which the iceberg location is updated. That is, if the iceberg location is updated every two hours, the recorded track is considered to be of a high accuracy. Otherwise, if the iceberg location is updated infrequently, say once every week, the iceberg's actual path is not a certainty. Hence, two sets of data were used to determine the ability of the tracker to accurately make iceberg detection associations, a sparse set that is input into the tracker, and a highly accurate set that represents the actual iceberg motion. With the highly accurate set, sparse sets with any degree of delay between detections can be generated through resampling.

A set of iceberg tracks that meets the criteria described above, is the track output from PAL's IDNS from 2000. The 2000 data set contains accurate tracks for targets near the Hibernia, Terra Nova, and White Rose locations (Figure 1.1). These tracks can be compared to the general direction of the associations being made in the wider area to determine the effectiveness of the MHT associations. As well, the data points in the

PAL IDNS (the position information from the individual tracks) can be used as inputs to the MHT and the results used to tune the system operation.

The PAL IDNS database from the 2000 ice season (PAL, 2000) provided a data set of closely monitored icebergs. From this database, a set of three days was selected such that the maximum number of iceberg targets were present. From the three days, detection sets were generated such that the iceberg detections had various mean times between detections. For testing purposes, sets consisting of three sensor scans, with mean times of 24 hours and 6 hours between detections, were used.

The system was unaware of which detections belonged to what iceberg. Ideally, the MHT system would associate detections that came from the same iceberg with each other. Intuitively chosen combinations of the statistics were used to determine the best association. Factors that affected the ability of the MHT system to perform correct associations include the amount of time between detections, the amount of cross over of the tracks, and the effect of some environmental forces that have not been accounted for, such as tidal effects, deep water current variations, and underwater iceberg profile anomalies.

The associations made from the 6 hour scans are shown in Figure 4.20. This figure depicts the iceberg detections, labeled in order of entry into the MHT program. The actual tracks can be seen in Figure 4.21. The two asterisks represent the Hibernia and

Terra Nova locations; the line represents the 100-m bathometric mark. The ranking for the correct hypotheses can be seen in Table 4.1

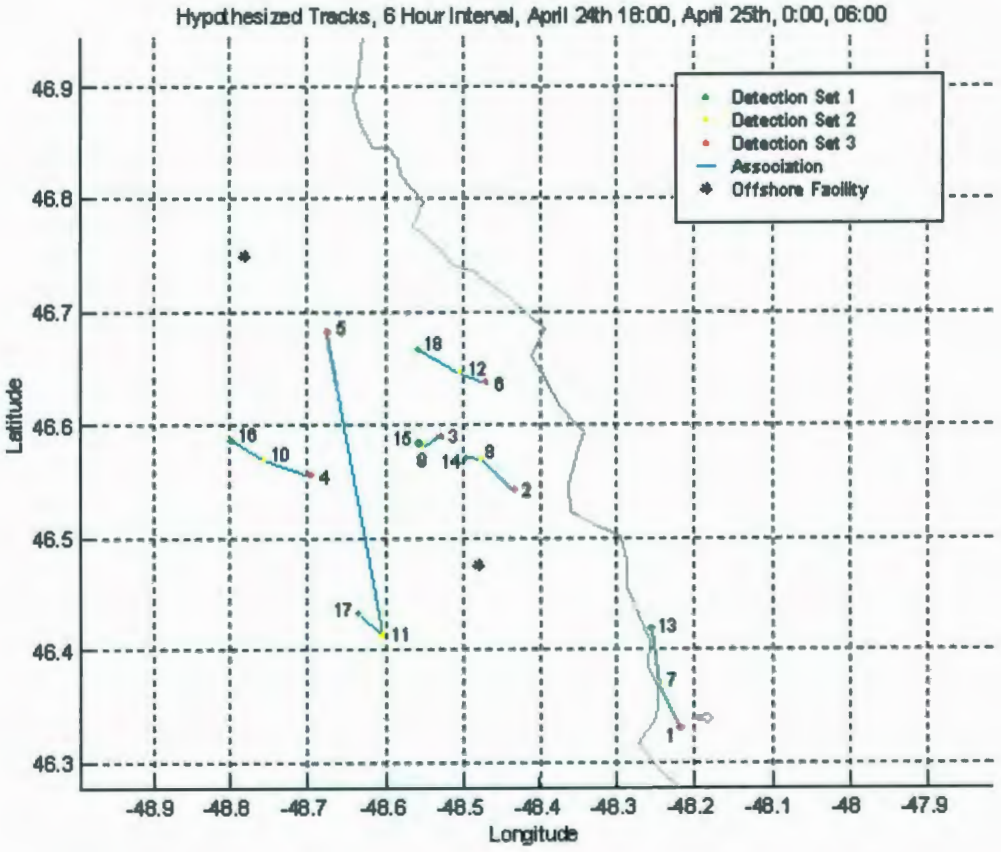

Figure 4.20: MHT Output, 6-Hour Intervals

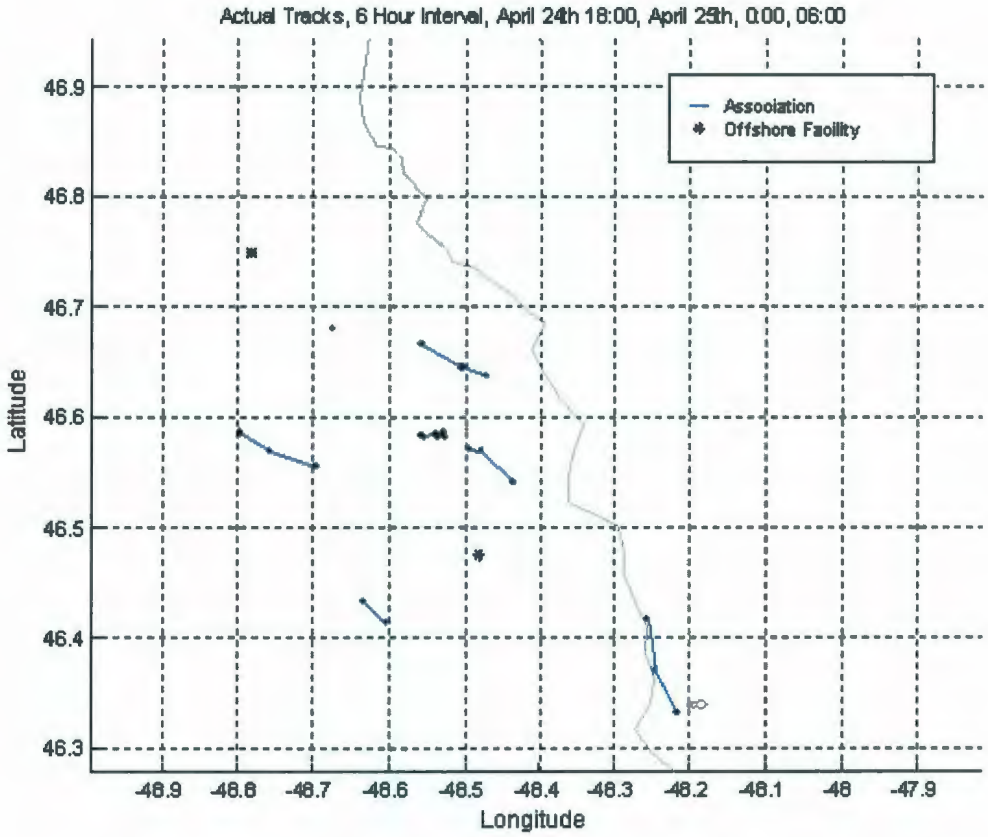

Figure 4.21: Actual Tracks, 6-Hour Intervals

Table 4.1: Hypotheses Rank List for 6-Hour Interval	
Correct Track Association	**Hypothesis Rank in Track List**
13 – 7 – 1	1
14 – 8 – 2	1
15 – 9 – 3	1
16 – 10 – 4	1
18 – 12 – 6	1

The associations in Figure 4.20 were correct for nearly all tracks involving three iceberg detections. The data set also contained partial tracks from icebergs that were not present in all three scans. Since every possible association was included, no matter how unlikely, the MHT algorithm generated a track that included the leftover partial tracks of different icebergs. The combined partial tracks are clearly visible as erratic, improbable tracks (e.g.. track 5-11-17), the correct partial two-point track can be seen in Figure 4.21

The associations made from the 24-hour scans can be seen in Figure 4.22. The results of this association are poorer than for the 6-hour. The actual tracks can be seen in Figure 4.23. While some associations are correct, the most likely hypothesis shown is not the completely correct set of associations. In this case, one of the possible eight tracks is correctly associated. To determine how the system would perform when functioning in an operational setting, the MHT system was setup to perform only the association of the last pair of the three detections for each track. This simulates an operational use of the system where a previous track is established with at least two detections and the next step is to link new detections to the established tracks. In this test of the system, three of the eight tracks were correctly associated. The results of the associations can be seen in Figure 4.24. Table 4.2 shows how far down the correct associations lay in the complete list of hypotheses for the unfixed cased.

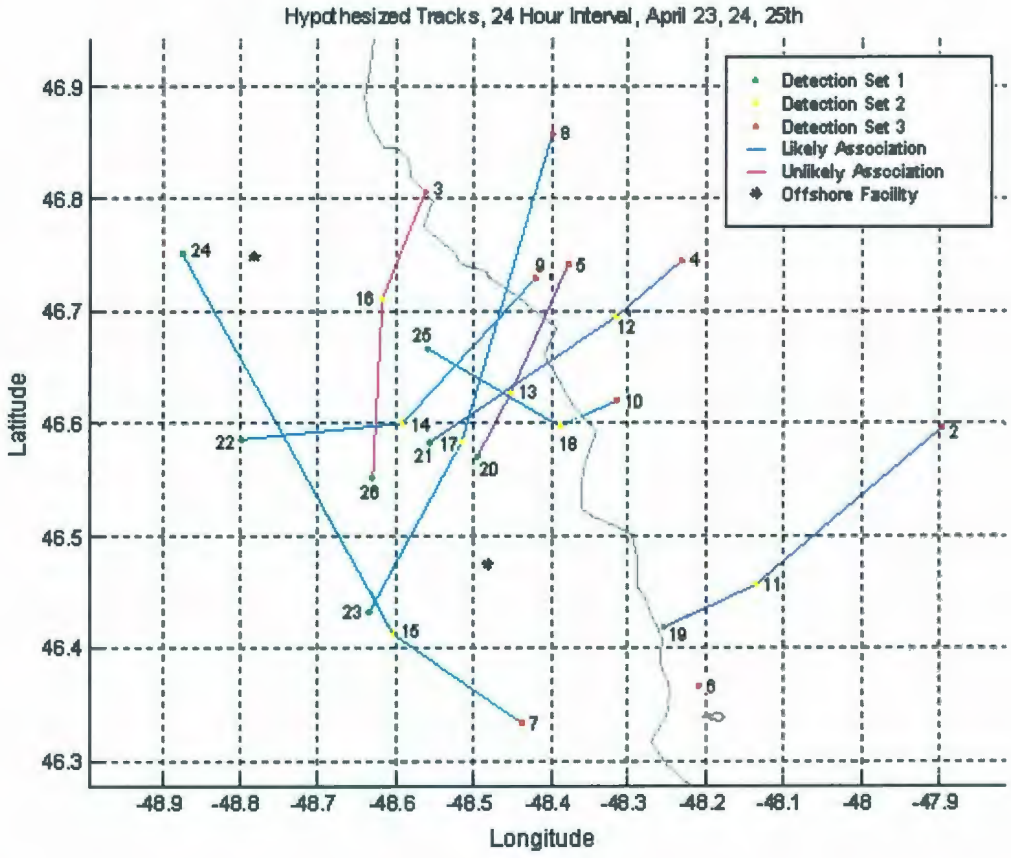

Figure 4.22: MHT Output 24-Hour Intervals

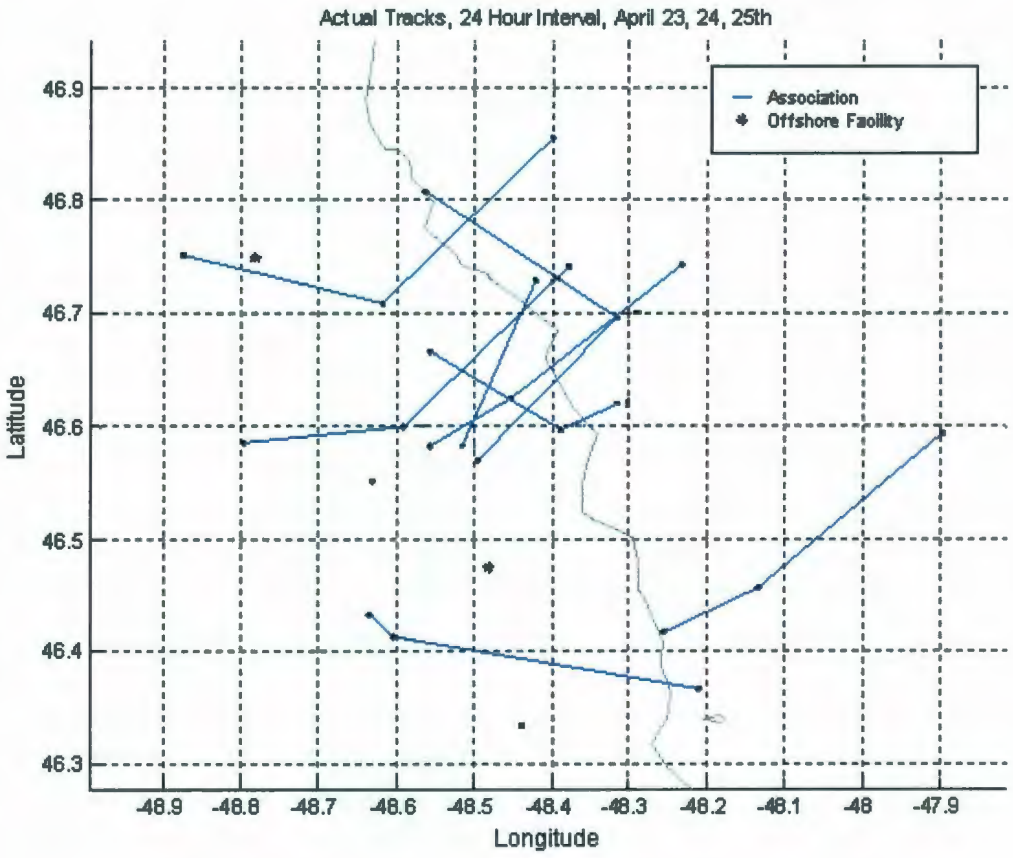

Figure 4.23: Actual Tracks, 24-Hour Intervals

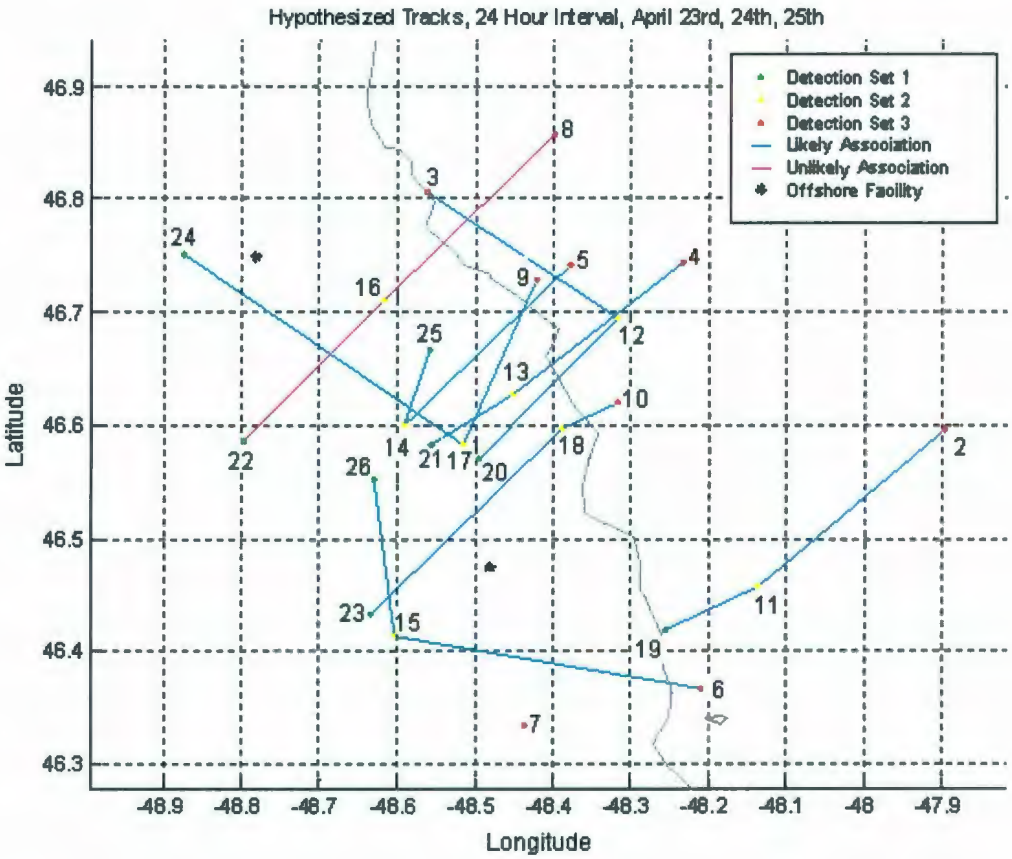

Figure 4.24: Actual Tracks, 24-Hour Intervals, First Association

Fixed

Table 4.2: Hypotheses Rank List for Unfixed 24-Hour Interval	
Correct Track Association	**Hypothesis Rank in Track List**
24 – 16 – 8	20
22 – 14 – 5	26
21 – 13 – 4	13
20 – 12 - 3	22
25 – 18 – 10	26
23 – 15 – 6	56
19 – 11 - 2	1

The reasons for the less accurate result when the two 24-hour tests are compared to the 6-hour test lies in the greater time-period between detections and the overlapping of tracks. The greater time-period results in a greater opportunity for icebergs to turn and change velocity. As well, they may be subjected to greater influence from unaccounted phenomenon (tidal effects, intermediate and deeper currents). Consequently, this poor association indicates the requirement for more complete and accurate data to be input into the MHT if it is to provide greater accuracy over the longer time period.

4.3.3 Assessment of Results

This multiple hypothesis tracking system defines an association probability between ice detections based on iceberg kinematics, namely angular and translational acceleration. Such an association system should be useful in either a tactical or a strategic planning environment.

The associations are made with sets of three detections to allow for the calculation of turning and acceleration statistics when provided only target position data. Due to this, there is a propensity to make associations to available 'other' icebergs when the actual iceberg may not have been detected or been outside the coverage of the sensor.

This association method worked well for the average iceberg movement over short periods, but does not sufficiently take into account the wide variations that environmental conditions can cause. Research on this method was stopped in favour of substituting the Canadian Ice Services (CIS) iceberg drift model in place of the maneuvering model based on historical statistics. This system is described in Section 4.4.

4.4 MHT Using Iceberg Drift Modeling

As an alternative to the statistical maneuvering model examined in Section 4.3, an additional model is examined. During the period of research for this thesis, this new iceberg drift prediction model, the Coupled Ice-Ocean (CIO) iceberg drift model, became available operationally from the CIS. The CIO model uses real-time environmental data and iceberg size to provide movement predictions. It is a logical step to use this as the basis an iceberg maneuvering model, since the CIO model sums forces on an iceberg in a similar way as was done for maneuvering based on historical statistics, that is, to sum historical forces (wind, wave, ocean currents, and surface currents) to determine future positions. The increased accuracy of the prediction drift model reduces the computational overhead requirement by decreasing the number of possible associations between previous detections and new targets.

4.4.1 Canadian Ice Services Drift Model

The CIS have been developing and improving the CIO model to determine sea-ice drift for use in producing ice charts. The inclusion of a physical model for iceberg drift has enabled operational iceberg forecasting with reasonable accuracy. The CIO iceberg drift model uses estimates of underwater iceberg profiles, scaled on waterline length, to generate a predicted path determined by the environmental forces. This is not the first attempt at creating such a model; however, it appears that recent advances in

environmental sensing and computation ability have translated into a model more accurate than previously available.

The model's inputs are: position, in latitude and longitude, time, and iceberg waterline length. The model outputs a set of latitudes, longitudes, and times for that iceberg. The model at this time does not account for shape parameters, and uses a generic underwater profile based solely on waterline length.

The model has been shown to have reasonable positional forecasting error in most cases and is an improvement over previous models (Carrieres et al., 2001, C-CORE, 2003a, and C-CORE, 2003b). This is significant since the accuracy of this model determines the gating size used in association and confidence calculations.

To illustrate the process through which information is added into the MHT, three iceberg aerial reconnaissance flights are examined. One detection from the first is chosen and the subsequent associations with that detection are illustrated. The three aerial flights are from April 17, 19, and 21, 2003.

Figure 4.25 shows a prediction for the iceberg designated HG03-017. This iceberg was a large tabular with a measured waterline length of 333 m. The prediction depicted is for 35 hours after the initial detection on April 15, at 01:20. The effect of size on drift prediction can be quite dramatic as is shown in Figure 4.26, which illustrates predictions for iceberg HG03-017 given different waterline lengths.

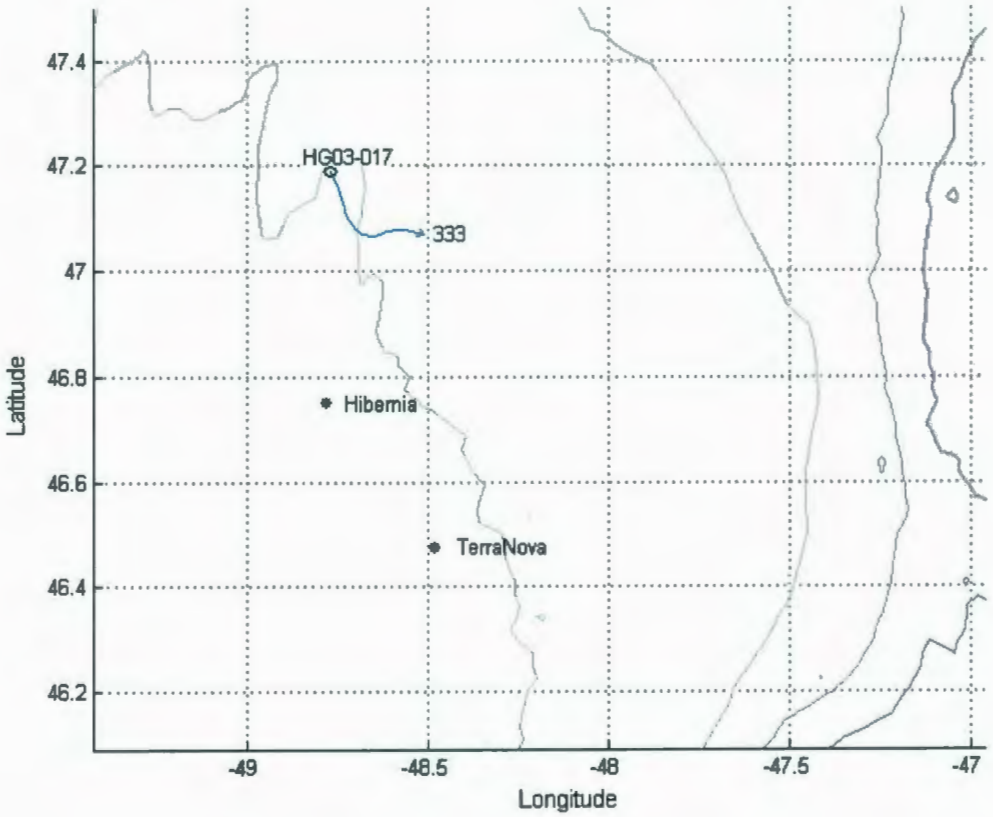

Figure 4.25: Iceberg Prediction HG03-017, 35 Hours, 333-meter Waterline Length.

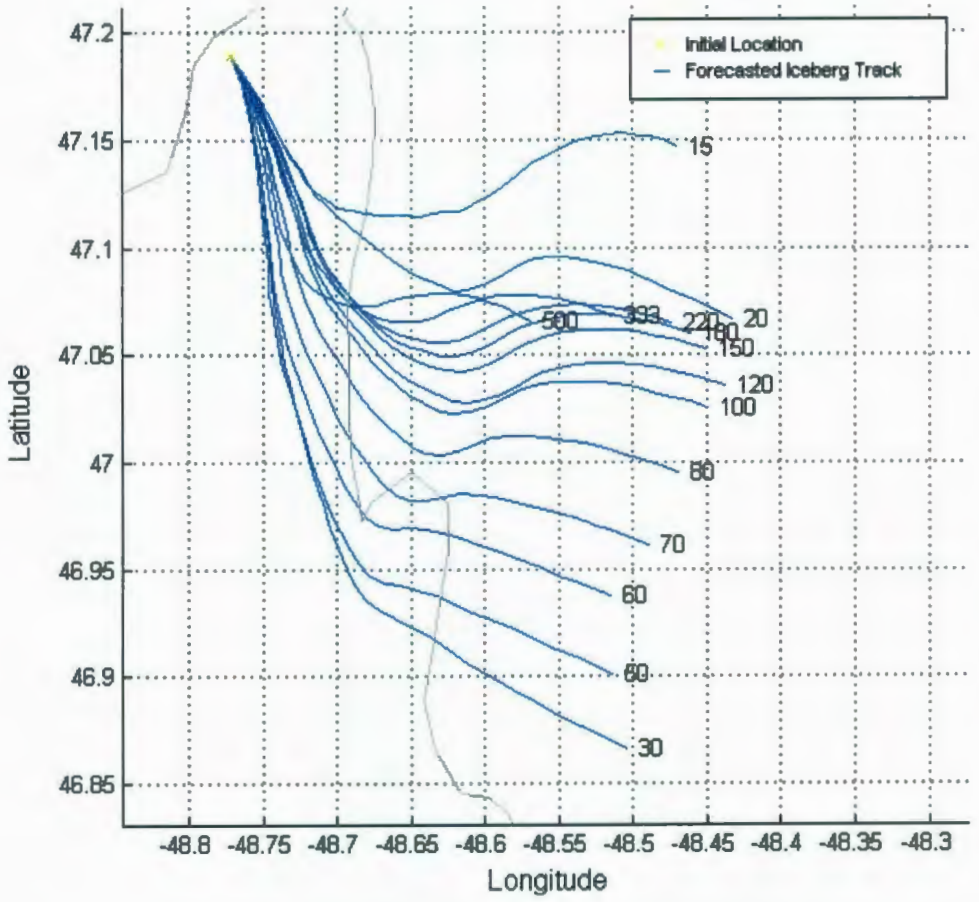

Figure 4.26: Iceberg Prediction Variation by Size in Meters

This sensitivity indicates a key parameter. The waterline length is extrapolated in the water column to form the third dimension of the iceberg. The interaction of the iceberg with various layers of the water column determines its drift.

4.4.2 Size Interpolation

From the initial analysis of the system, it was determined that the system can be used to help determine the size of an iceberg when no iceberg size data is available or where size information might have been misreported. By forecasting several icebergs from the same iceberg detection position, but with varying waterline lengths, a distribution of iceberg motion can be observed. The appropriate size is determined by finding which of these forecasts are substantiated by further iceberg detections. A size estimate could be determined by the relationship between the forecasts and the detected iceberg position, such as by interpolation between two forecasted paths.

From empirical examination, the distribution of movement appears somewhat logarithmically related to iceberg waterline length. Thus, three sizes were chosen for forecasting, 20, 100, and 300-meter lengths, to represent the range of iceberg drift for most circumstances.

4.4.3 Drifter Model Example

The following is an example of a tracking system using the CIO output as a maneuvering model and implemented in MATLAB®. As described in Section 4.2, the system must be capable of receiving data on position, heading, speed, and size of icebergs from many sensors, at irregular times, and from over a very large area. From these data, it must extrapolate a best estimate of the actual positions, heading, speed,

and size of icebergs at any point in time. It also must account for errors in the measurement systems and for the reliability of the data.

The system begins its analysis with some set of sensor data. Subsequently, new data are added and the relationships between the new data and those in the system are assessed.

For all data sets after the first, the data being added are associated with data already in the fusion database. The data in this case are those iceberg parameters that are available to be recorded. These will usually consist of latitude and longitude of detection, size and shape characteristics if available, the type of sensor from which the detection occurred. Given the type of sensor, the environmental conditions and the range from the target to the sensor, a probability of detection and a probability of false alarms can be determined. These parameters determine the sensor's ability to ensure confidence in the target.

Once new data become available, iceberg positions are predicted to the point in time that the new detections occurred. A gating area around the prediction point is determined. This area is proportional to the amount of error in the prediction model's accuracy. New detections that are within a previous detection's gate area are associated with that previous detection. The relative confidence in the new detection will affect the confidence in the previous associated target based on the track score calculations. The coverage area of the sensor is also taken into account. Should there have been no

association, the relative portion of the gating area that has been searched is used to diminish the confidence of the previous detection to which the gating area belonged.

Once associations have been made and confidence levels adjusted, the confidence levels or 'scores' are examined and prediction paths with low confidence are eliminated. Thus, new data are combined with old while taking into account the parameters of the sensors. The major benefit to such a methodology is the ability to use low confidence data from sensors whose parameters are less than optimal. The steps outlined in Section 4.2.2 are described in more detail below.

4.4.3.1 Gating

The gating area is a geographical area within which the predicted target should lie with a high degree of certainty. One method of calculating this is to take the estimated variance of the error of the model and use three standard deviations of this to produce a region that should contain the target in most cases. The variance is additive so that as the time from the last known position increases, the gating area increases as well. The shape of the gating area can vary; an ellipse is used in this implementation. The error in speed and rate of turn are estimated to form the major and semi-major axes of the ellipse. The large rate of turn that can be experienced by icebergs causes the quantification of the gating area to be difficult. One must choose whether the gating area should follow the prediction path, or the imaginary line from the predicted position to the last known position.

Figure 4.27 shows an example of a gating area computed using the detected position and the predicted position as an axis for the error ellipse. In the figure, the line leading away from the April 17, 2003 label indicates the detected position of the iceberg and the forecasted path. The circle on the line, next to the April 22, 2003 label, indicates the forecasted position on April 22, 2003. The ellipse centered on the small circle indicates the gating area. The orientation of the ellipse is with respect to the original position, as opposed to being orientated with the predicted direction of the iceberg's travel. The use of an ellipse orientated towards the original detection location is the current method for the implementation; it was chosen based on examination of actual and predicted paths, which indicate a larger error in the estimated speed of the iceberg than in its direction from the detection point.

4.4.3.2 Association and Coverage

Essential to the operation of the MHT is the association of new iceberg detections to previous detections that may be the same iceberg, detected at an earlier time. These associations are essential to account for all previously detected icebergs. The presence of icebergs that cannot be accounted for in the association process with previously detected icebergs can be an indication of potential 'gaps' in sensor geographical coverage. This can provide a means to decide if additional reconnaissance might be necessary to fill in the missing data.

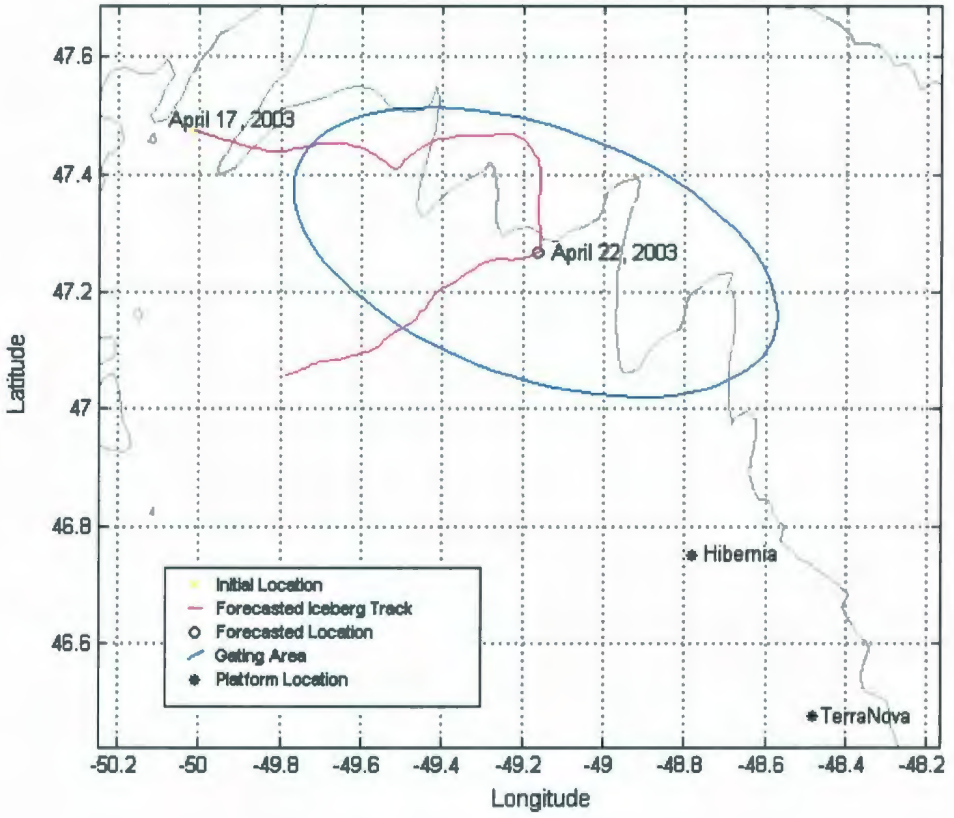

Figure 4.27: Gating Area/Error Estimation, 5 Days.

The gate area is used to determine which of the new iceberg detections can be associated to previously stored detections. For each previous detection, the gate area is determined through the maneuvering model at the time of the new detection. For that gate area, each new detection is examined to determine if it falls within the gate. Figure 4.28 shows several targets near the predicted location of a previous target. Two targets fall within the gating area, and solid green lines connect them to the predicted location. Additional targets are shown outside the gating area, but are not associated with the

previously detected iceberg. These targets are depicted as triangles and 'x's. The triangles represent visually confirmed icebergs and the 'x's represent detected radar targets which have not been visually confirmed as icebergs.

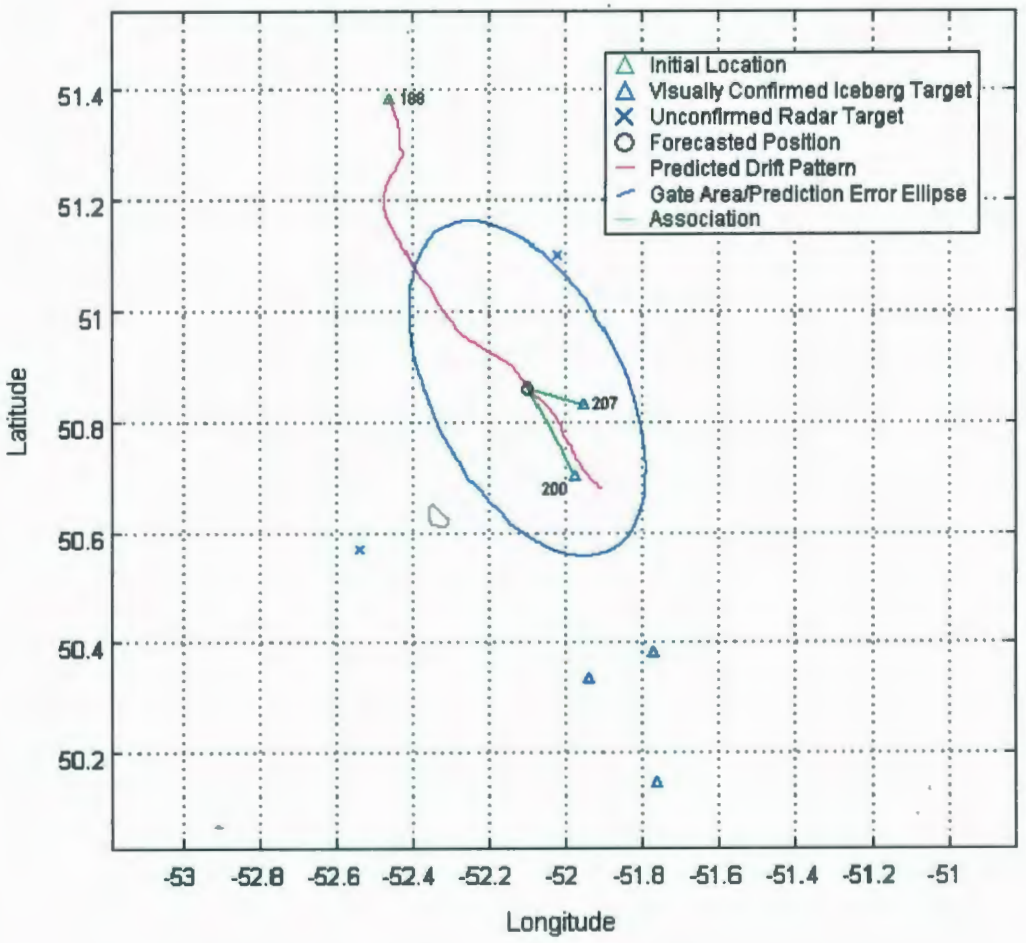

Figure 4.28: Association of Targets inside Gating Area.

Association of newly detected icebergs to previous ones is used as evidence to corroborate the previous targets, thus increasing confidence that a target exists at a

certain location. To aid in this, a confidence metric is used. Given that a detection does exist within the gate area, the confidence metric of the original detection is increased based on the parameters of the sensor and of the maneuvering model. That is, the ability of that sensor to detect targets or present false positives to the system is accounted for in the corroboration of the original detection based on the Bayes discussion in Section 4.2.3.

In addition to this, the adjustment of the confidence metric could include the error in prediction location, such as by being defined by the distance from the predicted position at the time of new detections in combination with the false positive (false alarm) rate of the most recently used sensor. Thus, new targets that are detected within the gating area, but far from the actual forecasted position will be less effective in increasing the confidence of the original target than new targets that are close to the predicted position. Likewise, sensors that generate many false positives will have a smaller effect on confidence than those that produce few false positives. Notably, the initial confidence score is set by the sensor used to find the original target, relative to its probability of detection of icebergs.

Should no association occur to a gate area, the area covered by the sensor is examined to determine if the gate area was included in the sensor scan. For example, Figure 4.29 shows the radar coverage and iceberg detections from an aerial reconnaissance flight. Note that this represents the radar area and not the area covered by visual observation

from the aircraft. The radar area is a function of the recorded altitude. If the gate area was included in the sensor scan and no target was observed, the confidence in the prediction is diminished.

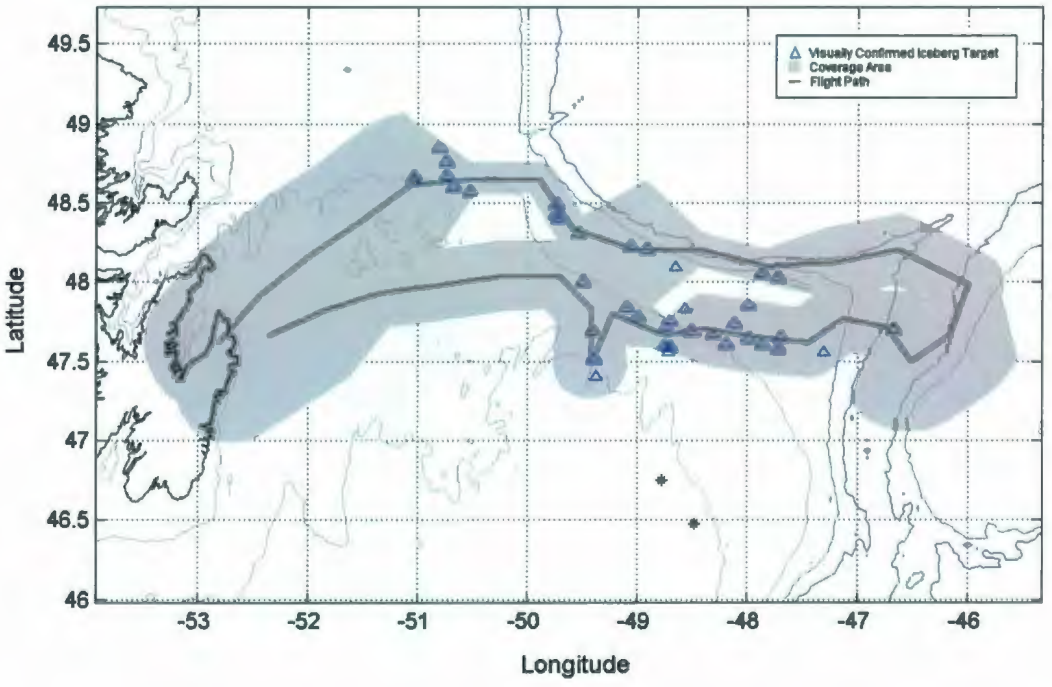

Figure 4.29: Radar Coverage from an Aerial Reconnaissance Flight.

4.4.3.3 Track Maintenance

The track maintenance function of the MHT refers to the management of the confidence, or track score, associated with each iceberg detection and the generation of a path from detection to detection through time. In particular, management of the confidence score implies the increasing and decreasing of a confidence score, the initialization of new detections with an appropriate confidence, and the de-activation of

detections whose confidence falls below a minimum. The rules for the confidence metric adjustment are based around Bayes Theorem. An example of the track score process was illustrated in Section 4.2.3. Bayes takes into account conditional probabilities. Through its use, the probability that a target exists can be adjusted by either increasing it, due to a positive result (subsequent detections), or decreasing it, due to a negative result (no further associated detections).

The initial values in this implementation are based on the sensor with which detection occurred. Currently, the probability of detection of icebergs by the given sensor is used as an initial value.

The lower limit for the confidence score is set empirically, prior to a detection being de-activated to stop further predictions and save processing resources. This is set low enough to allow false positives and other incorrect predictions to be removed easily but high enough to prevent accidental removal of predictions that should be kept.

4.4.3.4 System Output

The primary output consists of the positions of icebergs as determined from the combinations of sensor information entered into the system. False positives and other eliminated tracks can be removed leaving only the remaining 'likely' paths and associations. Utilizing the hypothetical nature of the MHT, multiple outputs can be generated. Each hypothesis displays combinations of the paths and associations from the multiple sensor data entries based on their degree of confidence.

In general, the results of the analysis of the system are available subsequent to the addition of new detection information – after every track maintenance iteration. As well, at intervals past this, the drift prediction system and gating functions defined here could be used to show areas where icebergs are likely to be located, allowing the planning of future sensor iterations.

In addition to this output, the coverage calculations can be used to define the geographical areas that require examination by sensors. The limits of this area would be defined by the sensors coverage contracted by limits of iceberg movement at the edges of the area based on the elapsed time. The limits of iceberg movement can be defined generically, or could be outputted by a query of the drift prediction model.

4.4.4 Drifter Model Maneuvering Application

The following is a sample application with the CIS maneuvering model and the MHT implementation described above. Figure 4.30 shows a forecast with the 20, 100, and 300-meter waterline length predictions; the estimated error ellipses related to the drift predictions are not shown. Iceberg with ID 87 was detected on March 3, 2003, the subsequent detection labeled 235, was detected on March 17, 2003. No detections were found near the estimates for the 20 or 300-m predictions, the only relevant detection was a single iceberg very close to the 100-m prediction. In this case, the iceberg was determined by ground truthing to have an effective size very close to 100 m in waterline length.

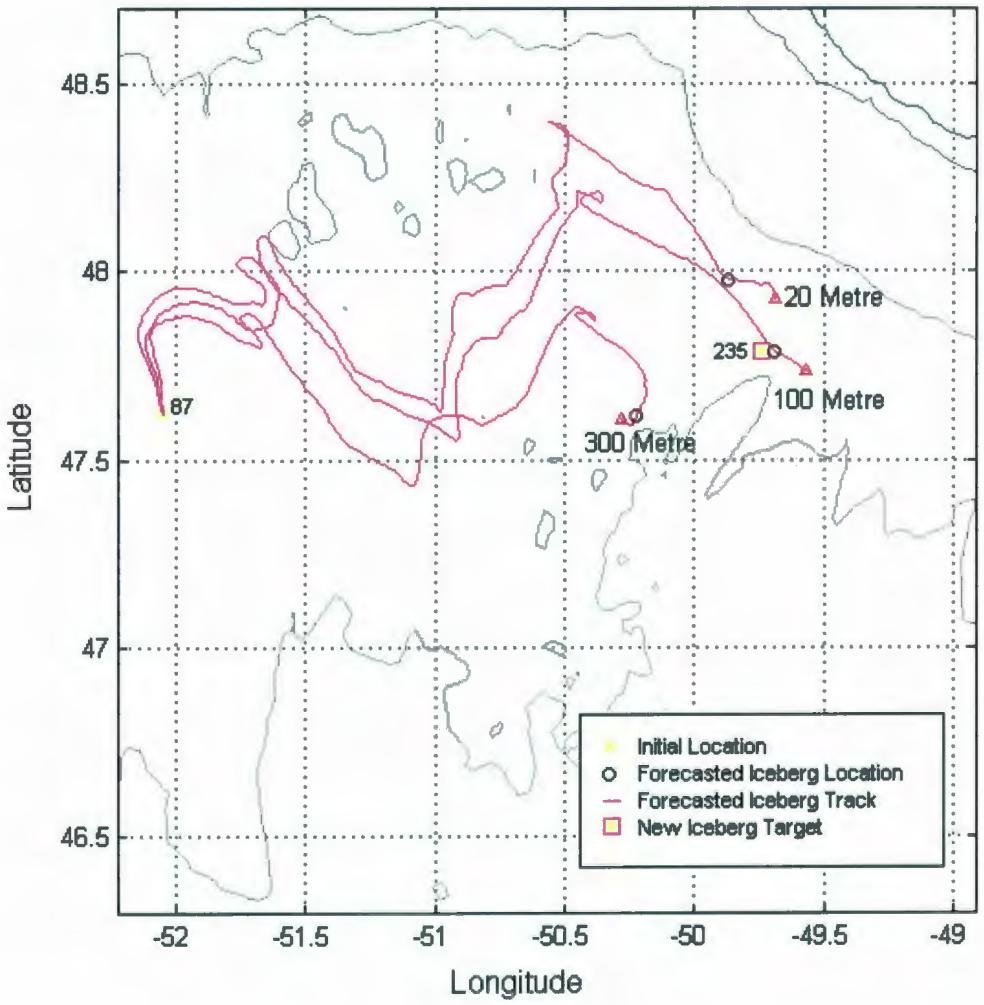

Figure 4.30: Iceberg Size Estimate.

Figure 4.31 shows the flight path of the April 17 flight, along with radar targets and visually confirmed iceberg targets. For purposes of illustration, the seventh iceberg from this set is examined more closely. This iceberg, ID 7, is shown in Figure 4.32 along with its predicted paths for 191 hours (7.9 Days).

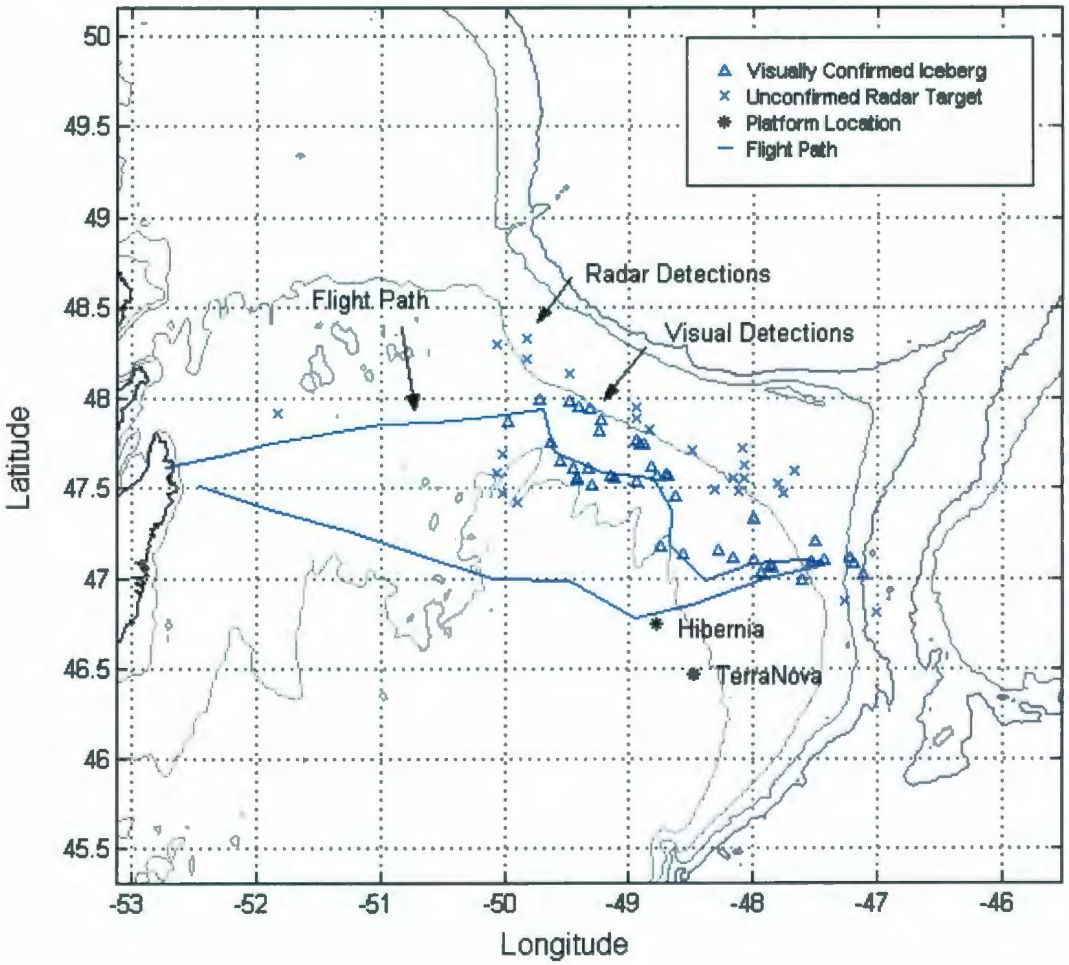

Figure 4.31: Aerial Reconnaissance Flight, April 17, 2003.

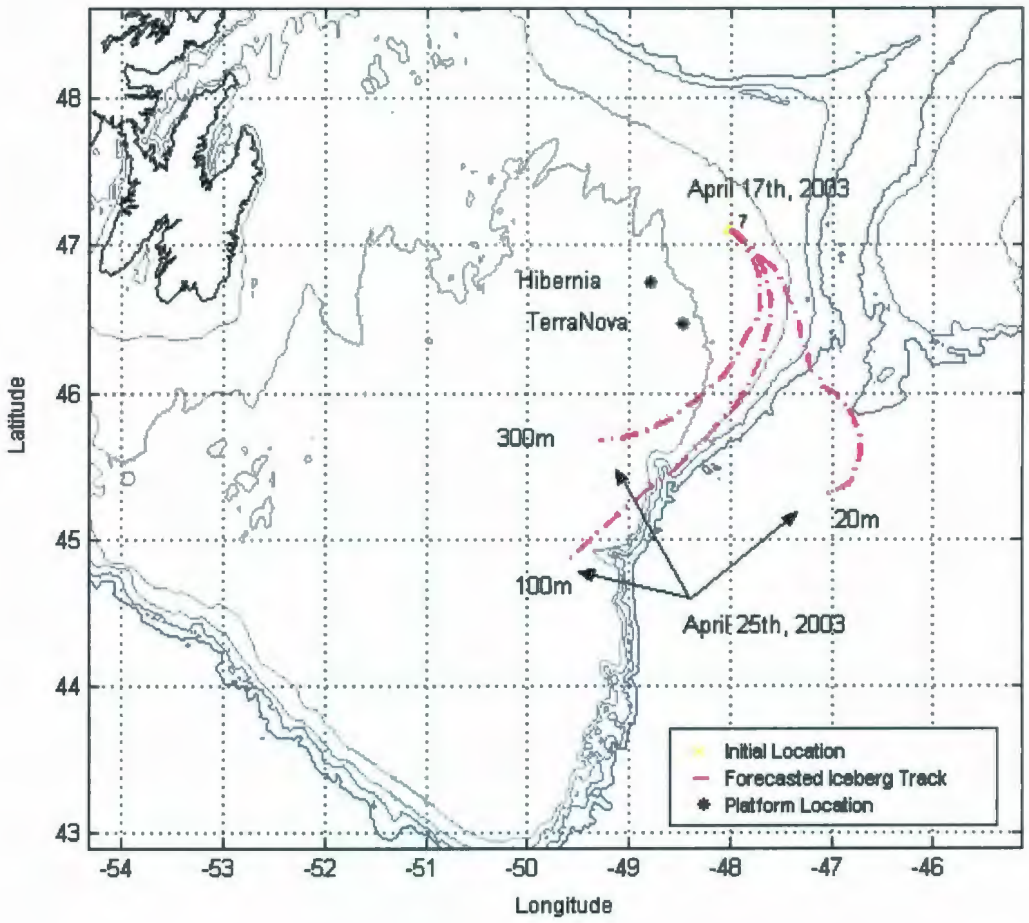

Figure 4.32: Berg #7 Predicted Paths, April 17 to April 25, 2003.

Once a second set of data is entered into the database, the appropriate predicted position from the first set is found and the gating area is determined. Figure 4.33 shows the gating areas at the time of the second detections, as well as iceberg ID 120, detected during the April 19 flight. Iceberg ID 120 is the only detection from April 19 that falls within the three gate areas for the three predicted iceberg lengths of iceberg ID 7.

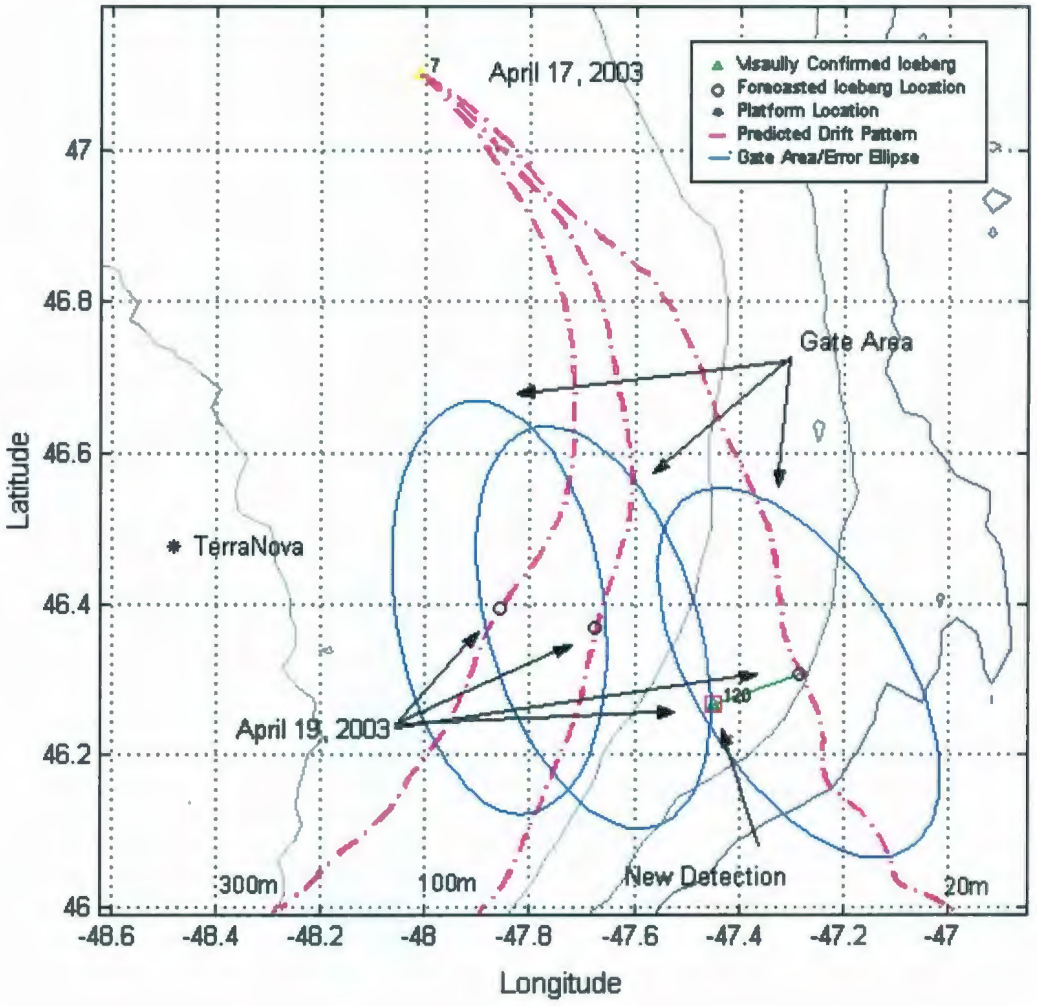

Figure 4.33: Berg #7 Gating Areas, Berg #120 Detection Position.

Circles on the dashed prediction tracks of iceberg ID 7 represent its predicted position at the time of iceberg ID 120's detection. A line connects iceberg ID 120 to the predicted position of iceberg ID 7 that represents the path of a 20-meter iceberg (the rightmost predicted path, see Figure 4.32).

The association of iceberg ID 120 to the 20-m prediction of iceberg ID 7 increases the confidence in that path. Likewise, the absence of detections with the 100 and 300-m paths decrease the confidence in those paths. The amount of the decrease is proportional to the amount of the gate area covered and the probability of detection of the sensor. If the flight's detection coverage does not contain any of the gate area, then no adjustment to the confidence of that particular path can be made.

Note that the detection of one association with the 20-m prediction of iceberg ID 7, and the lack of corroborating evidence for the 100 and 300-m paths, does not prevent the further prediction and analysis of these paths. Instead, the evidence causes an adjustment to the confidence scores; only when the confidence is reduced below a defined threshold does the prediction and analysis of a particular path stop. This allows multiple icebergs to be associated to a single iceberg and so forth. Additional routines are used to select the most probable set of associations from those available. These different hypotheses can be selected on criteria such as probability of association (proximity to forecasted position), confidence scores, or relative size indexes and shape parameters, if available.

Thus, when the information from the April 17 aerial reconnaissance is combined with the data from April 19, the April 19 set suggests iceberg ID 7 to be between 20 and 100 m, from Figure 4.33 the size can be estimated at approximately 40 m. Iceberg ID 7 was reported as having a waterline length between 15 and 60 m.

Three of the icebergs (ID 126, 140 and 141) from the April 21 aerial reconnaissance were found in the gate areas predicted for the detection times of the April 21 targets. The active gate area for this analysis now includes prediction paths from iceberg IDs 7 and 120. Although iceberg 120 was previously associated with iceberg 7, the gate areas from the paths of the two icebergs are provided so as not to rule out the possibility that 120 and 7 are not the same iceberg. Figure 4.34 shows the predicted paths from iceberg ID 120, April 19, and the associations from these to iceberg ID 126 from April 21. As can be seen from Figure 4.34 the most likely association is with the 100-m prediction from iceberg ID 120. Iceberg ID 141 is not depicted. Also present is the possible association with the 300-m prediction, though the 100-m appears far more likely. Iceberg ID 126 was reported as having an unknown size.

Figure 4.35 shows the predicted paths from iceberg ID 120 to iceberg 140, also detected on April 21. Again, the association with the 100-m path seems the most likely. Iceberg ID 140 was reported as having a size of 121–200 meters.

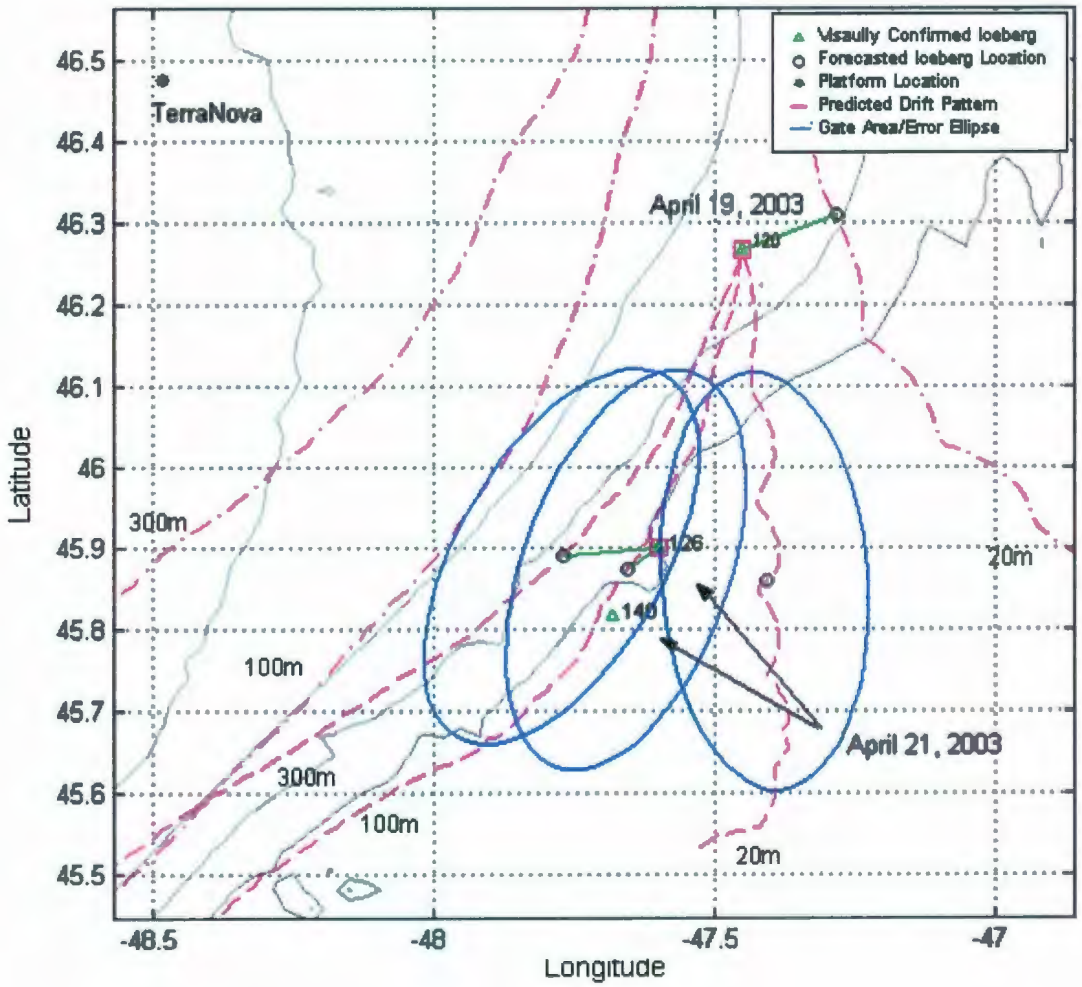

Figure 4.34: Berg #120 Gating Areas for Berg #126 Detection Position.

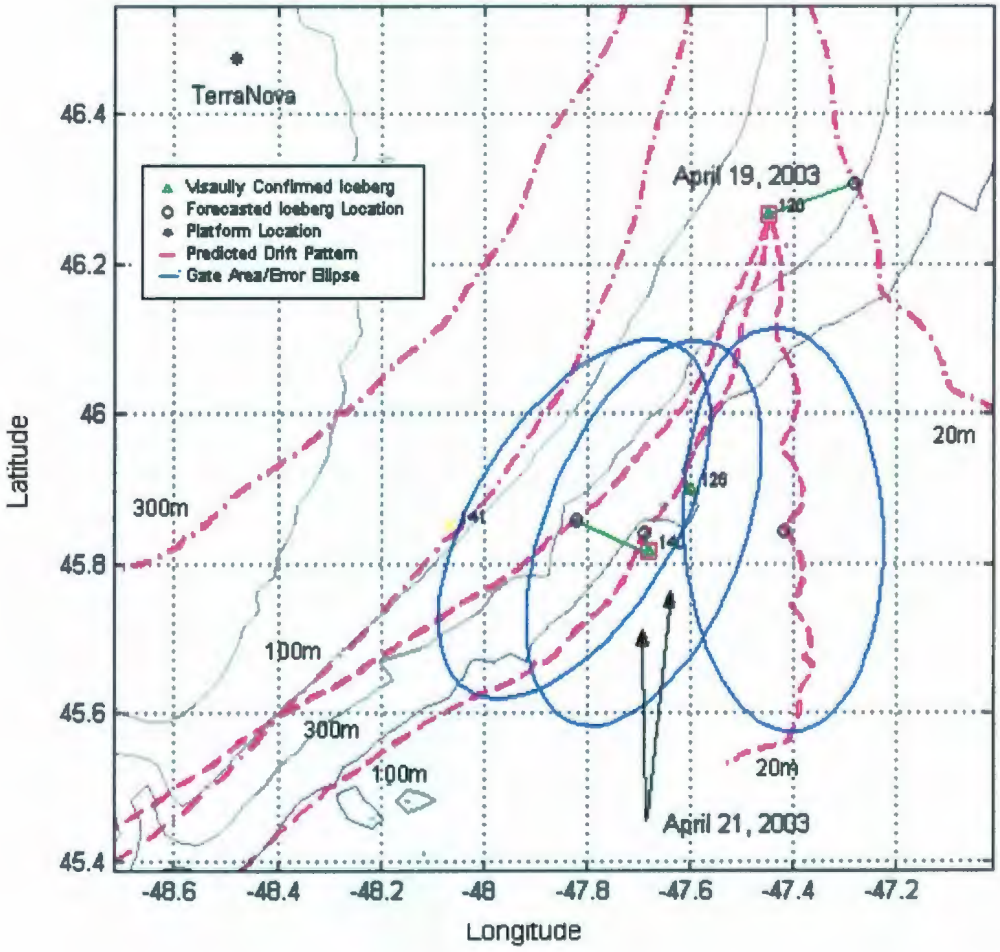

Figure 4.35: Berg #120 Gating Areas for Berg #140 Detection Position.

Figure 4.36 shows the predicted paths from iceberg ID 7, detected April 17, to iceberg ID 140, detected April 21, even though icebergs were detected in the general area April 19. Iceberg ID 141 is associated with both the 100-m and the 300-m predictions of iceberg ID 7. As can be seen in Figure 4.36, the association that is most likely is that with the 100-m path. Iceberg ID 141 was reported as having an unknown size.

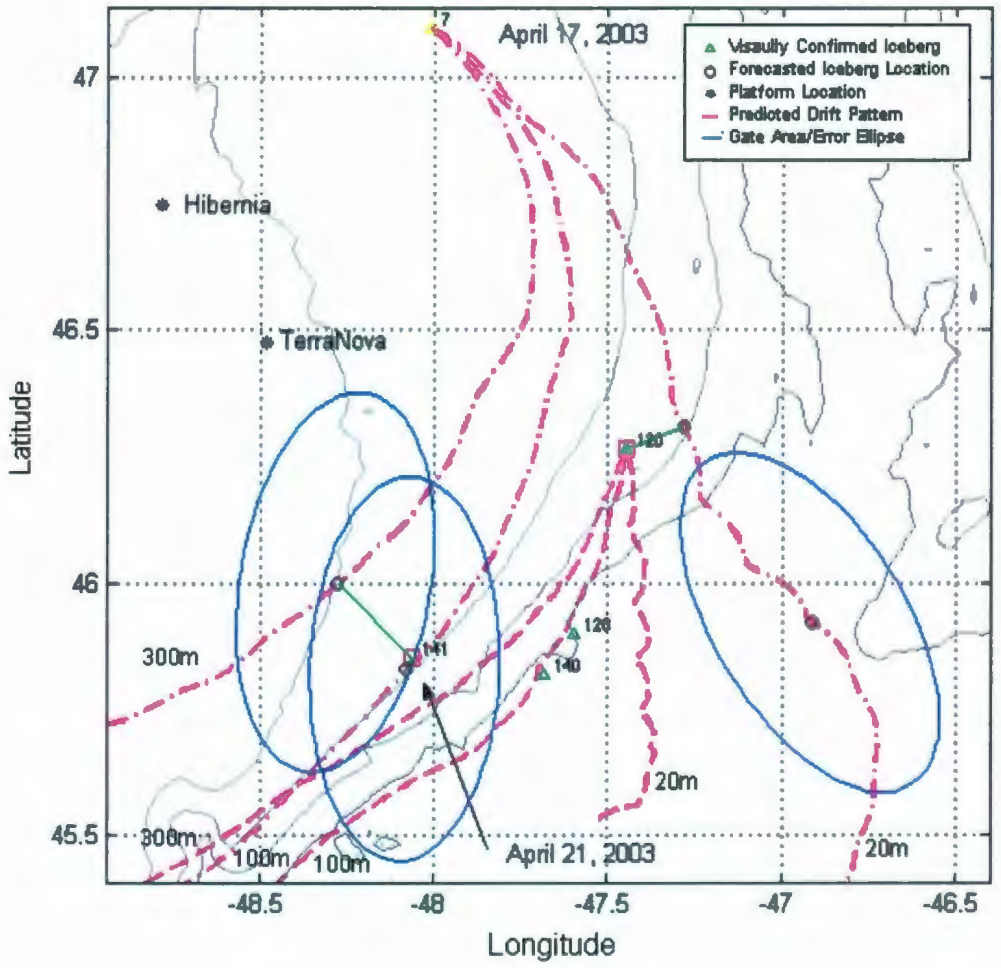

Figure 4.36: Berg #7 Gating Areas for Berg #141 Detection Position.

Given the associations available to iceberg ID 7 several hypothetical results are available. Note that there is some uncertainty in the sizes reported, as size estimates are difficult to gauge precisely, particularly from aircraft. As well, the predicted paths can have sizable errors; the gate area attempts to account for this, but cannot efficiently account for those cases where very large errors occur.

In this manner and as new information is added to the database, predicted paths, particularly various size estimates for single icebergs, will be de-activated. Essentially, these will be removed from those processed by the system, where processing refers to the prediction, and attempts to associate new detections with these previous detections. This will occur as more detection and sensor coverage data are entered, and some of the predicted paths remain uncorroborated. In a similar, manner low confidence detection data, for example from low probability of detection or high false positive sensors, can be used. Incorrect data supplied by these sensors will fail to have corroborating detections in future scans or from other sensors, while correct detections will have corroborating evidence, at least a portion of the time. Figure 4.37 shows the data collected for this small example, including the tracks de-activated by lack of corroborating evidence and those tracks that are still active and will continue to be predicted and have associations connected with them.

From the available associations, along with the parametric data collected such as size and shape, a 'most probable' set of associations can be selected. Figure 4.38 shows such an output for this case. Here, the size information along with the probability of association between predicted paths and detected icebergs is used to select the displayed paths and associations. Detections that had been associated, but are not in the final output seen in Figure 4.38, may be false positives, but are most likely other icebergs detected on April 17 from similar regions as iceberg ID 7. Notably, other icebergs from April 17 were associated with the excluded icebergs, ID 126 and 141.

However, the selection of the best representation is computationally intensive and not depicted here.

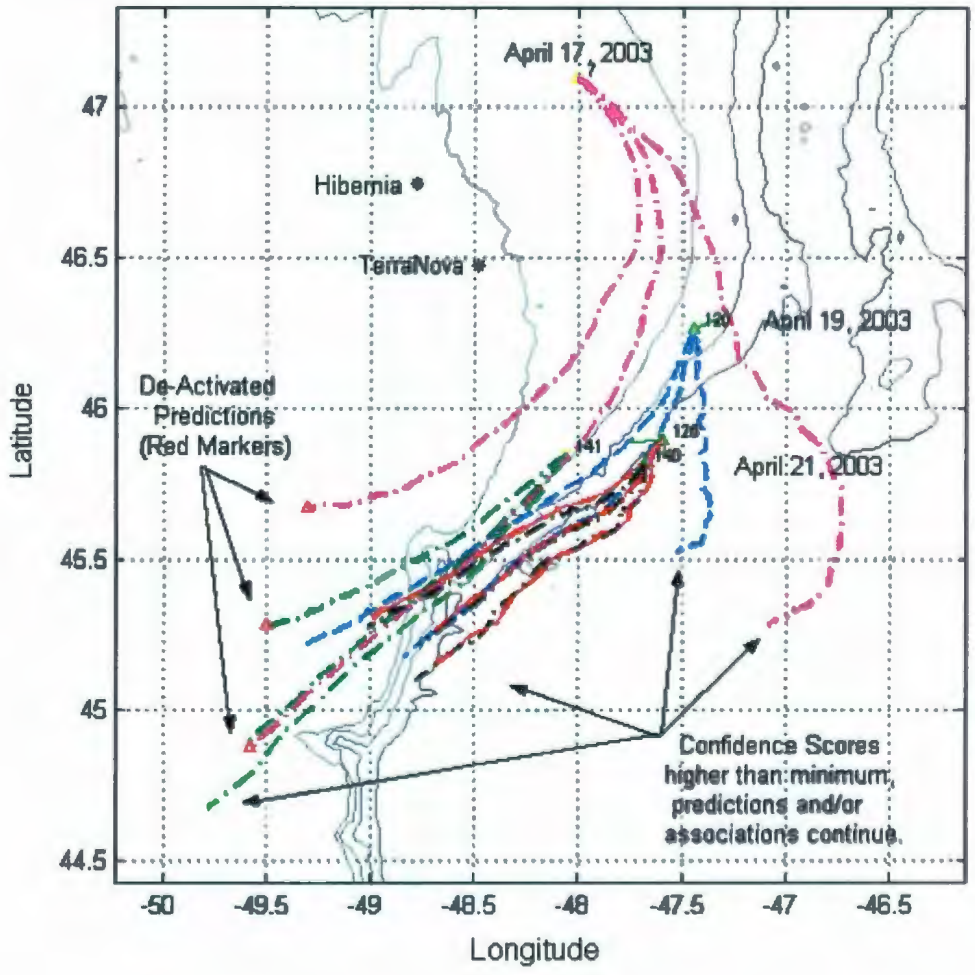

Figure 4.37: Berg #7 and Associations.

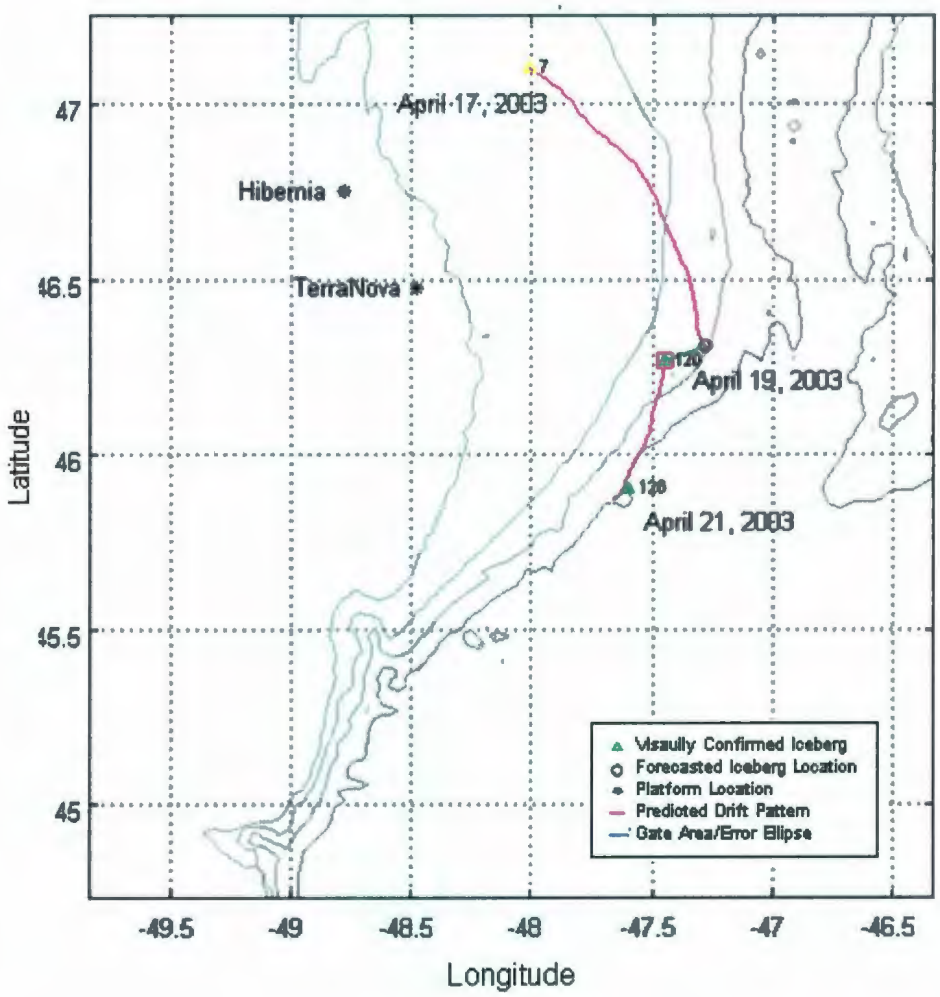

Figure 4.38: Most Probable Berg #7 Path.

The MHT software, written in MATLAB®, includes a visual interface. The interface is under development and modifications to increase its ease-of-use are best performed while it is used in an operational setting. Figure 4.39 shows a screen capture of the current interface and output window.

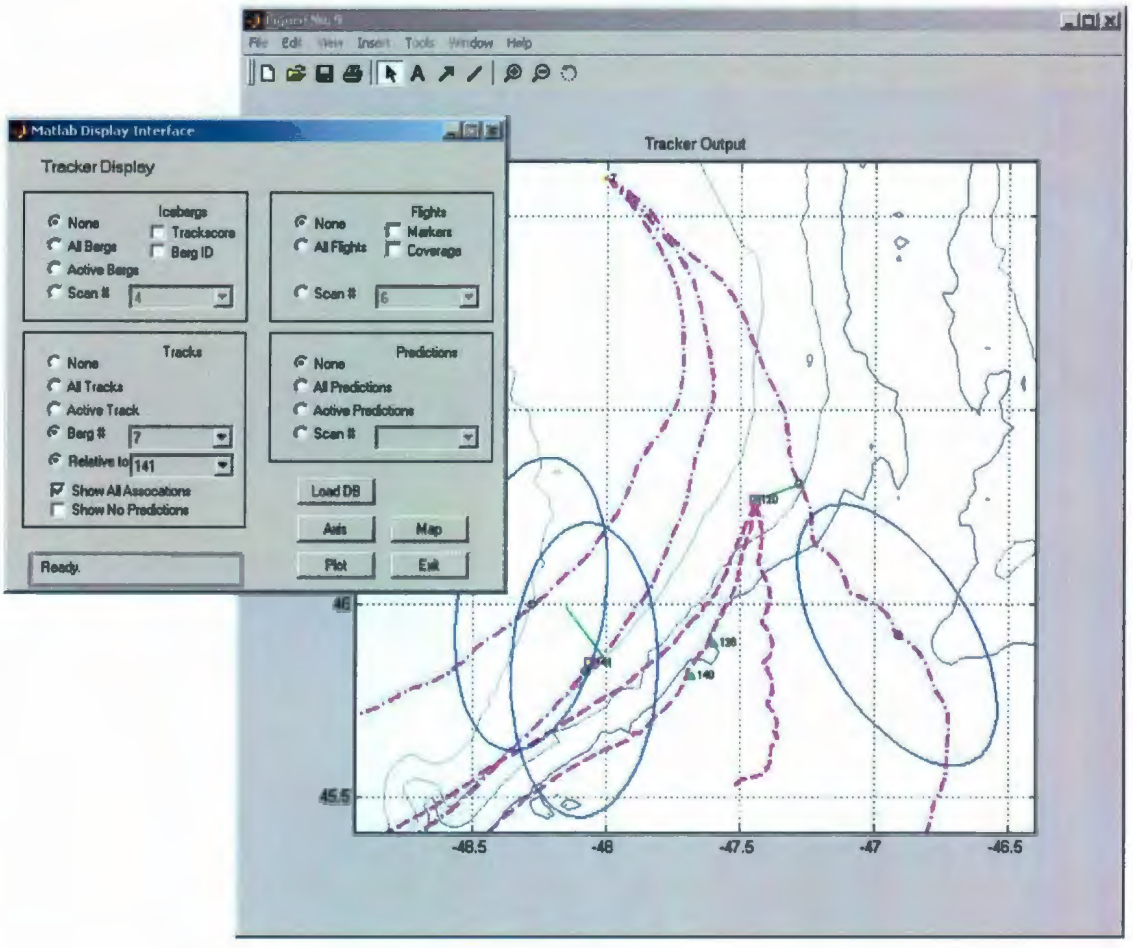

Figure 4.39: MHT MATLAB® Software Interface.

4.4.5 Assessment of Results

The MHT software outlined in this report has the capability to accept multiple inputs from a wide range of sensors and integrate them into a single data product. The sensors can be spread geographically and have a variety of performance levels. They can have various update rates from very frequent to rare, and at constant or sporadic intervals.

The use of the CIS CIO model appears to significantly improve the target association of the system. Empirically, the inference of the iceberg waterline length should allow for the system to tune itself to the behaviour of targets over multiple iterations.

As well as the functionality described above, there exists the capability to create multiple paths for any one iceberg. This may be done, for example, in cases where the size of the detected iceberg is unknown. In the case where multiple paths are followed, it is expected that the confidence in all but one path will reduce to such a point as multiple paths are eliminated. In this manner, size estimations of iceberg detections can be performed.

4.5 Analysis

The data fusion system differs from the sensor fusion method in that it acts solely with the combination of sensor data. That is, it is concerned with how to relate data points to one another. It makes use of the probability curves of the sensors themselves, but only to determine the certainty of the result.

The analysis of Bayesian statistics in application to the sensor data and the redetection of targets clearly indicate detection probability effectively increases over the long term. The iterations required to acquire a significant portion of targets is inversely proportional to Pr(det). The maximum maintainable real target tracks as a percentage of the actual tracks is inversely proportional to the track elimination value. The ratio of false tracks to real target tracks is inversely proportional to the track elimination score and Pr(det), and is proportional to PFA and Bayes prior value.

It is worth noting that the impact of PFA is generally underestimated and misunderstood. In the Bayes paradigm the PFA value is responsible for the rate at which sensor iterations that report a target provide an increase in the target confidence. Conversely, the Pr(det) is responsible for how quickly sensor iterations that do not report a target decrease confidence. Distinctions between statistical PFA and the PFA excluding false 'real' targets, such as ships identified as icebergs, need to be made.

The attempt to implement the statistics-based association portion of the tracking-based fusion system was hindered by problems relating to the adaptation of single point

target information to velocity and acceleration statistics. As well, it is clear that the movement of iceberg targets in periods greater than six hours was too complicated for the metrics used. This method may be applicable to other targets or in situations where frequent sensor iterations are guaranteed.

The implementation of a fusion system utilizing the CIS CIO prediction model for the generation of prediction and gating was largely successful in the tested application. A larger scale test of this system has been hindered by light ice seasons in years subsequent to the research.

This implementation has applications in both strategic and tactical ice management, and in the tasking of iceberg detection sensors. This methodology has the primary benefit of utilizing all available information. This is accomplished by taking into account the parameters of the sensor, such as probability of detection and probability of false positives.

Chapter 5 Summary

5.1 Conclusions

This thesis provides information on the application of sensor and data fusion to target detection, particularly to iceberg detection and redetection.

Within the context of this thesis sensor fusion has been defined as referring to the combination of sensor parameters, and data fusion has been defined as the combination of data from detection events.

Sensor fusion provides a means of evaluating the performance of a network of sensors. Presented herein has been an examination of methods that can be applied to provide for the combination of detection performance statistics for disparate sensors. Methods of dealing with data latency, geographical and temporal separation have been proposed. This methodology has applications in strategic planning and for risk analysis simulations. Stochastic simulation methods will likely provide additional versatility in analyzing more complex sensor arrangements.

This data fusion system can provide ice management operators with a tool to statistically and systematically combine detection information for a wide variety of sensors over a large geographical area. This document has examined a proposed simple track score method and demonstrated through simulation the significant benefits. Through this simulation it has been demonstrated that sensors currently considered to have low detection probability can be used reliably as a sensing method within a data fusion framework.

The simulation provides interesting insight into the detection problem. The key tradeoff to most applications will be the tolerance of false target tracks, which will persist for short durations within the system. As well, the use of Bayes points out the importance of PFA parameters in the assessment of a sensor's performance. In some applications, PFA will exceed Pr(det) as the key parameter considered when defining a sensor regime.

Additionally, two methods of target association have been implemented. The first utilizes historical kinematics to characterize the target movement; the second employs a third-party target drift model. These methods have been demonstrated and tested against real target data. Historical statistical kinematic modeling appears limited to short sub-day durations while more sophisticated target prediction models allow for longer sensor iteration periods.

For operational integration it should be possible to include metrics such as cost and practical availability into the evaluation for sensor selection and optimization studies.

The data fusion method described here may have effective applications in other fields, such as security and monitoring, or state space based applications.

5.2 Areas for Further Study

There are a number of areas that warrant further study and development, both in the sensor fusion application, and the data fusion application.

At a high level, new additional data sources are becoming available for inclusion in the data source set, which may provide additional detection capabilities and feature information. These new sensors include a new generation of multi-polarization, high resolution SAR satellites. These sensors will have to be taken into account when performing sensor fusion and in data fusion methodologies where their sensor data are to be included.

For sensor fusion methods, a wide variety of stochastic simulation methods could be applied, such as Monte Carlo analysis. Simulation methods will likely increase the adaptability of the methods presented here for handling the variety of configurations that may be possible in a modern sensor regime.

For data fusion, additional iceberg maneuvering models are becoming available that could improve the prediction and gating steps of iceberg tracking systems. Alternatives

to the CIS CIO model exist and new systems such as regional models based on the MERCATOR (2008) system may provide enhanced marine target prediction.

Although the easily implemented Bayes track score system defined here works quite well, a wide array of alternate track score methods exist. The investigations into the optimization of track initialization and elimination values should be part of the deployment of any practical system developed for real-world applications. Likewise, data handling in terms of the fusion and inference of feature information should be undertaken. Such information will help with identification of targets where target density is high and there is the possibility for track cross-over and target misidentification.

The natural progression of this research is a full practical test of the implementation during an ice season. Partial tests have been carried out with success, both technically and in terms of industry support. This level of implementation has been hindered in recent years by a lack of iceberg activity in the region of interest.

To be used on an industry level, the current implementation should be developed in a proper GIS software package with a supporting database. Such GIS interfaces are now the standard for mapping related applications. The current data fusion system has been prototyped in MATLAB®.

At a more general level, the data fusion work could be expanded and included in a wider threat assessment system that would examine the estimated iceberg conditions and determine the level of threat to offshore structures and vessels. Some progress has been made in this area by C-CORE.

Finally, the material presented here focused mainly on the application of ice detection in the Northwestern Atlantic Ocean. These methods certainly have other applications, specifically surveillance and monitoring for wide-area applications, and could be applied to security and sovereignty at regional and national levels.

References

Aldenderfer, Mark. S., and Blashfield Roger K. (1984), "Quantitative Applications in the Social Sciences", Sage University Paper 07-044, Sage Publications, London.

Allen, J.H. (1971). "Cruise report C.S.S. *Dawson* June 2-June 12, 1971", Faculty of Engineering and Applied Science, Memorial University of Newfoundland.

Berger, James O. (1985), *Statistical Decision Theory and Bayesian Analysis*, 2nd Edition, Springer-Verlag.

Bishop, Gary P. (1989), *Assessment of Iceberg Management for the Grand Banks Area: Analysis of Detection and Deflection Techniques*, Prepared for Mobil Oil Canada Properties, April 8, 1989.

Blackman, Samuel, and Robert Popoli (1999), *Design and Analysis of Modern Tracking Systems*, Artech House.

Bogler, Philip L., (1990), *Radar Principles with Applications to Tracking Systems*, John Wiley & Sons, Inc.

Brown, Pittard, and Spillane (1990), "A Simulation-Based Test Bed for Data Association Algorithms", *Sensor Fusion III, Proceedings of the SPIE Vol 1306*, pp58-68.

Brown, Robert Grover, and Patrick Y.C. Hwang (1992), *Introduction to Random Signals and Applied Kalman Fitltering*, Second Edition, John Wiley & Sons, Inc.

C-CORE (1992), *Design Criteria for Ice Loads on Floating Production Systems – Final Report*, C-CORE Contract Number 92-C13.

C-CORE (1999), *Integrated Ice Management R&D Initiative*, Contract Report for Chevron Canada Resources, Husky Oil Operations Ltd, Mobil Oil Canada Properties, Norsk Hydro Canada Oil & Gas Inc., Petro-Canada, North Atlantic Pipeline Partners, and Panel on Energy Research and Development. C-CORE Publication Number 99-C34, December, 1999.

C-CORE (2000), *Integrated Ice Management Initiative -Year 2000*, Contract Report for Chevron Canada Resources, Husky Oil Operations Ltd, Mobil Oil Canada Properties, Norsk Hydro Canada Oil & Gas Inc., Petro-Canada and Panel on Energy Research and Development. C-CORE Publication Number 00-C36, December, 2000.

C-CORE (2001), *Integrated Ice Management Initiative, 2001, Vol. 1 – Iceberg Detection*, Report No. R-01-24-605-V2, December 2001.

C-CORE (2003a), *Integrated Ice Management R&D Initiative, 2002*, R-02-026-110 v1.1, May, 2003.

C-CORE (2003b), *Integrated Ice Management R&D Initiative, 2003*, R-03-059-226 v2, December, 2003.

CANPOLAR Consultants Ltd. (1986). *Iceberg Detection by Airborne Radar: Technology Review and Proposed Field Programs. Environmental Studies Revolving Funds Report No. 045*, Ottawa, 135 pp.

Carrieres, T., Sayed, M., Savage, S. and Crocker, G. (2001). "Preliminary verification of an operational iceberg drift model", *POAC '01, Proceedings of the 16th International Conference on Port and Ocean Engineering under Arctic Conditions*, August 12-17, Ottawa, pp. 1107-1116.

Chankong, Vira, Yacov Y. Haimes, Herbert S. Rosenkranz and Julia Pet-Edwards (1985), "The Carcinogenicity prediction and battery selection (CPBS) method: a Bayesian approach", *Mutation Research, v153* pp. 135-166.

CIS (2002a). "Fact Sheet: Icebergs", Client Services, Canadian Ice Service, 373 promenade Sussex Drive, E-3 Ottawa, Ontario K1A.

CIS (2002b). "Education Corner-Icebergs-Iceberg Size", http://ice-glaces.ec.gc.ca/app/WsvPageDsp.cfm?ID=240&LnId=27&Lang=eng, Updated March 9, 2003.

Environment Canada (1989), *MANICE: Manual of Standard Procedures for Observing and Reporting Ice Conditions*, Seventh Edition, May 1989.

Grant, A.L. R.K. Hawkins, C.E. Livingstone, R. Lowry, R. Lawson, and R. Rawson. (1979), "The influence of incidence angle on microwave radar returns of 'targets' in an ocean background.", *Proceedings of 13th International Symposium on Remote Sensing of the Environment*, Ann Arbor, Michigan, pp 1815-1837.

Hall, David L. (1992), *Mathematical Techniques in Multisensor Data Fusion*, Artech House Inc., 1992.

Harvey, M.H. and J.P. Ryan. (1986). *Further studies on the assessment of marine radars for the detection of icebergs. Environmental Studies Revolving Funds Report No. 035*, Ottawa, 82 pp.

Heistrand et al. (1983), "An Automated Threat Value Model", *Proceedings of the 50th MORS*, March 1983.

Haykin, S., E. O. Lewis, R. K. Raney, and J. R. Rossiter (1994), *Remote Sensing of Sea Ice and Icebergs*, John Wiley and Sons.

IIP (2003a). "How do the Labrador and Gulf Stream currents affect icebergs in the North Atlantic Ocean?", http://www.uscg.mil/lantarea/iip/FAQ/Ocean_1.shtml, Updated Dec 10, 2003.

IIP (2003b). "Where do North Atlantic icebergs come from?", http://www.uscg.mil/lantarea/iip/FAQ/Icebergs_1.shtml, Updated Dec 10, 2003.

IIP (2003c). "Ice Patrol's Iceberg Counts", http://www.uscg.mil/lantarea/iip/General/icebergs.shtml, Updated Dec 10, 2003.

IIP (2003d). "IIP Picture Gallery", http://www.uscg.mil/lantarea/iip/Photo_Gallery/Thermite_Explosives_1.shtml, Updated Dec 11, 2003.

Joyce, James (2003). "Stanford Encyclopedia of Philosophy: Bayes's Theorem" http://plato.stanford.edu/entries/bayes-theorem/.

Manyika, James, Hugh Durrant-Wyte (1994). *Data Fusion and Sensor Management: a decentralized information theoretic approach*, Ellis Horwood Limited.

MERCATOR (2008). Website URL: http://www.mercator-ocean.fr/html/mercator/index_en.html.

MIROS (2008). Website URL: http://www.miros.no/wave_and_current_radar.php.

NIST SEMATECH (2001). "Assessing Product Reliability", Sect 8.1.10, *Engineering Statistics Handbook*, http://www.itl.nist.gov/div898/handbook/apr/section1/apr1a.htm.

PAL (2000). *The 2000 Iceberg Season on the Grand Banks, Final Report for The Grand Banks Ice Management Team.* PAL Environmental Services. November, 2000.

Peebles, Peyton Z., Jr. (2001). *Probability, Random Variables and Random Signal Principles*, 4th Ed., McGraw-Hill.

PERD (2001). "Update and Quality Assurance of the PERD Grand Banks Iceberg Database", prepared by Fleet Technology Limited for the National Research Council of Canada. PERD/CHC Report 20-59.

Petro-Canada (2002). Website URL: http://www.petro-canada.ca/en/about/741.aspx.

Robe, R.Q. and T.S. Ellis (1977), "Tagging of arctic icebergs", *Report of the International Ice Patrol in the North Atlantic Ocean (Season of 1977)*, Coast Guard Bulletin No. 63.

Robe, R.Q. and T.S. Ellis (1978), "Tagging of arctic icebergs", Arctic Bulletin, 2(14).

Rossiter, J.R., J. Guigne, C. Hill, R. Pilkington, E. Reimer, J. Ryan, and B. Wright, (1995), *Remote Sensing Ice Detection Capabilities – East Coast. Environmental Studies Revolving Funds Report No. 132*, Calgary, 172 pp.

RSI (RADARSAT International) (2001) Website URL: http://www.rsi.ca.

Ryan, J.P., M. Harvey, and A. Kent.(1985), *Assessment of Marine Radars for the Detection of Ice and Icebergs. Environmental Studies Revolving Funds Report No. 008*, Ottawa, 127 pp.

Ryan, Joseph P. (1985). *Enhancement of the Radar Detectability of Icebergs. Environmental Studies Revolving Funds Report No. 022*, Ottawa, 93 pp.

Appendix A Parameters of Iceberg Detection Sensors

This appendix briefly summarizes the parameters considered most important in the East Coast iceberg detection sensor regime.

A.1 Terms and Definitions

CFAR	Constance False Alarm Rate noise filtering
HF SWR	High Frequency Surface Wave Radar
PRF	Pulse Repetition Frequency, a radar parameter for the number of short electromagnetic bursts per second.
SAR	Synthetic Aperture Radar
STC	Sensitivity Time Control, a radar processing technique for removing range dependent clutter.
SWH	Significant Wave Height, a measure of sea roughness.

A.2 Parameters

The parameters considered most important are briefly defined below.

A.2.1 Coverage Area:

The area over which a sensor can provide a probably of detection as a function of iceberg size (for systems using higher frequencies that have negligible super-refraction (ducting) effects) can be approximated by calculating the 'line-of-sight' distance to the horizon:

$$Horizon(nmi) = \sqrt{5 \cdot height(m)} \qquad \text{Eq. A.1}$$

A.2.2 Probability of Detection:

The probability of detection of an iceberg. It is a function of range, sea state, and iceberg size.

A.2.3 Resolution

The ability of a system to determine the spatial location of a target.

A.2.4 Specificity:

Specificity is the probability of identifying correctly a negative detection (such as open water, as opposed to an iceberg).

A.2.5 Cost:

The operating costs of the sensor.

A.2.6 Update Frequency:

The rate at which information from the sensor is updated.

A.2.7 Data Latency:

The delay between data capture and data availability (most often due to processing of the data).

A.2.8 Availability:

The time period in which a sensor is available to operate or provides reliable data.

A.2.9 Reliability:

The susceptibility to adverse conditions (for example: fog for visual observation).

A.2.10 Ability to Classify:

The ability of the sensor to identify a target and provide relevant information such as direction, velocity, and size.

A.3 Sensors Discussed

The parameters for the following sensors are discussed here:

- Marine Radar
  - X-Band
  - S-Band
  - Enhanced Radar
    - Titan
    - SeaScan
- Airborne SAR (Litton APS-504 (V) 5)
- Satellite SAR (RADARSAT-1)
- HF SWR (Surface Wave Radar)
- Visual Observation
  - Ship based
  - Platform based
  - Airborne

A.4 Discussion of Parameters, Marine Radar, X-Band

A.4.1 Coverage Area:

The coverage area for marine radar is based on the line of sight to the horizon. For support vessels for the Hibernia platform having an antenna mounted at 15 meters this range is 17 km (9 nmi), for the Hibernia platform itself with a derrick mounted antenna the horizon is 48 km (26 nmi) radius [1]. X-Band is credited with longer range (then S-Band) [1].

A.4.2 Probability of Detection (Sensitivity)

Systems typically are capable of pulse to pulse integration and STC (Sensitivity Time Control) which remove range dependent clutter.

A.4.2.1 Growlers:

Undetectable [3].

A.4.2.2 Bergy Bits

Undetectable [3].

A.4.2.3 Small Icebergs

MV Polar Circle, 1985: 9-13 km (5 to 7 nmi) with the average detection at 11 km for average sizes of 40 m wide by 9 m (X and S-Bands) [1].

20 m bergs detectable up to 23 km at significant wave height (SWH) 1 m, 60 m bergs detectable up to 36 km at SWH 9 m [3].

A.4.2.4 Medium Icebergs

MV Polar Circle, 1985: Ranges from 12 to 24 km (6.4 to 13.3 nmi), average detection at 16 km (10 nmi). Average sizes were 26 m high and 100 m wide. X and S-Band. [1:102]

A.4.2.5 Large Icebergs

Presumably as good or better then smaller icebergs.

A.4.3 Resolution

One percent of the range used for detection [1]. X-Band has a horizontal beamwidth of 0.8° [1:107].

A.4.4 Specificity

No data.

A.4.5 Cost

Operating costs would primarily consist of only an operator's salary.

A.4.6 Update Frequency

Real time. (1600 PRF, 30 RPM [1:107])

A.4.7 Data Latency

None.

A.4.8 Availability

Constant.

A.4.9 Reliability

X-Band is adversely affected by rain and heavy fog. [1]

A.4.10 Ability to Classify

Operator interpretation. The monitoring of detections can determine the speed and direction of the object detected.

Speed is a reliable method of identifying an iceberg, assuming that all ships are moving. However, anchored or drifting ships may be mistaken for icebergs until they are once again underway.

A.5 Discussion of Parameters, Marine Radar, S-Band

A.5.1 Coverage Area

The coverage area for marine radar is based on the line of sight to the horizon. For support vessels for the Hibernia platform having an antenna mounted at 15 meters this range is 17 km (9 nmi), for the Hibernia platform itself with a derrick mounted antenna the horizon is 48 km (26 nmi) radius [1].

A.5.2 Probability of Detection (Sensitivity)

Systems typically are capable of pulse to pulse integration and STC, which removes range dependent clutter.

A.5.2.1 Growlers

Insufficient data [1]. Undetectable [3].

A.5.2.2 Bergy Bits

Insufficient data [1]. Detectable up to 13 km by platform mount systems, 6.5 km for vessel mounted systems [3].

A.5.2.3 Small Icebergs

MV Polar Circle, 1985: 9-13 km (5 to 7 nmi) with the average detection at 11 km for average sizes of 40 m wide by 9 m (X and S-Bands) [1].

In the region of 5 to 20 km, sea clutter presents a significant decrease in the ability to detect icebergs [1:107].

Twenty meter bergs detectable up to 19 km at SWH 1 m, 60 m bergs detectable 31 km at SWH of 9 m [3].

A.5.2.4 Medium Icebergs

ERSF No. 22, 1991: Reliable at ranges for S-Band of 25 to 31 km (13.5 to 16.7 nmi) [1:61]

MV Polar Circle, 1985: Ranges from 12 to 24 km (6.4 to 13.3 nmi), average detection at 16 km (10 nmi). Average size was 26 m heights and 100 m widths (X and S-Band) [1:102].

A.5.2.5 Large Icebergs

Presumably as good or better then smaller icebergs.

A.5.3 Resolution

1% of the range used for detection [1]. S-Band has a horizontal beamwidth of 2.0° [1:107].

A.5.4 Specificity

No data.

A.5.5 Cost

Operating costs would primarily consist of only an operator's salary.

A.5.6 Update Frequency

Real time. (1600 PRF, 30 RPM [1:107])

A.5.7 Data Latency

None.

A.5.8 Availability

Constant.

A.5.9 Reliability

S-Band provides better performance than X in sea clutter and adverse weather conditions. Provides good penetration through moderate rain (4 mm/h). Adversely affected by heavy rain (16 mm/h). [1]

A.5.10 Ability to Classify

Operator interpretation. The monitoring of detections can determine the speed and direction of the object detected.

Speed is a reliable method of identifying an iceberg, assuming that all ships are moving. However, anchored or drifting ships may be mistaken for icebergs until they are once again underway.

A.6 Discussion of Parameters, Marine Radar, Enhanced

These systems are based on conventional X-Band and S-Band system, but include additional computer processing of the radar returns..

A.6.1 Coverage Area

Same as for the X or S-Band Radar.

A.6.2 Probability of Detection (Sensitivity)

Systems typically are capable of pulse to pulse integration and STC, which remove range dependent clutter. This is then scan to scan averaged. For the Titan 16 scans can be averaged.

Probability of detection graphs in [1] implies that even with a non-enhanced probability of detection of 10% is boosted to 100% using the TITAN system.

A.6.2.1 Growlers

No specific data. Presumably undetectable as it relies on a conventional X or S-Band radar.

A.6.2.2 Bergy Bits

Presumably as good or better then the source X or S-Band system for this size iceberg.

A.6.2.3 Small Icebergs

The Titan has a 100% capability of detecting a 30 m iceberg to as far as 26 km [1:115].

A.6.2.4 Medium Icebergs

Presumably as good or better then performance on smaller icebergs.

A.6.2.5 Large Icebergs

Presumably as good or better then performance on smaller icebergs.

A.6.3 Resolution

Dependent on whether the source of the data is X or S-Band radar. (Typically 37.5 m, 0.8° or 2.0° horizontal beamwidth [1])

A.6.4 Specificity

No Data.

A.6.5 Cost

Operating costs would primarily consist of only an operator's salary.

A.6.6 Update Frequency

Real time. (1600 PRF, 30 RPM [1:107])

A.6.7 Data Latency

Practically none. (Some latency could be accounted for by scan averaging. For example, 32 seconds for a 16 scan average with a 30 RPM radar. This is negligible).

A.6.8 Availability

Constant.

A.6.9 Reliability

Susceptible to the same interference as regular X and S-Band system on which it is based.

Due to CFAR averaging, icebergs covered in interference by precipitation or fog will appear as clear ocean.

A.6.10 Ability to Classify

The same as un-enhanced marine radar. Additionally, the software may have some features that make tracking easier or automated.

A.7 Discussion of Parameters, Marine Radar, SeaScan Enhanced Radar

These systems are based on conventional X-Band and S-Band system, but include additional computer processing of the radar returns.

A.7.1 Coverage Area

Same as for the X or S-Band Radar. The SeaScan will be installed on the Terra Nova production platform at a height of 45 m, giving a radar horizon of 15 nmi [6].

A.7.2 Probability of Detection (Sensitivity)

Systems typically are capable of pulse to pulse integration and which remove range dependent clutter. This is then scan to scan averaged.

A.7.2.1 Growlers

Detectable to a maximum range of 3.8 nmi (radar installed at a height of 90 m) [6].

A.7.2.2 Bergy Bits

Detectable to a maximum range of 18 nmi (radar installed at a height of 90 m) [6]. Reliably detected bergy bits and small icebergs in sea states reaching 3 to 4 m with winds of 50 km/h gusting to 64 km/h [6].

A.7.2.3 Small Icebergs

Consistently detected to the radar horizon of the test [6]. Reliably detected bergy bits and small icebergs in sea states reaching 3 to 4 m with winds of 50 km/h gusting to 64 km/h [6].

A.7.2.4 Medium Icebergs

Consistently detected to the radar horizon of the test [6].

A.7.2.5 Large Icebergs

Consistently detected to the radar horizon of the test [6].

A.7.3 Resolution

Dependent on whether the source of the data is X or S-Band radar. (Typically 37.5 m, 0.8° (X) or 2.0° (S) horizontal beamwidth [1])

A.7.4 Specificity

No Data.

A.7.5 Cost

Operating costs would primarily consist of only an operator's salary.

A.7.6 Update Frequency

Real time. (1600 PRF [1:107], 120 RPM)

A.7.7 Data Latency

Practically none. (Some latency could be accounted for by scan averaging, but this is negligible).

A.7.8 Availability

Constant.

A.7.9 Reliability

Susceptible to the same interference as regular X and S-Band system on which it is based.

Due to CFAR averaging icebergs covered in interference by precipitation or fog will appear as clear ocean.

A.7.10 Ability to Classify

The same as un-enhanced marine radar. Additionally, the software may have some features that make tracking easier or automated.

A.8 Discussion of Parameters, Airborne SAR (Litton APS-504(V)5)

The only radar in use at the time of this report is the Litton APS-504(V)5, a SAR search radar [2]. This radar is also used by the International Ice Patrol [1]

A.8.1 Coverage Area

The Litton search radar is found most effective at 150 to 450 m altitude. At his height it has a radar horizon of 50–87 km (27 to 47 nmi) [1].

A.8.2 Probability of Detection (Sensitivity)

The Litton APS-504 uses pulse to pulse and scan to scan integration, CFAR and STC [1:108].

A.8.2.1 Growlers

Detectable up to 29 km at a SWH of 1 m [3].

A.8.2.2 Bergy Bits

Detectable up to 39 km at a SWH 1 m for 10 m bergs [3].

A.8.2.3 Small Icebergs

Detected with up to 80% reliability up to sea state 5 for a line spacing of 37 km (20 nmi) [1:103]. 20 m bergs detected up to 46 km at SWH of 5m. Bergs detectable up to 58 km at a SWH of 15 m for 60 m waterline length [3].

A.8.2.4 Medium Icebergs

No specific data, presumably as good or better performance as smaller.

A.8.2.5 Large Icebergs

No specific data, presumably as good or better performance as smaller.

A.8.3 Resolution

The system has a range resolution of 4.5 m (it has 7 range options, 3, 6, 12, 25, 50, 100, 200 nmi) [1]. The positional accuracy is 200 m^2, given a 100 m accuracy of aircraft GPS navigation and a radar ranging error of 2% at the shortest range (3 nmi) [1]. Horizontal beamwidth of 2.3° [1:108].

A.8.4 Specificity

No Data.

A.8.5 Cost

Provincial Airlines Environmental Services operates chartered flights at a cost of approximately $4,500 to $5,000 per hour.

A.8.6 Update Frequency

Real time. (PRF 1350 Hz, 30 RPM)

A.8.7 Data Latency

The operator could relay data from the radar almost instantaneously over radio channels. However, if the data were not delivered until the end of the flight the latency could on the order of several hours.

When the plane is not over a particular area the data will become outdated proportionally.

A.8.8 Availability

Obviously the plane must be in the air to be of any use. Flights are relatively frequent and could be scheduled as needed given the resources. As well, areas of particular interested could be prioritized.

A.8.9 Reliability

The Litton operates over 16 frequencies in the range of 8.9 to 9.4 GHz (it uses frequency agility to improve performance) [1]. As such it is susceptible to the interferences that will disturb other X-Band systems.

Also the effects of fog and poor weather on aircraft flights must be considered.

A.8.10 Ability to Classify

The system is usually verified by visual confirmation whenever possible. There does not appear to be a quantitative analysis of this available.

Considering the short dwell time, velocity measurement and subsequent identification from this data is likely not feasible.

Radar return amplitude would give some indication as to the size of the target.

A.9 Discussion of Parameters, Satellite SAR (RADARSAT-1-1)

RADARSAT-1 offers five modes of operation, offering a tradeoff between coverage area and resolution. Of these two, ScanSAR Narrow and Wide, provide the most useful coverage to area tradeoff.

A.9.1 Coverage Area

ScanSAR Narrow: 300 km x 300 km coverage.

Wide: 150 km x 150 km coverage.

A.9.2 Probability of Detection (Sensitivity)

A.9.2.1 Growlers

Undetectable given the resolution of the modes in use.

A.9.2.2 Bergy Bits

Undetectable given the resolution of the modes in use.

A.9.2.3 Small Icebergs

Icebergs over 30m are detectable with a 98.1% accuracy using visual identification and 90% using software [4]. These probabilities were determined by comparison of RADARSAT-1 imagery to ground truthed data. As such they most likely represent favorable weather conditions and may deteriorate somewhat in poorer sea states.

A.9.2.4 Medium Icebergs

Similar or better than smaller icebergs.

A.9.2.5 Large Icebergs

Similar or better than smaller icebergs.

A.9.3 Resolution

ScanSAR Narrow: 50 m resolution [4]

Wide: 30 m resolution [4]

A.9.4 Specificity

No data.

A.9.5 Cost

For RADARSAT-1 imagery ordered well in advance (min. 3 days) and returned as quickly as possible (3 hours), the cost would be approximately $2,025 (cdn) [5].

A.9.6 Update Frequency

RADARSAT-1 has a 24-day repeat pattern [5]. However, with antenna redirection a three-day revisit schedule for any one point can be obtained [1]. Each visit consists of both an ascending and descending pass within one day of each other [5].

A.9.7 Data Latency

"Real time" data turn around (3 hours) can be purchased at a premium, see cost.

A.9.8 Availability

RADARSAT-1 data is available at a cost whenever the satellite passes over the area of interest. However, if a particular scan mode is desired, the satellite must be tasked ahead of time. Hence, planning days ahead is required.

A.9.9 Reliability

Operating in the C-Band, RADARSAT-1 is not affected by cloud cover. As well, due to it's high angle of incidence, there is little or no interference from precipitation attenuation [5].

A.9.10 Ability to Classify

The size of objects can be determined easily with an accuracy dependent on the resolution size.

With no data on motion the identity of the objects is somewhat difficult to ascertain. As metallic ships are much better reflectors of radar signals then icebergs, an examination of the mean and variance of pixel intensities can be useful for identifying objects that cover an area of several pixels. Small or non-metallic objects are particularly difficult to identify.

A.10 Discussion of Parameters, HF Surface Wave Radar

A.10.1 Coverage Area

Covers approximately 200,000 km^2. Out to approximately 200 nmi for medium sized icebergs [4]. Maximum coverage area is 120° wide and out to 250 nmi.

A.10.2 Probability of Detection (Sensitivity)

A.10.2.1 Growlers

Undetectable except at very close range [4].

A.10.2.2 Bergy Bits

Undetectable except at very close range [4].

A.10.2.3 Small Icebergs

Ten percent probability of detection in the 150 to 250 nmi range at an average SWH 1.25 to 2.5 [4].

A.10.2.4 Medium Icebergs

Twenty five percent probability of detection in the 150 to 250 nmi range at an average SWH 1.25 to 2.5 [4].

A.10.2.5 Large Icebergs

Sixty-five percent probability of detection in the 150 to 250 nmi range at an average SWH 1.25 to 2.5 [4].

A.10.2.6 Very Large Icebergs

One-hundred percent probability of detection in the 150 to 250 nmi range at an average SWH 1.25 to 2.5 [4].

A.10.3 Resolution

No Data.

A.10.4 Specificity

No Data.

A.10.5 Cost

Operator's salary, electrical power costs may become significant over long periods of time.

A.10.6 Update Frequency

Immediate.

A.10.7 Data Latency

Data processing can be from 6 to 20 minutes.

A.10.8 Availability

Daytime, during favorable ionosphere conditions.

A.10.9 Reliability

Not affected by weather conditions due to the operation at low frequencies.

A.10.10 Ability to Classify

HF SWR is able to determine velocity of the target. Given observation over a period of time it should be reliable to determine if a target is an iceberg, vessel, or false alarm.

Like other radar systems, the size of the HF SWR return indicates the radar cross section of the target; radar returns are a good indication of the target size.

A.11 Discussion of Parameters, Visual Observation, Ship

A.11.1 Coverage Area

Governed by the visible horizon, same formula as with radar horizon. For ship based, approximately 17 km [1].

A.11.2 Probability of Detection (Sensitivity)

No Data.

A.11.3 Resolution

The spatial resolution (minimum separation) of the human eye is 0.3 mrad [1:125], 5.1 m at 17 km.

A.11.4 Specificity

No data.

A.11.5 Cost

Cost of salary as a function of time spent on ice observation.

A.11.6 Update Frequency

For all intensive purposes instantaneous (25Hz) [1:125].

A.11.7 Data Latency

None.

A.11.8 Availability

Daytime.

A.11.9 Reliability

As with all visual observations they are adversely affected by poor weather (fog, precipitation, etc).

A.11.10 Ability to Classify

Given a visual sighting, classification of identity is almost 100% certain. However, track and speed information can be difficult to ascertain.

A.12 Discussion of Parameters, Visual Observation, Platform

A.12.1 Coverage Area

Governed by the visible horizon, same formula as with radar horizon. For platform based, approximately 48 km [1].

A.12.2 Probability of Detection (Sensitivity)

No Data.

A.12.3 Resolution

The spatial resolution (minimum separation) of the human eye is 0.3 mrad [1:125], 14.4 m at 48 km.

A.12.4 Specificity

No data.

A.12.5 Cost

Cost of salary as a function of time spent on ice observation.

A.12.6 Update Frequency

For all intensive purposes instantaneous (25Hz) [1:125].

A.12.7 Data Latency

None

A.12.8 Availability

Daytime.

A.12.9 Reliability

As with all visual observations they are adversely affected by poor weather (fog, precipitation, etc).

A.12.10 Ability to Classify

Given a visual sighting, classification of identity is almost 100% certain. However, track and speed information can be difficult to ascertain.

A.13 Discussion of Parameters, Visual Observation, Airborne

A.13.1 Coverage Area

Governed by the visible horizon, same formula as with radar horizon. At 150 to 450 m altitude the horizon is at 50–87 km (27 to 47 nmi) [1].

A.13.2 Probability of Detection (Sensitivity)

No Data.

A.13.3 Resolution

The spatial resolution (minimum separation) of the human eye is 0.3 mrad [1:125], 26.1 m at 87 km.

A.13.4 Specificity

No data.

A.13.5 Cost

Cost of salary as a function of time spent on ice observation plus flight costs of approximately $4,500 to $5,000 per hour.

A.13.6 Update Frequency

For all intensive purposes instantaneous (25Hz) [1:125].

A.13.7 Data Latency

Depends on when data is reported. Theoretically, if the observation were 'radioed in' immediately there would be no latency. However, if reports are not submitted until the end of a flight the latency could be in the order of several hours.

A.13.8 Availability

Flights can be scheduled on an as required basis, typically one per day during the iceberg season. However, for visual observation these must be during the day.

A.13.9 Reliability

As with any flight, it can be grounded by poor weather (fog, snow, heavy rain). As well, low cloud cover will prevent visual observation.

A.13.10 Ability to Classify

Given a visual sighting, classification of identity is almost 100% certain. However, track and speed information can be difficult to ascertain.

A.14 References

1. Rossiter, J.R., J. Guigne, C. Hill, R. Pilkington, E. Reimer, J. Ryan, and B. Wright. 1995. Remote Sensing Ice Detection Capabilities – East Coast. *Environmental Studies Research Funds Report No. 132*, Calgary, 172pp.
2. Private communication with Pip Rutkin, Provincial Airlines, June 8, 2001.
3. C-CORE. 1992. Design Criteria for Ice Loads on Floating Production Systems. Contract report for Petro-Canada, Contract No.92-C13. (Referenced in [1]).
4. C-CORE. 2000. "Integrated Ice Management R&D Initiative – Year 2000", Contract Report for Chevron Canada Resources, Huskey Oil Operations limited, Mobil Oil Canada Properties, Norsk Hydro Canada Oil & Gas Inc., Petro-Canada and Panel on Energy Research and Development. C-CORE Publication 00-C36, December 2000.
5. RSI (RADARSAT-1 International). 2001. http://www.rsi.ca/.
6. C-CORE, "Integrated Ice Management R& D Initiative", Contract Report for Chevron Canada Resources, Husky Oil Operations Ltd., Mobil Oil Canada Properties, Norsk Hydro Canada Oil & Gas Inc., Petro-Canada, North Atlantic Pipeline Partners, and Panel on Energy Research and Development. Publication Number 99-C34, December 1999.

Appendix B CPBS Method

This generalization of the CPBS method is based on the document:

Chankong, Vira, Yacov Y. Haimes, Herbert S. Rosenkranz and Julia Pet-Edwards, The Carcinogenicity prediction and battery selection (CPBS) method: a Bayesian approach, *Mutation Research*, v153 (1985) pp135-166

B.1 Terms and Definitions

Sensitivity	The fraction of positive elements correctly identified. (i.e. the fraction of icebergs correctly identified by a sensor; the fraction of tests correctly returned positive).
Selectivity	The characteristics which are represented by the parameters of sensitivity and specificity. It indicates the ability to correctly identify positive and negative elements.
Specificity	The fraction of negative elements correctly identified (i.e. the area of open sea, correctly identified (e.g. not mistaken for an iceberg) divided by the total area of open sea; the fraction of tests correctly return negative).
Predictivity	The degree of confidence (reliability) of the positive or negative outcome of a test (sensor output).
Elements	A set of positive and negative elements, that is, a set containing both icebergs and ocean. Please note that when Empty Ocean is referred to it only indicates a section of ocean devoid of icebergs. The existence of other non-iceberg objects (ships, buoys, etc.) is possible.
E_P	A positive element (i.e. an area of ocean with an iceberg).
E_N	A negative element (i.e. an area of ocean without an iceberg).

B.2 Summary

The CPBS method, as published, consists generally of five tasks:

1. Data Consolidation
2. Parameter estimation
3. Predictivity Calculation
4. Battery Selection
5. Risk Assessment

The original CPBS method defined a set of tests, which returned either positive or negative, and had an associated degree of confidence as to this result. The confidence of the test is calculated from its selective and predictive statistics.

The goal is to choose a battery of tests that have the most confident outcome from the whole set of tests.

For our purposes these 'tests' are actually sensor returns, indicating the existence of an iceberg (positive element) or open water (negative element). This distinction between positive elements and negative elements is made because we are not only detecting icebergs, but open water as well. Misidentify open water (i.e. a false alarm) will have an implication on the performance of a sensor.

This document attempts to apply the CPBS method to iceberg detection. That is, instead of tests and assays on suspected carcinogens; we will be examining the results of sensors on ocean suspected of containing icebergs. Hence, not all aspects of the

CPBS method examined in the original document are applicable here. Only those aspects of relevance are examined and even then may they not be entirely necessary for integration into an iceberg sensor system.

B.3 Introduction to this Application

There exists a need for quantifying the predictivity of sensors used in iceberg detection. This quality implies a quantifiable certainty in a positive or negative result, if an iceberg is detected by a sensor or group of sensors we want to be confident that the detection is correct and relatively certain that icebergs do not exists where they have not been detected. To this end the CPBS method may be of use.

The method has two purposes: to develop a method for determining the reliability and predictive capability of individual short-term tests and batteries of such tests, and to develop a strategy for formulating and selecting batteries of these.

To begin, the appropriate performance measure for each test must be determined. These are generally sensitivity, and specificity. These two together are indicative of the selective property of the test.

The information of sensitivity and specificity constitute a criterion for selecting essays to form a battery of tests that is highly selective and predictive. Selectivity indicates the probability that an iceberg will be detected or not, given one is or is not present. Predictivity indicates the probability that an iceberg is present or not, given one was

detected or not detected respectively. They also provide a basis for predicting the nature of an element (i.e. positive or negative) through a Bayesian approach based on sensor results. An *a priori* probability that an iceberg is present can be used to improve this calculation; this can be provided by intuitive feeling, knowledge of prevalence, and/or other statistical information.

To determine the predictive capability of a test or a battery of tests we need to know with what degree of confidence a positive or negative result would correctly determine the nature of an element (i.e. whether there truly exists a positive element or a negative element). These make up the measures of predictivity. The predictivity of one or more sensors can be computed using the above information and Bayes' Theorem.

B.4 Selectivity of an Assay

Selectivity is easily measured and is used to calculate predictivity. A test is said to be perfectly selective if it always shows a positive response for a positive element and always a negative response for a negative element.

$$\alpha^{+} \equiv \Pr(+ \mid E_P) = \frac{\#\,of\ correct\ positive\ responses}{total\ number\ of\ positive\ elelments} \qquad \text{Eq. B.1}$$

Sensitivity (α^{+}) is the probability that the sensor return will indicate an iceberg (positive result) given that an iceberg is present (positive element).

$$\alpha^{-} \equiv \Pr(- \mid E_N) = \frac{\#\,of\ correct\ negative\ responses}{total\ number\ of\ negative\ elelments} \qquad \text{Eq. B.2}$$

Specificity (α^{-}) is the probability that the sensor return will indicate a section of open water, and not a false alarm, (negative result) given there is no iceberg (negative element).

For assays where the selectivity is unknown, the parameters can be determined and confirmed through testing. Because the assays that give the same positive and negative responses on a set of elements should have the same sensitivities and specificities, there exists a method of determining whether the approximate sensitivities and specificity actually reflect the true specificity and sensitivity. This involves assuming that assays that are determined to be within one group have the same sensitivity and the same specificity. If the sensitivity and/or specificity of an assay within the group are known with a high degree of assurance, than the estimates of the other assays within the group can be strengthened by this information. The method consists of four steps:

1. Estimate the sensitivity and specificity of each assay employing the above equations.
2. Compute the confidence interface for sensitivity and selectivity as:

$$\hat{p} - z_{\gamma/2}\sqrt{\frac{\hat{p}(1-\hat{p})}{n}} < p < \hat{p} + z_{\gamma/2}\sqrt{\frac{\hat{p}(1-\hat{p})}{n}} \qquad \text{Eq. B.3}$$

Where, n is the number of elements used in the calculation. $\hat{p}$ is the estimate for sensitivity or specificity and p is the true value. γ is the level of significance, and z is the standard normal variate (this shows how 'good' the estimate is).

3. Use cluster analysis on the database to group the assays by similarity of responses.
4. Try to 'improve' the estimates for the specificity and sensitivity using the information provided by cluster analysis.

This allows more accurate estimations of the selectivity statistics to be made.

B.5 Predictivity of an Assay

An assay is said to be predictive if, based on the results alone, we can conclude with a reasonable degree of confidence that the positive or negative element returned is correct.

The degree of confidence associated with the correctness of an assay's prediction reflects a measure of its predictivity.

$$\Theta^{+} \equiv \Pr(E_p \mid +) = \begin{array}{l}\text{probability that a positive element} \\ \text{actually exists given a positive result.}\end{array} \qquad \text{Eq. B.4}$$

$$\Theta^{-} \equiv \Pr(E_n \mid -) = \begin{array}{l}\text{probability that a negative element} \\ \text{actually exists given a negative result.}\end{array} \qquad \text{Eq. B.5}$$

With the sensitivity, specificity, and the expectation that a positive element, $Pr(E_P)$, exists (the Bayes prior), the associated predictivity indices of an assay can be computed using Bayes' formula as follows:

$$\Theta^{+} \equiv \Pr(E_P \mid +) \qquad \text{Eq. B.6}$$

$$= \frac{\Pr(E_P)\Pr(+ \mid E_P)}{\Pr(E_P)\Pr(+ \mid E_P) + \Pr(E_N)\Pr(+ \mid E_N)} \qquad \text{Eq. B.7}$$

$$\Theta^{-} \equiv \Pr(E_N \mid -) \qquad \text{Eq. B.8}$$

$$= \frac{\Pr(E_N)\Pr(- \mid E_N)}{\Pr(E_N)\Pr(- \mid E_N) + \Pr(E_P)\Pr(- \mid E_P)} \qquad \text{Eq. B.9}$$

Θ^{+} is the probability that a iceberg actually exists given a positive result, Θ^{-} is the probability that there is no iceberg present given a negative result.

If a good estimate of $Pr(E_P)$ is not available, a worst case estimate may be made (i.e. $Pr(E_P) = 0.5$). Thus, a positive or negative result will modify the original estimate of an iceberg being present. The test result can be viewed as an aid that helps us improve a subjective judgment or enhances the present state of knowledge.

B.6 Strategy for Battery Selection

An assay with high sensitivity ($\alpha^{+} \approx 1$) but with low to moderate specificity ($\alpha^{-} \approx 0.7$) will be highly selective for icebergs (E_P), but not for clear ocean (E_N). This means that the assay will give a positive result when it encounters an iceberg and can give a positive or negative response when it encounters open water. That is to say, it may generate a

'false alarm'. Thus, if we use such a sensor to predict the existence of an iceberg, a positive response can occur from an iceberg or misclassified empty ocean, and a negative response occurs only from empty ocean. This implies that a sensor with high sensitivity and low specificity is a good predictor of empty ocean and a poor-to-moderate predictor of icebergs.

From this we see that sensors can be divided into 4 classes:

Table B.1: Classes of Assays

Potential Use	Class I $0.75 < \alpha^+ < 1$ $0.75 < \alpha^- < 1$	Class II $0.75 < \alpha^+ < 1$ $0 < \alpha^- < 0.75$	Class III $0 < \alpha^+ < 0.75$ $0.75 < \alpha^- < 1$	Class IV $0 < \alpha^+ < 0.75$ $0 < \alpha^- < 0.75$
Detecting Icebergs	Moderate to Good	Moderate to Good	Poor to Moderate	Poor to Moderate
Detecting Open Water	Moderate to Good	Poor to Moderate	Moderate to Good	Poor to Moderate
Predicting Icebergs	Moderate to Good	Poor to Moderate	Moderate to Good	Poor to Moderate
Predicting Open Water	Moderate to Good	Moderate to Good	Poor to Moderate	Poor to Moderate

NOTE: the use of 0.75 as a boundary for a 'good' assay is arbitrary. As well the division into four classes is also arbitrary, that is, more classes could be used, and this would increase the complexity exponentially.

From the above we can conclude:

1. Use as many sensors of Class I as possible.
2. Combine sensors of Class II with Class III.
3. Do not use sensors of Class IV.

The final selection will depend on the estimated predictivity and specificity indices and associated costs, including the cost of misclassification.

B.6.1 Statistical Independence and Association of Assays

Totally statistically dependent tests will consistently give exactly the same result on a given set of elements. A test battery consisting of these two assays is no better than using either one of them alone since each gives exactly the same information about the elements. Partially dependent assays may furnish partially overlapping information. Hence to maximize the amount of information obtainable from the tests, statistically independent assays should be used.

Formally, two assays are said to be statistically independent if knowing the test results of one assay on a set of elements does not alter the likelihood of getting a certain set of outcomes when the other assay is applied to the same set. Knowing the test result of one will neither improve nor decrease the probabilities of the second.

B.6.2 Determining the Performance of the Test Battery

The performance of a battery is measured as a function of the predictivity and selectivity of the battery. This method of combining multiple tests to find the effective overall selectivity may be useful in sensor fusion methods.

To compute the selectivity of a test package, we must first decide on how we wish to interpret the test results.

Because the test result of each individual assay is independent of the other assay results, the probability of occurrence of each combination can then be easily computed using the multiplication law of probability. For example if a best two-of-three scheme is used and if the test returns a positive element then the probability that combination No.1 (of the chart below) will occur can be found as described below:

$$\begin{aligned} \Pr(No.1 \mid E_P) &= \Pr(A_1 = + \mid E_P)\Pr(A_2 = + \mid E_P)\Pr(A_3 = + \mid E_P) \\ &= 0.8 \cdot 0.9 \cdot 0.6 = 0.432 \end{aligned} \qquad \text{Eq. B.10}$$

Similarly ,the results of all the possible battery outcomes can be written as in Table B.2.

Table B.2: Battery Example						
Combination No.	Possible result			Conclusion of Test Package	$Pr(No.i \mid E_P)$	$Pr(No.i \mid E_N)$
	A_1	A_2	A_3			
1	+	+	+	+	0.432	0.008
2	+	+	-	+	0.048	0.072
3	+	-	+	+	0.288	0.012
4	+	-	-	-	0.032	0.108
5	-	+	+	+	0.108	0.032
6	-	+	-	-	0.012	0.288
7	-	-	+	-	0.072	0.048
8	-	-	-	-	0.008	0.432

Then, the sensitivity and specificity can be found for the combinations of these three tests:

$$sensitivity = \Pr(+ \mid E_P) = 0.432 + 0.048 + 0.288 + 0.108 = 0.876 \qquad \text{Eq. B.11}$$

$$specificity = \Pr(- \mid E_N) = 0.108 + 0.288 + 0.048 + 0.432 = 0.876 \quad \text{Eq. B.12}$$

This result is subjective however, due to the two-of-three criteria. If one-of-three criteria were chosen the results would be different, for example

$$sensitivity = \Pr(+ \mid E_P) = 0.432 + 0.048 + 0.288 + 0.032 + 0.108 + 0.012 + 0.072 = 0.992 \quad \text{Eq. B.13}$$

$$specificity = \Pr(- \mid E_N) = 0.432 \quad \text{Eq. B.14}$$

As well, the predictivity of the test package can be determined. As per our previous equation:

$$\Theta^+ \equiv \Pr(E_P \mid +) \quad \text{Eq. B.15}$$

$$= \frac{\Pr(E_P)\Pr(+ \mid E_P)}{\Pr(E_P)\Pr(+ \mid E_P) + \Pr(E_N)\Pr(+ \mid E_N)} \quad \text{Eq. B.16}$$

$$= \frac{0.876 \cdot \Pr(E_P)}{0.124 - 0.752 \cdot \Pr(E_P)} \quad \text{Eq. B.17}$$

Given total uncertainty of the existence of an element, $\Pr(E_P)=0.5$, then the probability of an iceberg existing, given an overall positive result of this battery of tests is:

$$\Theta^+ = \frac{0.876 \cdot \Pr(E_P)}{0.124 - 0.752 \cdot \Pr(E_P)} = \frac{0.876 \cdot (0.5)}{0.124 - 0.752 \cdot (0.5)} = 0.876 \quad \text{Eq. B.18}$$

Likewise the probability that no iceberg is present given a negative result can be determined.

B.7 Iterative CPBS Method

The above method can be performed iteratively. Staring with a certainty of existence, subsequent sensor results either improve or decrease the certainty of the overall result. This approach may be very useful for the integration of sensor data: data fusion.

Consider a series of tests A_1, A_2, ... A_n, whose sensitivities α^+_1, α^+_2, ... α^+_n and specificities α^-_1, α^-_2, ... α^-_n are known. Let these tests be applied sequentially.

Let Θ^+_i be the estimate of $Pr(E_P)$, given the results of the first i tests. Mathematically Θ^+_i can be written as $Pr(E_P \mid A_1, A_2, \ldots A_i)$, where $A_1, A_2, \ldots A_i$ represent the results of the first i tests. Let Θ^+_0 be our initial guess of the likelihood of a positive element.

If A_1 shows positive, it can be derived:

$$\Theta_1^+ \equiv \Pr(E_P \mid A_1 = +) \qquad \text{Eq. B.19}$$

$$= \frac{\Pr(E_P)\Pr(A_1 = + \mid E_P)}{\Pr(E_P)\Pr(A_1 = + \mid E_P) + \Pr(E_N)\Pr(A_1 = + \mid E_N)} \qquad \text{Eq. B.20}$$

Repeated application of Bayes' theorem in the above manner yields a general recursive formula for positive element predictivity.

For a positive result:

$$\Theta_i^+ = \frac{\alpha_i^+ \Theta_{i-1}^+}{(1-\alpha_i^-) + (\alpha_i^+ + \alpha_i^- - 1)\Theta_{i-1}^+} \qquad \text{Eq. B.21}$$

For a negative result:

$$\Theta_i^- = \frac{(1-\alpha_i^+)\Theta_{i-1}^+}{\alpha_i^- - (\alpha_i^+ + \alpha_i^- - 1)\Theta_{i-1}^+} \qquad \text{Eq. B.22}$$

In this manner multiple sensor inputs could be added one after another, ad infinitum. The general formulae can be used to calculate predictivity indices for any combinations and any number of assays (assuming that the assays are independent). The problem of predicting the existence of an iceberg on the basis of the assay results already available in a database can also be easily handled.

B.8 Conclusions

The CPBS method could provide a method for the addition of multiple sensor outputs over a quantified geographical area. The results of sensor iterations could be overlaid geographically and processed by area to determine a combined result and associated confidence.

As well, sensor outputs over quantified periods of time might be combined as a method of integrating with respect to time.